

AI

Annex I: Atlas of Global and Regional Climate Projections

Editorial Team:

Geert Jan van Oldenborgh (Netherlands), Matthew Collins (UK), Julie Arblaster (Australia), Jens Hesselbjerg Christensen (Denmark), Jochem Marotzke (Germany), Scott B. Power (Australia), Markku Rummukainen (Sweden), Tianjun Zhou (China)

Advisory Board:

David Wratt (New Zealand), Francis Zwiers (Canada), Bruce Hewitson (South Africa)

Review Editor Team:

Pascale Delecluse (France), John Fyfe (Canada), Karl Taylor (USA)

This annex should be cited as:

IPCC, 2013: Annex I: Atlas of Global and Regional Climate Projections [van Oldenborgh, G.J., M. Collins, J. Arblaster, J.H. Christensen, J. Marotzke, S.B. Power, M. Rummukainen and T. Zhou (eds.)]. In: *Climate Change 2013: The Physical Science Basis. Contribution of Working Group I to the Fifth Assessment Report of the Intergovernmental Panel on Climate Change* [Stocker, T.F., D. Qin, G.-K. Plattner, M. Tignor, S.K. Allen, J. Boschung, A. Nauels, Y. Xia, V. Bex and P.M. Midgley (eds.)]. Cambridge University Press, Cambridge, United Kingdom and New York, NY, USA.

Table of Contents

AI

Introduction and Scope 1313

Technical Notes 1313

References 1314

Atlas 1317

Figures AI.4 to AI.7: World 1318

Figures AI.8 to AI.11: Arctic 1322

Figures AI.12 to AI.15: High latitudes 1326

Figures AI.16 to AI.19: North America (West) 1330

Figures AI.20 to AI.23: North America (East) 1334

Figures AI.24 to AI.27: Central America and Caribbean 1338

Figures AI.28 to AI.31: Northern South America 1342

Figures AI.32 to AI.35: Southern South America 1346

Figures AI.36 to AI.39: North and Central Europe 1350

Figures AI.40 to AI.43: Mediterranean and Sahara 1354

Figures AI.44 to AI.47: West and East Africa 1358

Figures AI.48 to AI.51: Southern Africa and West Indian Ocean 1362

Figures AI.52 to AI.55: West and Central Asia 1366

Figures AI.56 to AI.59: Eastern Asia and Tibetan Plateau 1370

Figures AI.60 to AI.63: South Asia 1374

Figures AI.64 to AI.67: Southeast Asia 1378

Figures AI.68 to AI.71: Australia and New Zealand 1382

Figures AI.72 to AI.75: Pacific Islands region 1386

Figures AI.76 to AI.79: Antarctica 1390

Supplementary Material

Supplementary Material is available in online versions of the report.

Introduction and Scope

This Annex presents a series of figures showing global and regional patterns of climate change computed from global climate model output gathered as part of the Coupled Model Intercomparison Project Phase 5 (CMIP5; Taylor et al., 2012). Maps of surface air temperature change and relative precipitation change (i.e., change expressed as a percentage of mean precipitation) in different seasons are presented for the globe and for a number of different sub-continental-scale regions. Twenty-year average changes for the near term (2016–2035), for the mid term (2046–2065) and for the long term (2081–2100) are given, relative to a reference period of 1986–2005. Time series for temperature and relative precipitation changes are shown for global land and sea averages, the 26 sub-continental SREX (IPCC Special Report on Managing the Risks of Extreme Events and Disasters to Advance Climate Change Adaptation) regions (IPCC, 2012) augmented with polar regions and the Caribbean, two Indian Ocean and three Pacific Ocean regions. In total this Annex gives projections for 35 regions, 2 variables and 2 seasons. The projections are made under the Representative Concentration Pathway (RCP) scenarios, which are introduced in Chapter 1 with more technical detail given in Section 12.3 (also note the discussion of near-term biases in Sections 11.3.5.1 and 11.3.6.1). Maps are shown only for the RCP4.5 scenario; however, the time series presented show how the area-average response varies among the RCP2.6, RCP4.5, RCP6.0 and RCP8.5 scenarios. Spatial maps for the other RCP scenarios and additional seasons are presented in the Annex I Supplementary Material. Figures AI.1 and AI.2 give a graphical explanation of aspects of both the time series plots and the spatial maps. While some of the background to the information presented is given here, discussion of the maps and time series, as well as important additional background, is provided in Chapters 9, 11, 12 and 14. Figure captions on each page of the Atlas reference the specific sub-sections in the report relevant to the regions considered on that page.

The projection of future climate change involves the careful evaluation of models, taking into account uncertainties in observations and consideration of the physical basis of the findings, in order to characterize the credibility of the projections and assess their sensitivity to uncertainties. As discussed in Chapter 9, different climate models have varying degrees of success in simulating past climate variability and mean state when compared to observations. Verification of regional trends is discussed in Box 11.2 and provides further information on the credibility of model projections. The information presented in this Annex is based entirely on all available CMIP5 model output with equal weight given to each model or version with different parameterizations.

Complementary methods for making quantitative projections, in which model output is combined with information about model performance using statistical techniques, exist and should be considered in impacts studies (see Sections 9.8.3, 11.3.1 and 12.2.2 to 12.2.3). Although results from the application of such methods can be assessed alongside the projections from CMIP5 presented here, it is beyond the scope of this Annex. Nor do the simple maps provided represent a robust estimate of the uncertainty associated with the projections. Here the range of model spread is provided as a simple, albeit imperfect, guide to the range of possible futures (including the effect of natural variability). Alternative approaches used to estimate projection uncertainty

are discussed in Sections 11.3.1 and 12.2.2 to 12.2.3. The reliability of past trends is assessed in Box 11.2, which concludes that the time series and maps cannot be interpreted literally as probability density functions. They should not be interpreted as ‘forecasts’.

Projections of future climate change are conditional on assumptions of climate forcing, affected by shortcomings of climate models and inevitably also subject to internal variability when considering specific periods. Projected patterns of climate change may differ from one climate model generation to the next due to improvements in models. Some model-inadequacies are common to all models, but so are many patterns of change across successive generations of models, which gives some confidence in projections. The information presented is intended to be only a starting point for anyone interested in more detailed information on projections of future climate change and complements the assessment in Chapters 11, 12 and 14.

Technical Notes

Data and Processing: The figures have been constructed using the CMIP5 model output available at the time of the AR5 cut-off for accepted papers (15 March 2013). This data set comprises 32/42/25/39 scenario experiments for RCP2.6/4.5/6.0/8.5 from 42 climate models (Table AI.1). Only concentration-driven experiments are used (i.e., those in which concentrations rather than emissions of greenhouse gases are prescribed) and only one ensemble member from each model is selected, even if multiple realizations exist with different initial conditions and different realizations of natural variability. Hence each model is given equal weight. Maps from only one scenario (RCP4.5) are shown but time series are included from all four RCPs. Maps from other RCPs are presented in the Annex I Supplementary Material.

Reference Period: Projections are expressed as anomalies with respect to the reference period of 1986–2005 for both time series and spatial maps (i.e., differences between the future period and the reference period). Thus the changes are relative to the climate change that has already occurred since the pre-industrial period and which is discussed in Chapters 2 and 10. For quantities where the trend is larger than the natural variability such as large-area temperature changes, a more recent reference period would give better estimates (see Section 11.3.6.1); for quantities where the natural variability is much larger than the trend a longer reference period would be preferable.

Equal Model Weighting: Model evaluation uses a multitude of techniques (see Chapter 9) and there is no consensus in the community about how to use this information to assign likelihood to different model projections. Consequently, the different CMIP5 models used for the projections in the Atlas are all considered to give equally likely projections in the sense of ‘one model, one vote’. Models with variations in physical parameterization schemes are treated as distinct models.

Variables: Two variables have been plotted: surface air temperature change and relative precipitation change. The relative precipitation change is defined as the percentage change from the 1986–2005 reference period in each ensemble member. For the time series, the variables are first averaged over the domain and then the changes from the reference period are computed. This implies that in regions with

large climatological precipitation gradients, the change is generally dominated by the areas with the most precipitation.

Seasons: For temperature, the standard meteorological seasons June to August and December to February are shown, as these often correspond roughly with the warmest and coldest seasons. The annual mean and remaining seasons, March to May and September to October can be found in the Annex I Supplementary Material. For precipitation, the half-years April to September and October to March are shown so that in most monsoon areas the local rain seasons are entirely contained within the seasonal range plotted. Because the seasonal average is computed first, followed by the percentile change, these numbers are dominated by the rainy months within the half-year. The annual means are included in the Supplementary Material.

Regions: In addition to the global maps, the areas defined in the SREX (IPCC, 2012) are plotted with the addition of six regions containing the Caribbean, Indian Ocean and Pacific Island States and land and sea areas of the two polar regions. For regions containing large land-areas, averages are computed only over land grid points only. For ocean regions, averages are computed over both land and ocean grid points (see figure captions). A grid box is considered land if the land fraction is larger than 50% and sea if it is smaller than this. SREX regions with long coastlines (west coast of South America, North Europe, Southeast Asia) therefore include some influence of the ocean. Note that temperature and precipitation over islands may be very different from those over the surrounding sea.

Time Series: For each of the resulting areas the areal mean is computed on the original model grid using land, sea or all points, depending on the definition of the region (see above). As an indication of the model uncertainty and natural variability, the time series of each model and scenario over the common period 1900–2100 are shown on the top of the page as anomalies relative to 1986–2005 (the seasons December to February and October to March are counted towards the second year in the interval). The multi-model ensemble means are also shown. Finally, for the period 2081–2100, the 20-year means are computed and the box-and-whisker plots show the 5th, 25th, 50th (median), 75th and 95th percentiles sampled over the distribution of the 20-year means of the model time series indicated in Table AI.1, including both natural variability and model spread. In the 20-year means the natural variability is suppressed relative to the annual values in the time series whereas the model uncertainty is the same. Note that owing to a smaller number of models, the box-and-whisker plots for the RCP2.6 scenario and especially the RCP6.0 scenario are less certain than those for RCP4.5 and RCP8.5.

Spatial Maps: The maps in the Atlas show, for an area encompassing two or three regions, the difference between the periods 2016–2035, 2046–2065 and 2081–2100 and the reference period 1986–2005. As local projections of climate change are uncertain, a measure of the range of model projections is shown in addition to the median response of the model ensemble interpolated to a common 2.5° grid (the interpolation was done bilinearly for surface air temperature and first order conservatively for precipitation). It should again be emphasized (see above) that this range does not represent the full uncertainty in the projection. On the left, the 25th percentile of the distribution

of ensemble members is shown, on the right the 75th percentile. The median is shown in the middle (different from similar plots in Chapters 11 and 12 and the time series which show the multi-model mean). The distribution combines the effects of natural variability and model spread. The colour scale is kept constant over all maps.

Hatching: Hatching indicates regions where the magnitude of the change of the 20-year mean is less than 1 standard deviation of model-estimated present-day natural variability of 20-year mean differences. The natural variability is estimated using all pre-industrial control runs which are at least 500 years long. The first 100 years of the pre-industrial are ignored. The natural variability is then calculated for every grid point as the standard deviation of non-overlapping 20-year means after a quadratic fit is subtracted at every grid point to eliminate model drift. This is multiplied by the square root of 2, a factor that arises as the comparison is between two distributions of numbers. The median across all models of that quantity is used. This characterizes the typical difference between two 20-year averages that would be expected due to unforced internal variability. The hatching is applied to all maps so, for example, if the 25th percentile of the distribution of model projections is less than 1 standard deviation of natural variability, it is hatched.

The hatching can be interpreted as some indication of the strength of the future anomalies from present-day climate, when compared to the strength of present day internal 20-year variability. It either means that the change is relatively small or that there is little agreement between models on the sign of the change. It is presented only as a guide to assessing the strength of change as the difference between two 20-year intervals. Using other measures of natural variability would give smaller or larger hatched areas, but the colours underneath the hatching would not be very different. Other methods of hatching and stippling are possible (see Box 12.1) and, in cases where such information is critical, it is recommended that thorough attention is paid to assessing significance using a statistical test appropriate to the problem being considered.

Scenarios: Spatial patterns of changes for scenarios other than RCP4.5 can be found in the Annex I Supplementary Material.

References

- IPCC, 2012: *Managing the Risks of Extreme Events and Disasters to Advance Climate Change Adaptation*. A Special Report of Working Groups I and II of the Intergovernmental Panel on Climate Change [C. B. Field, V. Barros, T. F. Stocker, D. Qin, D. J. Dokken, K. L. Ebi, M. D. Mastrandrea, K. J. Mach, G.-K. Plattner, S. K. Allen, M. Tignor and P. M. Midgley (eds.)]. Cambridge University Press, Cambridge, United Kingdom, and New York, NY, USA, 582 pp.
 Taylor, K. E., R. J. Stouffer, and G. A. Meehl, 2012: A summary of the CMIP5 experiment design. *Bull. Am. Meteorol. Soc.*, 93, 485–498.

Table AI.1 | The CMIP5 models used in this Annex for each of the historical and RCP scenario experiments. A number in each column is the identifier of the single ensemble member from that model that is used. A blank indicates no run was used, usually because that scenario run was not available. For the pre-industrial control column (piControl), a ‘tas’ indicates that those control simulations are used in the estimate of internal variability of surface air temperature and a ‘pr’ indicates that those control simulations are used in the estimate of precipitation internal variability.

CMIP5 Model Name	piControl	Historical	RCP2.6	RCP4.5	RCP6.0	RCP8.5
ACCESS1-0	tas/pr	1		1		1
ACCESS1-3	tas/pr	1		1		1
bcc-csm1-1	tas/pr	1	1	1	1	1
bcc-csm1-1-m		1	1	1	1	
BNU-ESM	tas/pr	1	1	1		1
CanESM2	tas/pr	1	1	1		1
CCSM4	tas/pr	1	1	1	1	1
CESM1-BGC	tas/pr	1		1		1
CESM1-CAM5		1	1	1	1	1
CMCC-CM		1		1		1
CMCC-CMS	tas/pr	1		1		1
CNRM-CM5	tas/pr	1	1	1		1
CSIRO-Mk3-6-0	tas/pr	1	1	1	1	1
EC-EARTH		8	8	8		8
FGOALS-g2	tas/pr	1	1	1		1
FIO-ESM	tas/pr	1	1	1	1	1
GFDL-CM3	tas/pr	1	1	1	1	1
GFDL-ESM2G	tas/pr	1	1	1	1	1
GFDL-ESM2M	tas/pr	1	1	1	1	1
GISS-E2-H p1		1	1	1	1	1
GISS-E2-H p2	tas/pr	1	1	1	1	1
GISS-E2-H p3	tas/pr	1	1	1	1	1
GISS-E2-H-CC		1		1		
GISS-E2-R p1		1	1	1	1	1
GISS-E2-R p2	pr	1	1	1	1	1
GISS-E2-R p3	pr	1	1	1	1	1
GISS-E2-R-CC		1		1		
HadGEM2-AO		1	1	1	1	1
HadGEM2-CC		1		1		1
HadGEM2-ES		2	2	2	2	2
inmcm4	tas/pr	1		1		1
IPSL-CM5A-LR	tas/pr	1	1	1	1	1
IPSL-CM5A-MR		1	1	1	1	1
IPSL-CM5B-LR		1		1		1
MIROC5	tas/pr	1	1	1	1	1
MIROC-ESM	tas/pr	1	1	1	1	1
MIROC-ESM-CHEM		1	1	1	1	1
MPI-ESM-LR	tas/pr	1	1	1		1
MPI-ESM-MR	tas/pr	1	1	1		1
MPI-ESM-P	tas/pr					
MRI-CGCM3	tas/pr	1	1	1	1	1
NorESM1-M	tas/pr	1	1	1	1	1
NorESM1-ME		1	1	1	1	1
Number of models		42	32	42	25	39

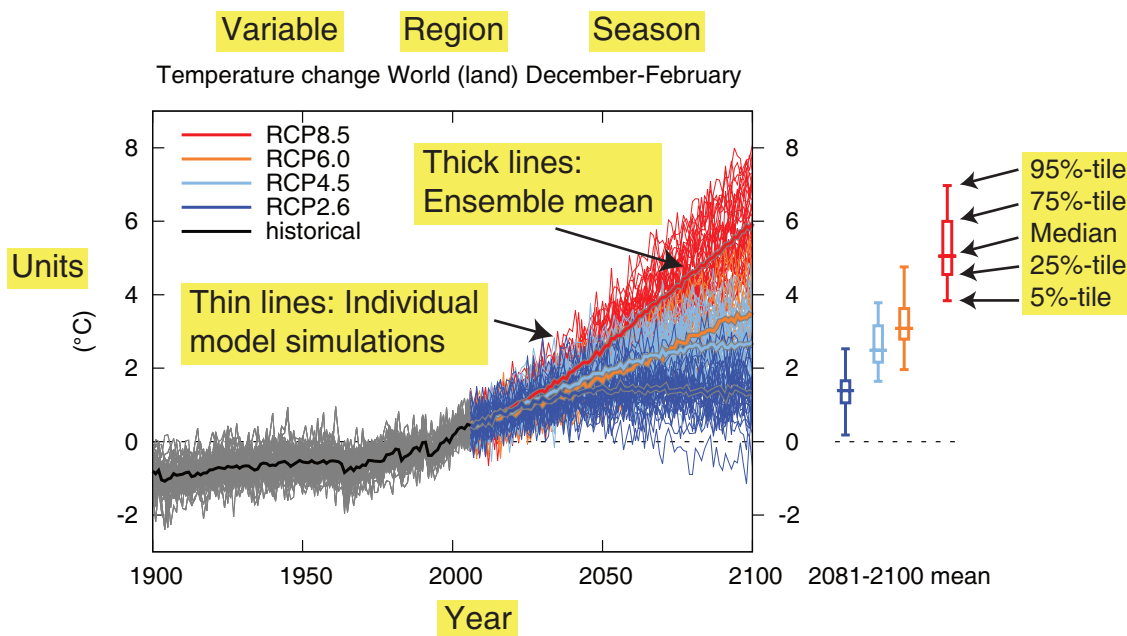


Figure AI.1 | Explanation of the features of a typical time series figure presented in Annex I.

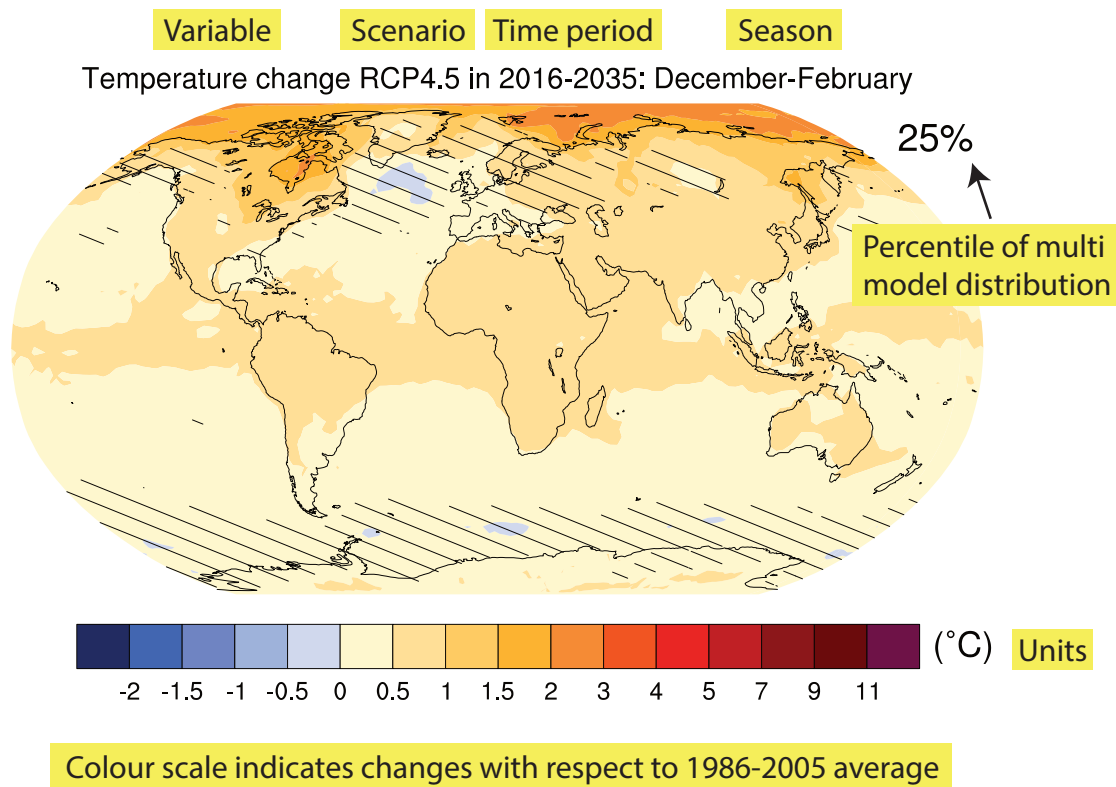
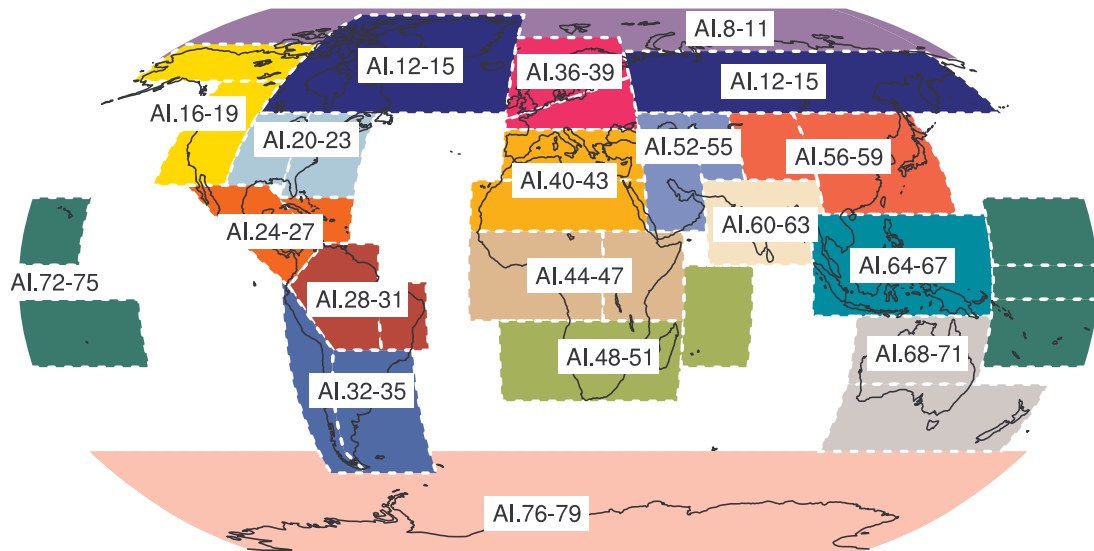


Figure AI.2 | Explanation of the features of a typical spatial map presented in Annex I. Hatching indicates regions where the magnitude of the 25th, median or 75th percentile of the 20-year mean change is less than 1 standard deviation of model-estimated natural variability of 20-year mean differences.

Atlas



AI

Figure AI.3 | Overview of the SREX, ocean and polar regions used.

Figures AI.4 to AI.7: World
 Figures AI.8 to AI.11: Arctic
 Figures AI.12 to AI.15: High latitudes
 Figures AI.16 to AI.19: North America (West)
 Figures AI.20 to AI.23: North America (East)
 Figures AI.24 to AI.27: Central America and Caribbean
 Figures AI.28 to AI.31: Northern South America
 Figures AI.32 to AI.35: Southern South America
 Figures AI.36 to AI.39: North and Central Europe
 Figures AI.40 to AI.43: Mediterranean and Sahara

Figures AI.44 to AI.47: West and East Africa
 Figures AI.48 to AI.51: Southern Africa and West Indian Ocean
 Figures AI.52 to AI.55: West and Central Asia
 Figures AI.56 to AI.59: Eastern Asia and Tibetan Plateau
 Figures AI.60 to AI.63: South Asia
 Figures AI.64 to AI.67: Southeast Asia
 Figures AI.68 to AI.71: Australia and New Zealand
 Figures AI.72 to AI.75: Pacific Islands region
 Figures AI.76 to AI.79: Antarctica

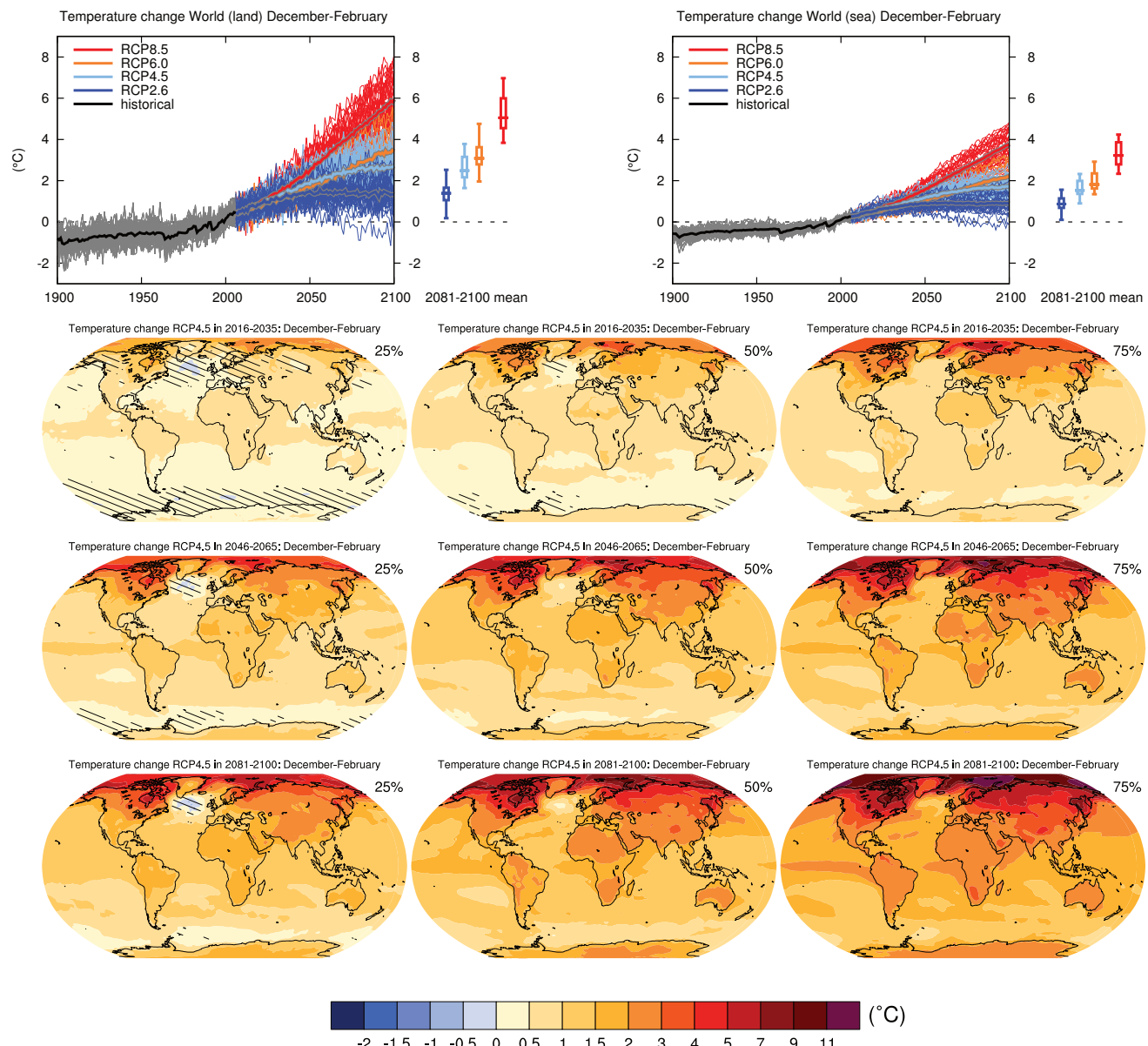


Figure AI.4 | (Top left) Time series of temperature change relative to 1986–2005 averaged over land grid points over the globe in December to February. (Top right) Same for sea grid points. Thin lines denote one ensemble member per model, thick lines the CMIP5 multi-model mean. On the right-hand side the 5th, 25th, 50th (median), 75th and 95th percentiles of the distribution of 20-year mean changes are given for 2081–2100 in the four RCP scenarios.

(Below) Maps of temperature changes in 2016–2035, 2046–2065 and 2081–2100 with respect to 1986–2005 in the RCP4.5 scenario. For each point, the 25th, 50th and 75th percentiles of the distribution of the CMIP5 ensemble are shown; this includes both natural variability and inter-model spread. Hatching denotes areas where the 20-year mean differences of the percentiles are less than the standard deviation of model-estimated present-day natural variability of 20-year mean differences.

Sections 9.4.1.1, 9.6.1.1, 10.3.1.1.4, 11.3.2.1.2, 11.3.3.1, Box 11.2, 12.4.3.1 and 12.4.7 contain relevant information regarding the evaluation of models in this region, the model spread in the context of other methods of projecting changes and the role of modes of variability and other climate phenomena.

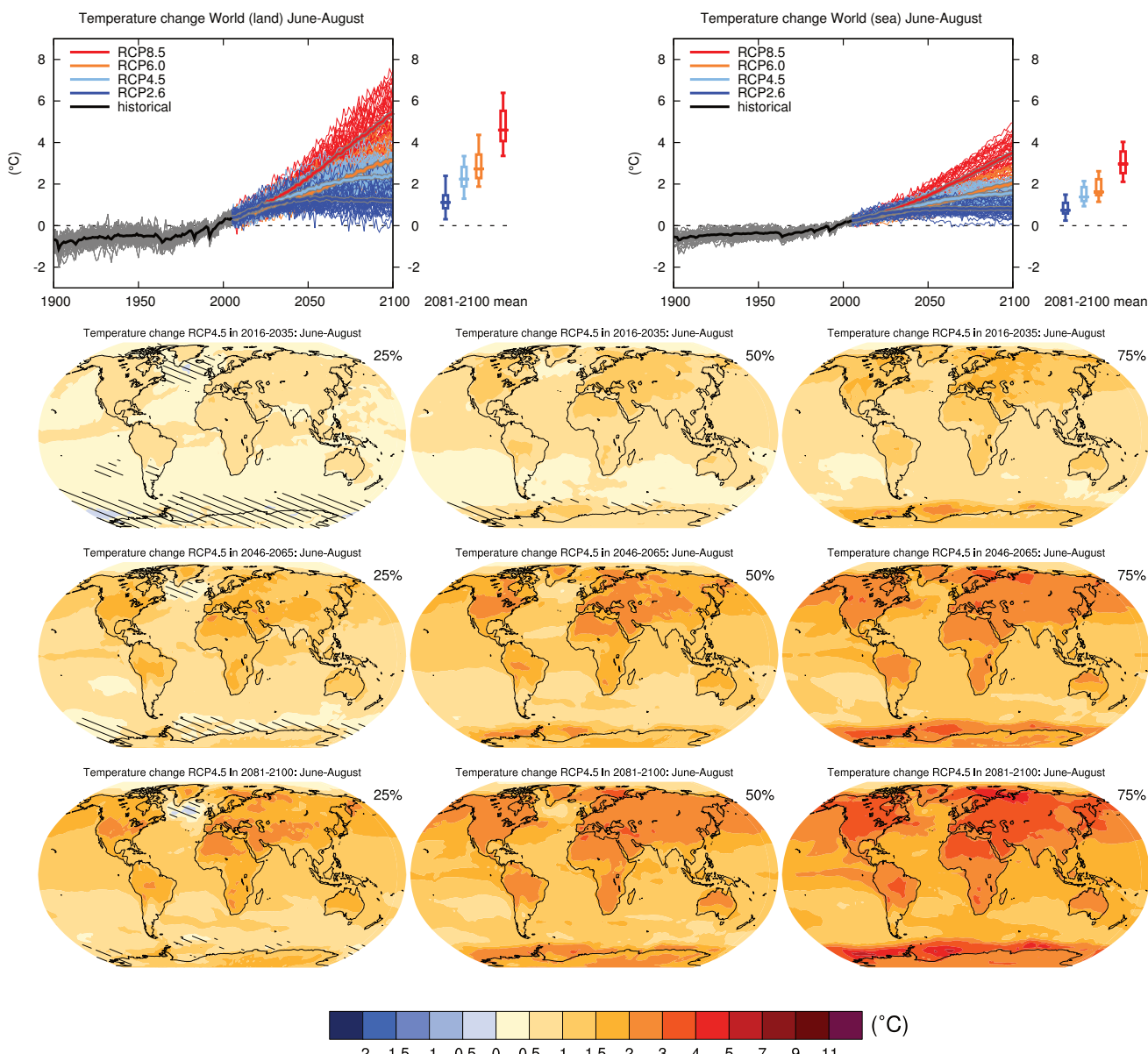


Figure AI.5 | (Top left) Time series of temperature change relative to 1986–2005 averaged over land grid points over the globe in June to August. (Top right) Same for sea grid points. Thin lines denote one ensemble member per model, thick lines the CMIP5 multi-model mean. On the right-hand side the 5th, 25th, 50th (median), 75th and 95th percentiles of the distribution of 20-year mean changes are given for 2081–2100 in the four RCP scenarios.

(Below) Maps of temperature changes in 2016–2035, 2046–2065 and 2081–2100 with respect to 1986–2005 in the RCP4.5 scenario. For each point, the 25th, 50th and 75th percentiles of the distribution of the CMIP5 ensemble are shown; this includes both natural variability and inter-model spread. Hatching denotes areas where the 20-year mean differences of the percentiles are less than the standard deviation of model-estimated present-day natural variability of 20-year mean differences.

Sections 9.4.1.1, 9.6.1.1, 10.3.1.1.4, 11.3.2.1.2, 11.3.3.1, Box 11.2, 12.4.3.1 and 12.4.7 contain relevant information regarding the evaluation of models in this region, the model spread in the context of other methods of projecting changes and the role of modes of variability and other climate phenomena.

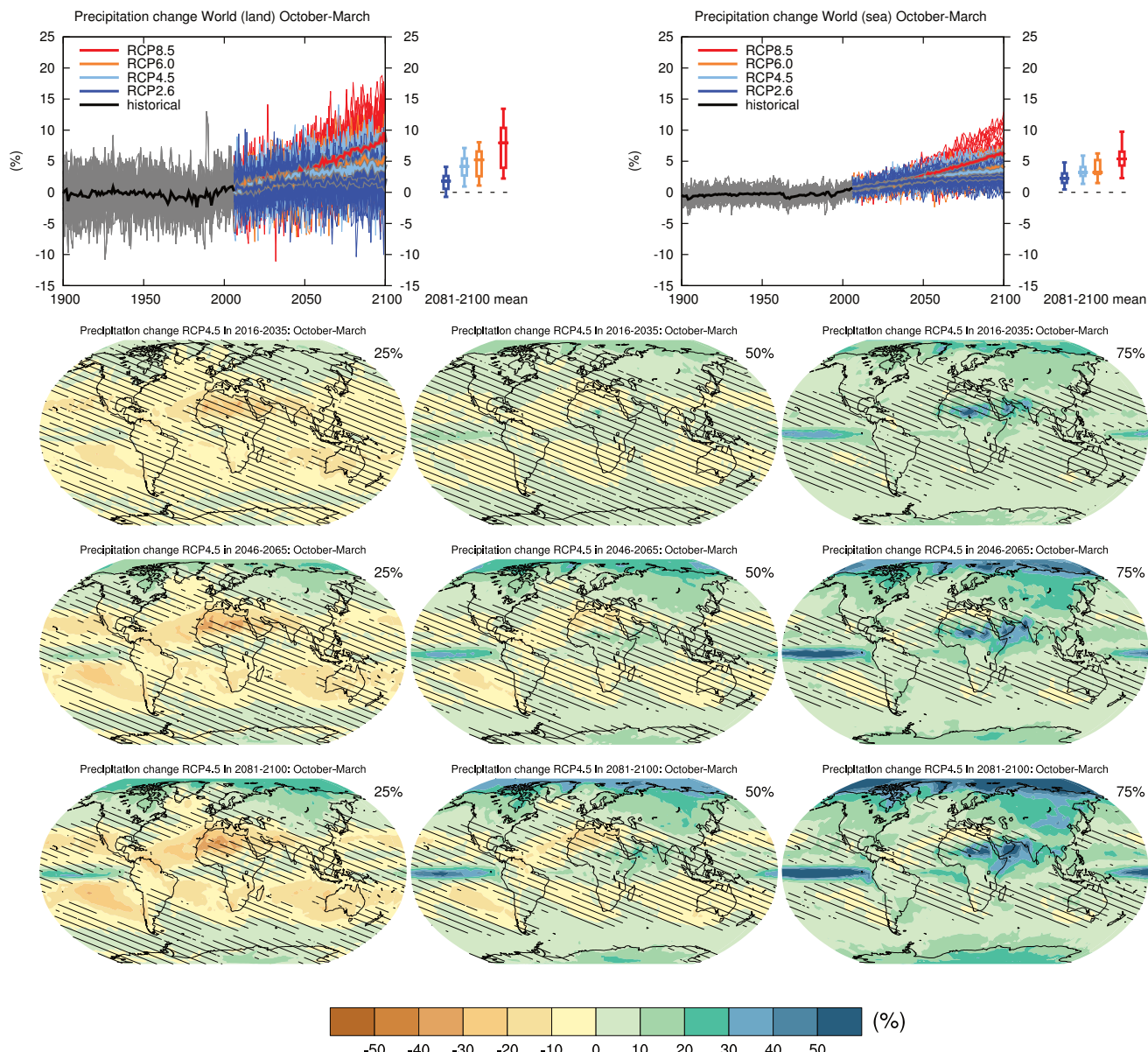


Figure AI.6 | (Top left) Time series of relative change relative to 1986–2005 in precipitation averaged over land grid points over the globe in October to March. (Top right) Same for sea grid points. Thin lines denote one ensemble member per model, thick lines the CMIP5 multi-model mean. On the right-hand side the 5th, 25th, 50th (median), 75th and 95th percentiles of the distribution of 20-year mean changes are given for 2081–2100 in the four RCP scenarios.

(Below) Maps of precipitation changes in 2016–2035, 2046–2065 and 2081–2100 with respect to 1986–2005 in the RCP4.5 scenario. For each point, the 25th, 50th and 75th percentiles of the distribution of the CMIP5 ensemble are shown; this includes both natural variability and inter-model spread. Hatching denotes areas where the 20-year mean differences of the percentiles are less than the standard deviation of model-estimated present-day natural variability of 20-year mean differences.

Sections 9.4.1.1, 9.6.1.1, 10.3.2.2, 11.3.2.3.1, Box 11.2, 12.4.5.2, 14.2 contain relevant information regarding the evaluation of models in this region, the model spread in the context of other methods of projecting changes and the role of modes of variability and other climate phenomena.

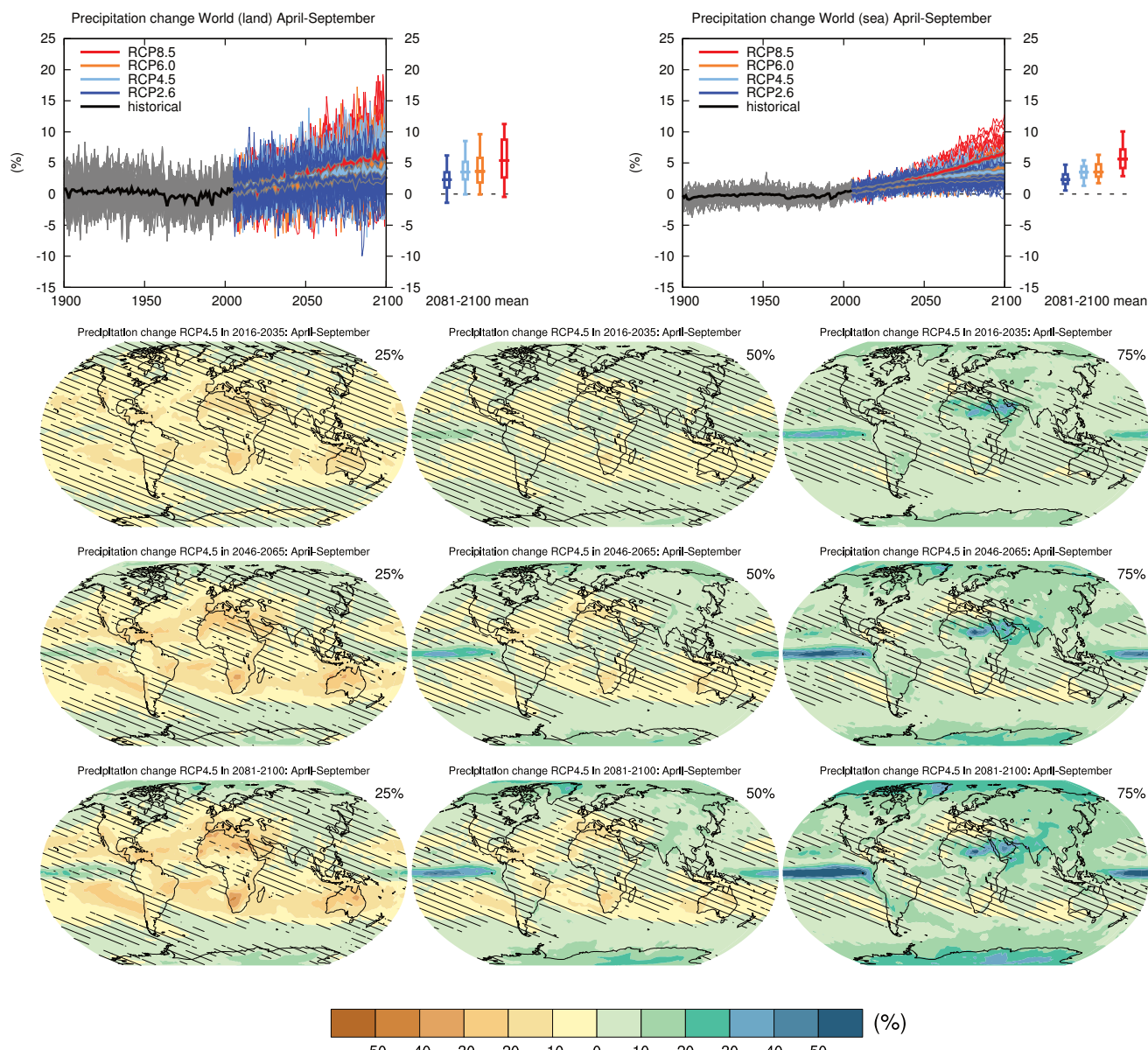


Figure AI.7 | (Top left) Time series of relative change relative to 1986–2005 in precipitation averaged over land grid points over the globe in April to September. (Top right) Same for sea grid points. Thin lines denote one ensemble member per model, thick lines the CMIP5 multi-model mean. On the right-hand side the 5th, 25th, 50th (median), 75th and 95th percentiles of the distribution of 20-year mean changes are given for 2081–2100 in the four RCP scenarios.

(Below) Maps of precipitation changes in 2016–2035, 2046–2065 and 2081–2100 with respect to 1986–2005 in the RCP4.5 scenario. For each point, the 25th, 50th and 75th percentiles of the distribution of the CMIP5 ensemble are shown; this includes both natural variability and inter-model spread. Hatching denotes areas where the 20-year mean differences of the percentiles are less than the standard deviation of model-estimated present-day natural variability of 20-year mean differences.

Sections 9.4.1.1, 9.6.1.1, 10.3.2.2, 11.3.2.3.1, Box 11.2, 12.4.5.2, 14.2 contain relevant information regarding the evaluation of models in this region, the model spread in the context of other methods of projecting changes and the role of modes of variability and other climate phenomena.

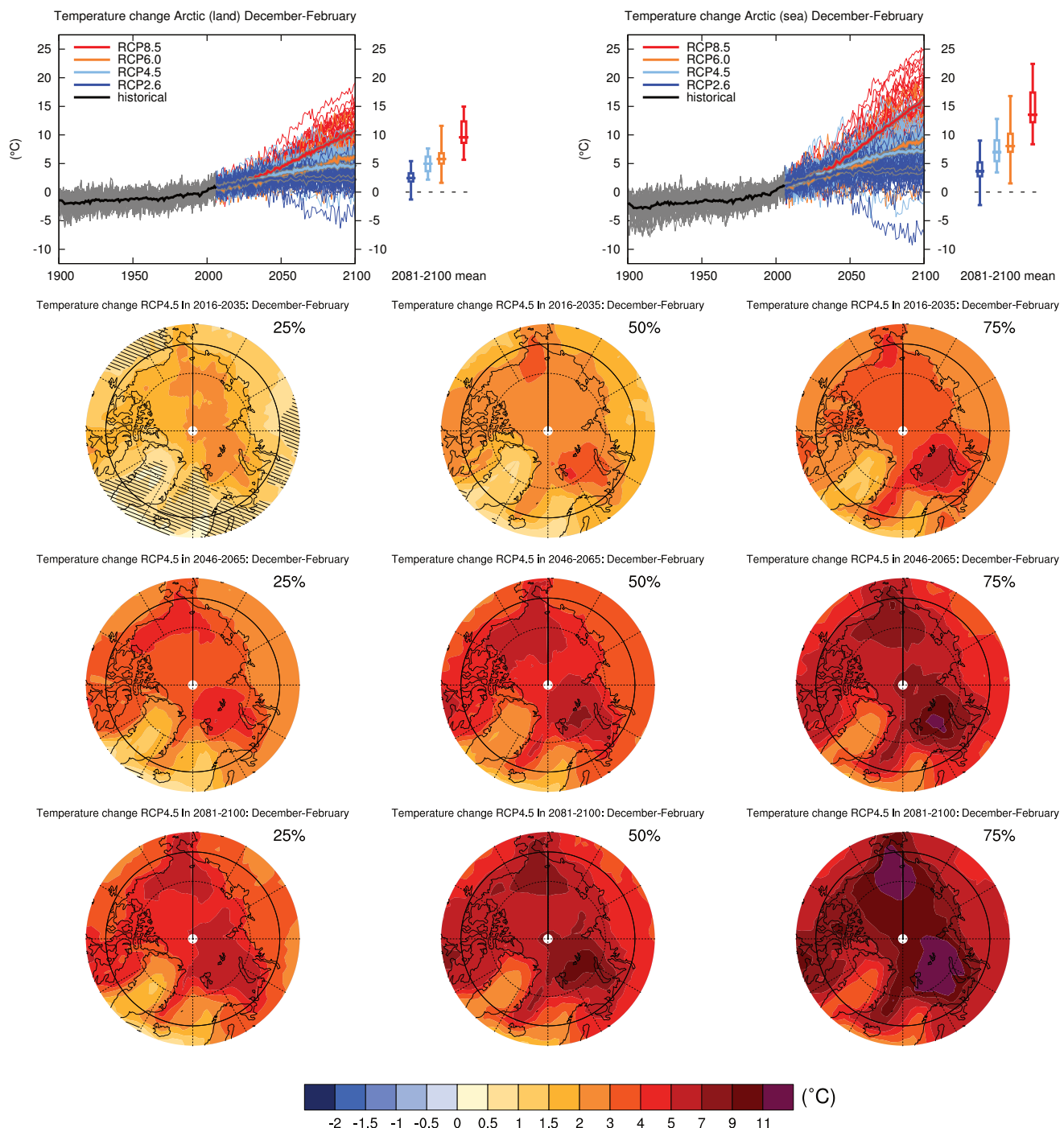


Figure AI.8 | (Top left) Time series of temperature change relative to 1986–2005 averaged over land grid points in the Arctic (67.5°N to 90°N) in December to February. (Top right) Same for sea grid points. Thin lines denote one ensemble member per model, thick lines the CMIP5 multi-model mean. On the right-hand side the 5th, 25th, 50th (median), 75th and 95th percentiles of the distribution of 20-year mean changes are given for 2081–2100 in the four RCP scenarios.

(Below) Maps of temperature changes in 2016–2035, 2046–2065 and 2081–2100 with respect to 1986–2005 in the RCP4.5 scenario. For each point, the 25th, 50th and 75th percentiles of the distribution of the CMIP5 ensemble are shown; this includes both natural variability and inter-model spread. Hatching denotes areas where the 20-year mean differences of the percentiles are less than the standard deviation of model-estimated present-day natural variability of 20-year mean differences.

Sections 9.4.1.1, 9.6.1.1, 10.3.1.1.4, 11.3.2.1.2, Box 11.2, 12.4.3.1, 14.8.2 contain relevant information regarding the evaluation of models in this region, the model spread in the context of other methods of projecting changes and the role of modes of variability and other climate phenomena.

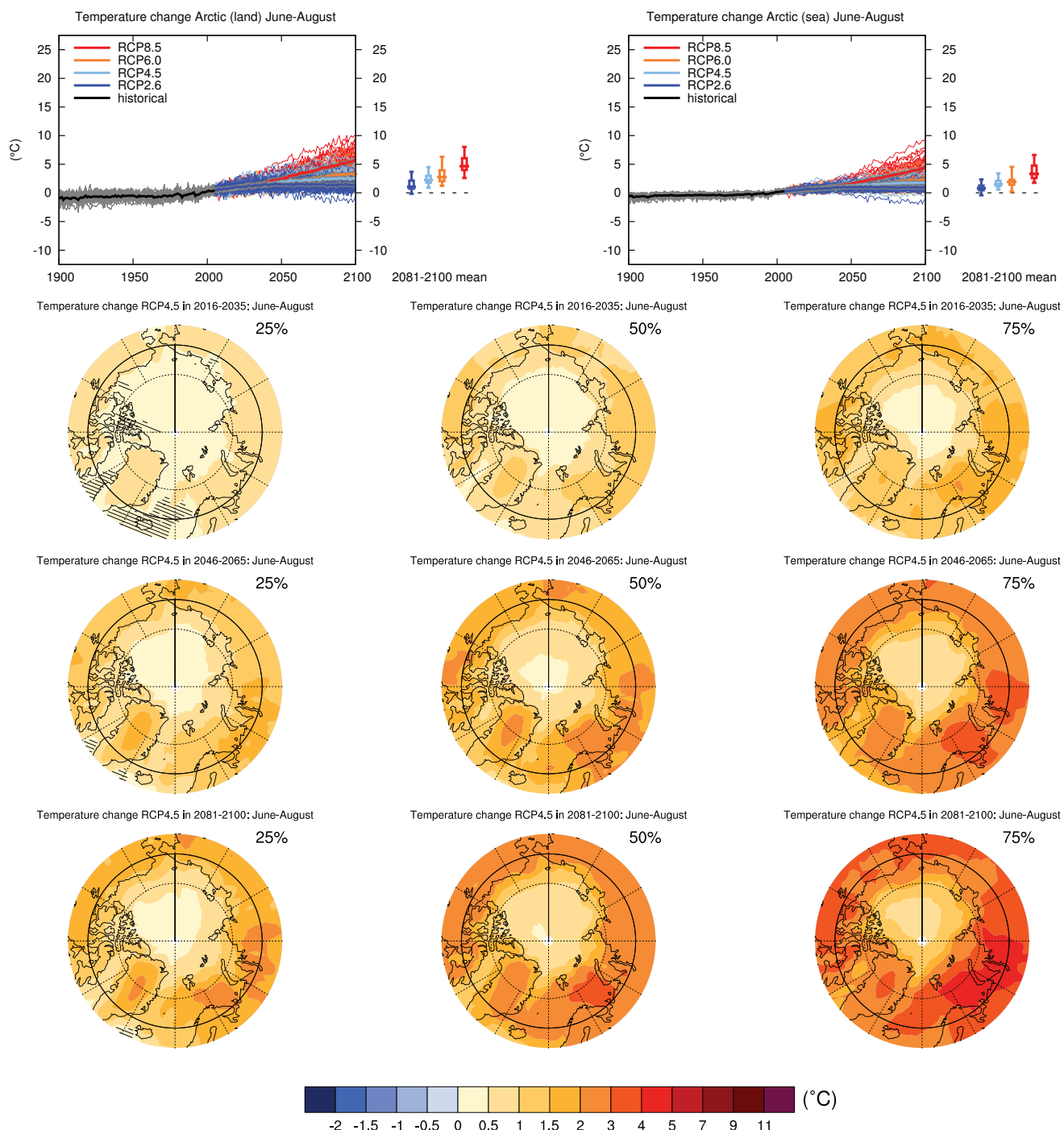


Figure AI.9 | (Top left) Time series of temperature change relative to 1986–2005 averaged over land grid points in the Arctic (67.5°N to 90°N) in June to August. (Top right) Same for sea grid points. Thin lines denote one ensemble member per model, thick lines the CMIP5 multi-model mean. On the right-hand side the 5th, 25th, 50th (median), 75th and 95th percentiles of the distribution of 20-year mean changes are given for 2081–2100 in the four RCP scenarios.

(Below) Maps of temperature changes in 2016–2035, 2046–2065 and 2081–2100 with respect to 1986–2005 in the RCP4.5 scenario. For each point, the 25th, 50th and 75th percentiles of the distribution of the CMIP5 ensemble are shown; this includes both natural variability and inter-model spread. Hatching denotes areas where the 20-year mean differences of the percentiles are less than the standard deviation of model-estimated present-day natural variability of 20-year mean differences.

Sections 9.4.1.1, 9.6.1.1, 10.3.1.1.4, 11.3.2.1.2, Box 11.2, 12.4.3.1, 14.8.2 contain relevant information regarding the evaluation of models in this region, the model spread in the context of other methods of projecting changes and the role of modes of variability and other climate phenomena.

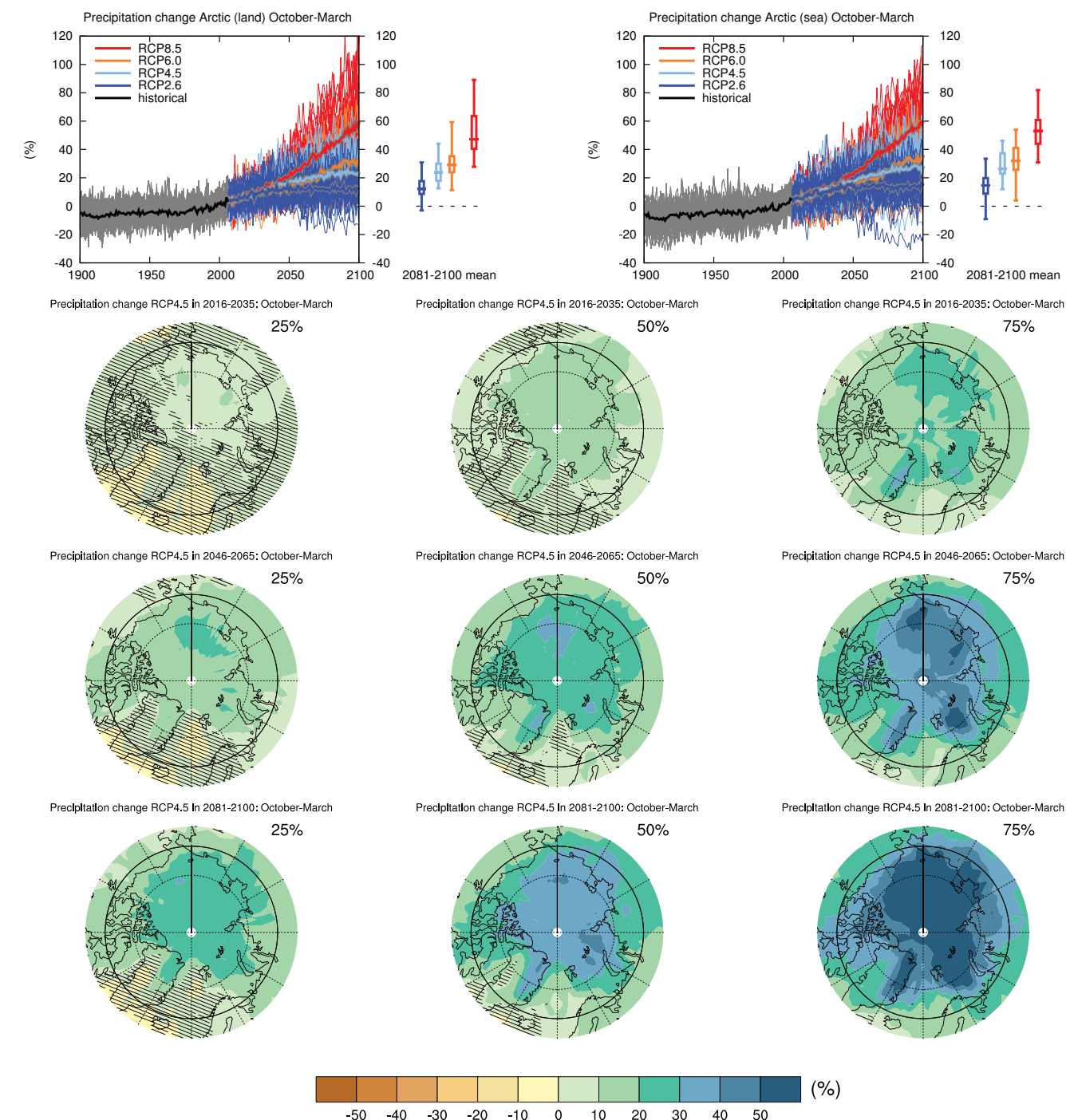


Figure AI.10 | (Top left) Time series of relative change relative to 1986–2005 in precipitation averaged over land grid points in the Arctic (67.5°N to 90°N) in October to March. (Top right) Same for sea grid points. Thin lines denote one ensemble member per model, thick lines the CMIP5 multi-model mean. On the right-hand side the 5th, 25th, 50th (median), 75th and 95th percentiles of the distribution of 20-year mean changes are given for 2081–2100 in the four RCP scenarios.

(Below) Maps of precipitation changes in 2016–2035, 2046–2065 and 2081–2100 with respect to 1986–2005 in the RCP4.5 scenario. For each point, the 25th, 50th and 75th percentiles of the distribution of the CMIP5 ensemble are shown; this includes both natural variability and inter-model spread. Hatching denotes areas where the 20-year mean differences of the percentiles are less than the standard deviation of model-estimated present-day natural variability of 20-year mean differences.

Sections 9.4.1.1, 9.6.1.1, 11.3.2.3.1, Box 11.2, 12.4.5.2, 14.8.2 contain relevant information regarding the evaluation of models in this region, the model spread in the context of other methods of projecting changes and the role of modes of variability and other climate phenomena.

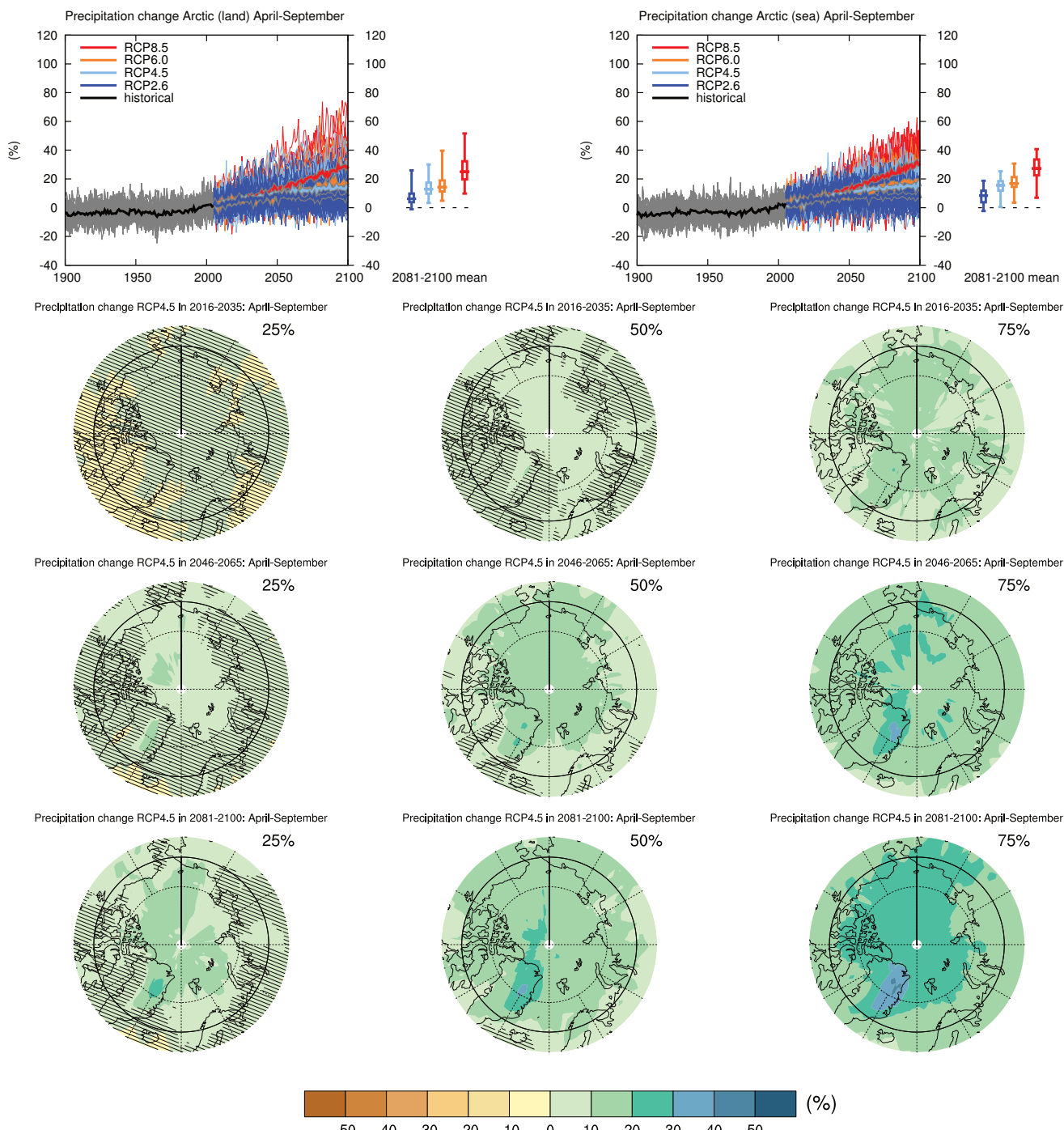


Figure AI.11 | (Top left) Time series of relative change relative to 1986–2005 in precipitation averaged over land grid points in the Arctic (67.5°N to 90°N) in April to September. (Top right) Same for sea grid points. Thin lines denote one ensemble member per model, thick lines the CMIP5 multi-model mean. On the right-hand side the 5th, 25th, 50th (median), 75th and 95th percentiles of the distribution of 20-year mean changes are given for 2081–2100 in the four RCP scenarios.

(Below) Maps of precipitation changes in 2016–2035, 2046–2065 and 2081–2100 with respect to 1986–2005 in the RCP4.5 scenario. For each point, the 25th, 50th and 75th percentiles of the distribution of the CMIP5 ensemble are shown; this includes both natural variability and inter-model spread. Hatching denotes areas where the 20-year mean differences of the percentiles are less than the standard deviation of model-estimated present-day natural variability of 20-year mean differences.

Sections 9.4.1.1, 9.6.1.1, 11.3.2.3.1, Box 11.2, 12.4.5.2, 14.8.2 contain relevant information regarding the evaluation of models in this region, the model spread in the context of other methods of projecting changes and the role of modes of variability and other climate phenomena.

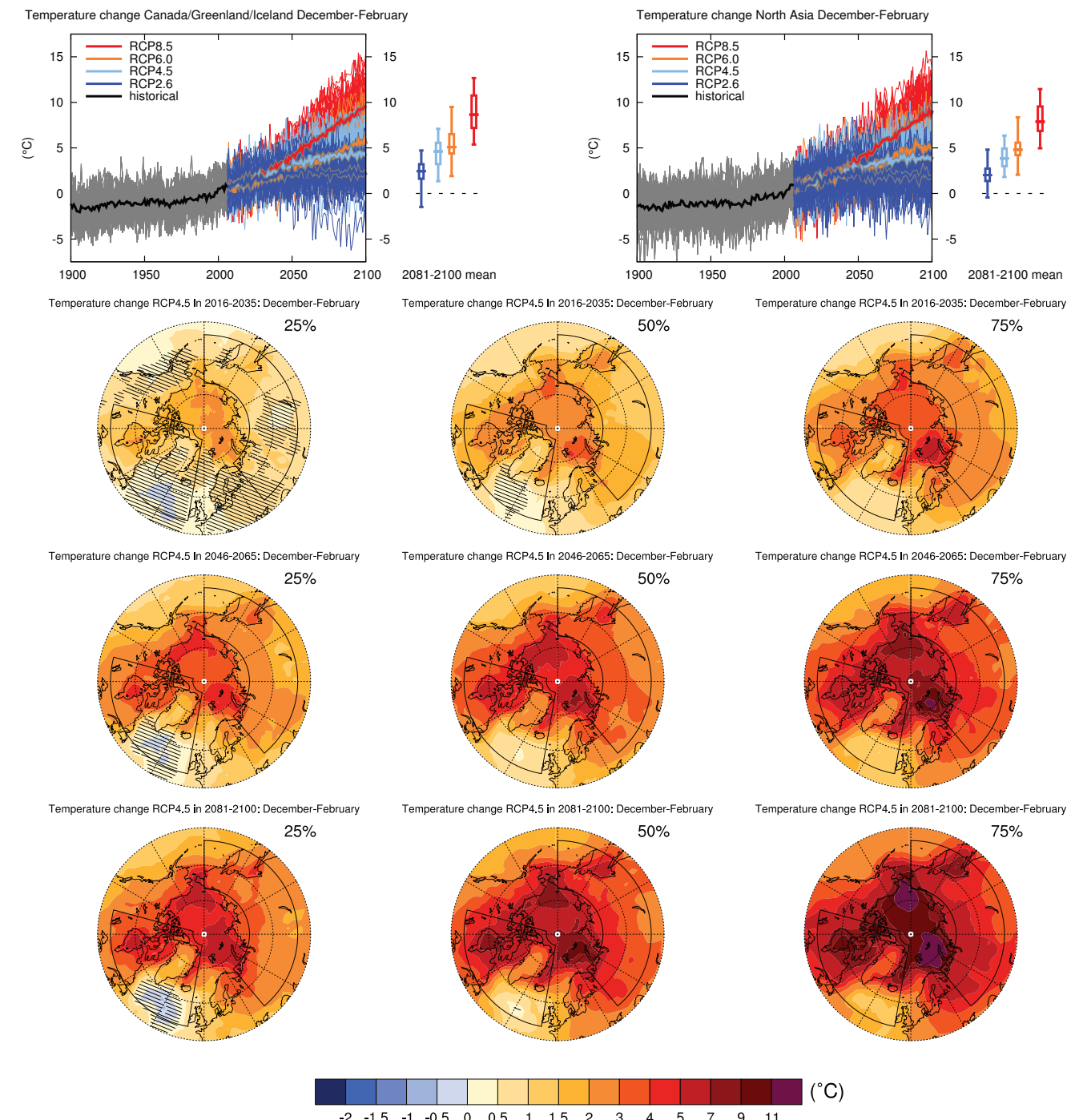


Figure AI.12 | (Top left) Time series of temperature change relative to 1986–2005 averaged over land grid points in Canada/Greenland/Iceland (50°N to 85°N , 105°W to 10°W) in December to February. (Top right) Same for land grid points in North Asia (50°N to 70°N , 40°E to 180°E). Thin lines denote one ensemble member per model, thick lines the CMIP5 multi-model mean. On the right-hand side the 5th, 25th, 50th (median), 75th and 95th percentiles of the distribution of 20-year mean changes are given for 2081–2100 in the four RCP scenarios.

(Below) Maps of temperature changes in 2016–2035, 2046–2065 and 2081–2100 with respect to 1986–2005 in the RCP4.5 scenario. For each point, the 25th, 50th and 75th percentiles of the distribution of the CMIP5 ensemble are shown; this includes both natural variability and inter-model spread. Hatching denotes areas where the 20-year mean differences of the percentiles are less than the standard deviation of model-estimated present-day natural variability of 20-year mean differences.

Sections 9.4.1.1, 9.6.1.1, 10.3.1.1.4, 11.3.2.1.2, Box 11.2, 14.8.2, 14.8.8 contain relevant information regarding the evaluation of models in this region, the model spread in the context of other methods of projecting changes and the role of modes of variability and other climate phenomena.

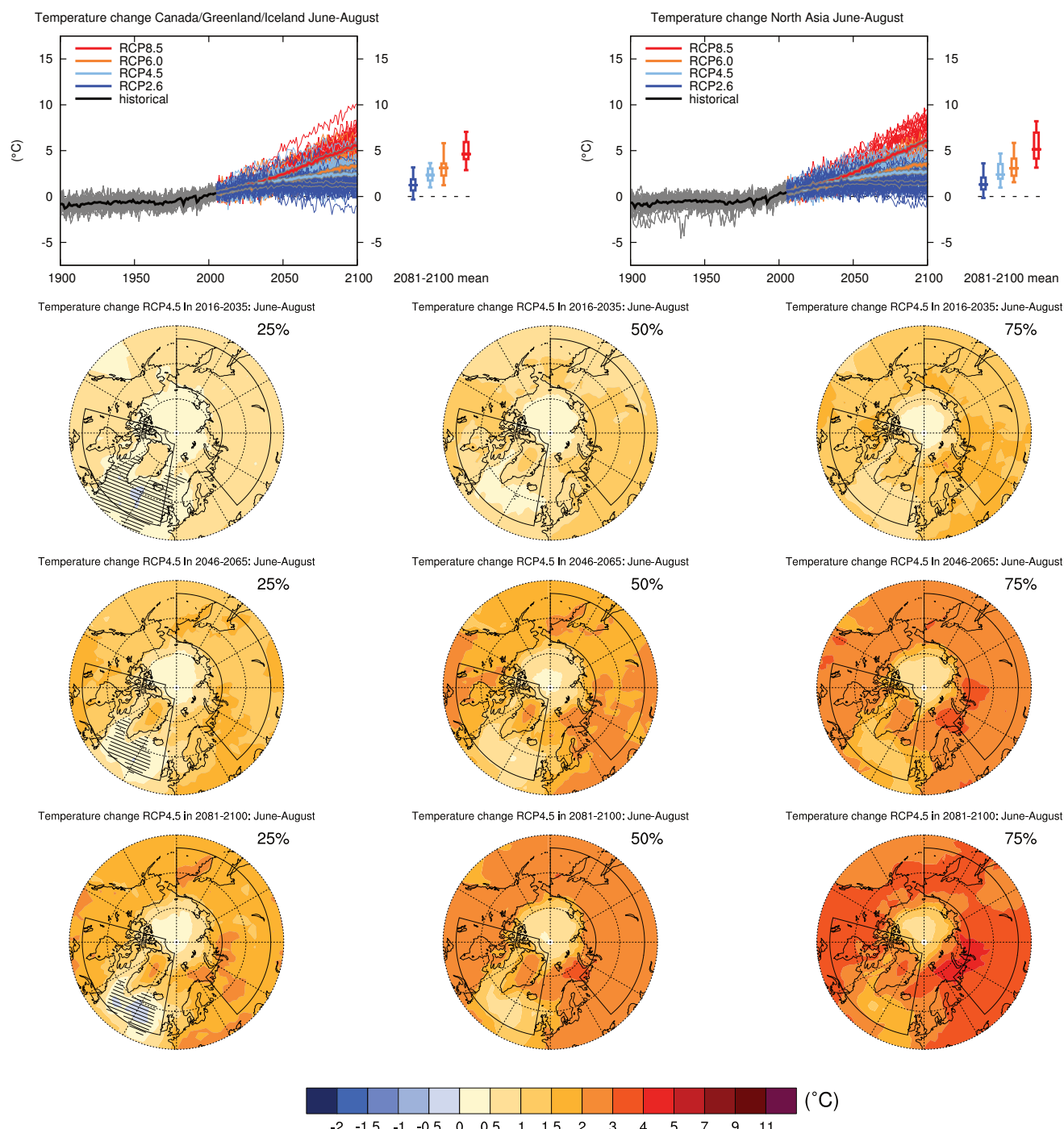


Figure AI.13 | (Top left) Time series of temperature change relative to 1986–2005 averaged over land grid points in Canada/Greenland/Iceland (50°N to 85°N , 105°W to 10°W) in June to August. (Top right) Same for land grid points in North Asia (50°N to 70°N , 40°E to 180°E). Thin lines denote one ensemble member per model, thick lines the CMIP5 multi-model mean. On the right-hand side the 5th, 25th, 50th (median), 75th and 95th percentiles of the distribution of 20-year mean changes are given for 2081–2100 in the four RCP scenarios.

(Below) Maps of temperature changes in 2016–2035, 2046–2065 and 2081–2100 with respect to 1986–2005 in the RCP4.5 scenario. For each point, the 25th, 50th and 75th percentiles of the distribution of the CMIP5 ensemble are shown; this includes both natural variability and inter-model spread. Hatching denotes areas where the 20-year mean differences of the percentiles are less than the standard deviation of model-estimated present-day natural variability of 20-year mean differences.

Sections 9.4.1.1, 9.6.1.1, 10.3.1.1.4, 11.3.2.1.2, Box 11.2, 14.8.2, 14.8.8 contain relevant information regarding the evaluation of models in this region, the model spread in the context of other methods of projecting changes and the role of modes of variability and other climate phenomena.

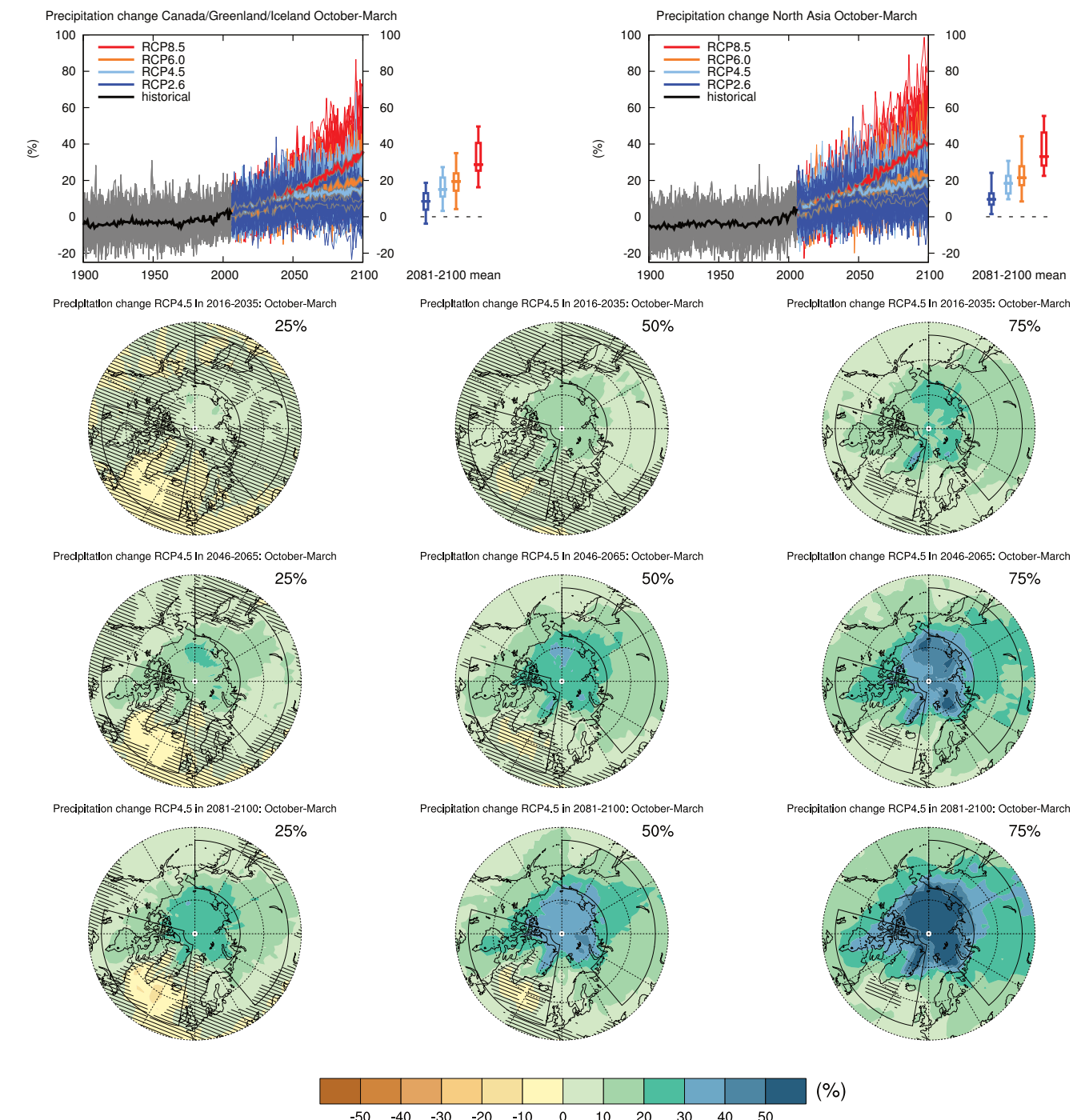


Figure AI.14 | (Top left) Time series of relative change relative to 1986–2005 in precipitation averaged over land grid points in Canada/Greenland/Iceland (50°N to 85°N , 105°W to 10°W) in October to March. (Top right) Same for land grid points in North Asia (50°N to 70°N , 40°E to 180°E). Thin lines denote one ensemble member per model, thick lines the CMIP5 multi-model mean. On the right-hand side the 5th, 25th, 50th (median), 75th and 95th percentiles of the distribution of 20-year mean changes are given for 2081–2100 in the four RCP scenarios.

(Below) Maps of precipitation changes in 2016–2035, 2046–2065 and 2081–2100 with respect to 1986–2005 in the RCP4.5 scenario. For each point, the 25th, 50th and 75th percentiles of the distribution of the CMIP5 ensemble are shown; this includes both natural variability and inter-model spread. Hatching denotes areas where the 20-year mean differences of the percentiles are less than the standard deviation of model-estimated present-day natural variability of 20-year mean differences.

Sections 9.4.1.1, 9.6.1.1, 10.3.2.2, 11.3.2.3.1, Box 11.2, 12.4.5.2, 14.8.2, 14.8.8 contain relevant information regarding the evaluation of models in this region, the model spread in the context of other methods of projecting changes and the role of modes of variability and other climate phenomena.

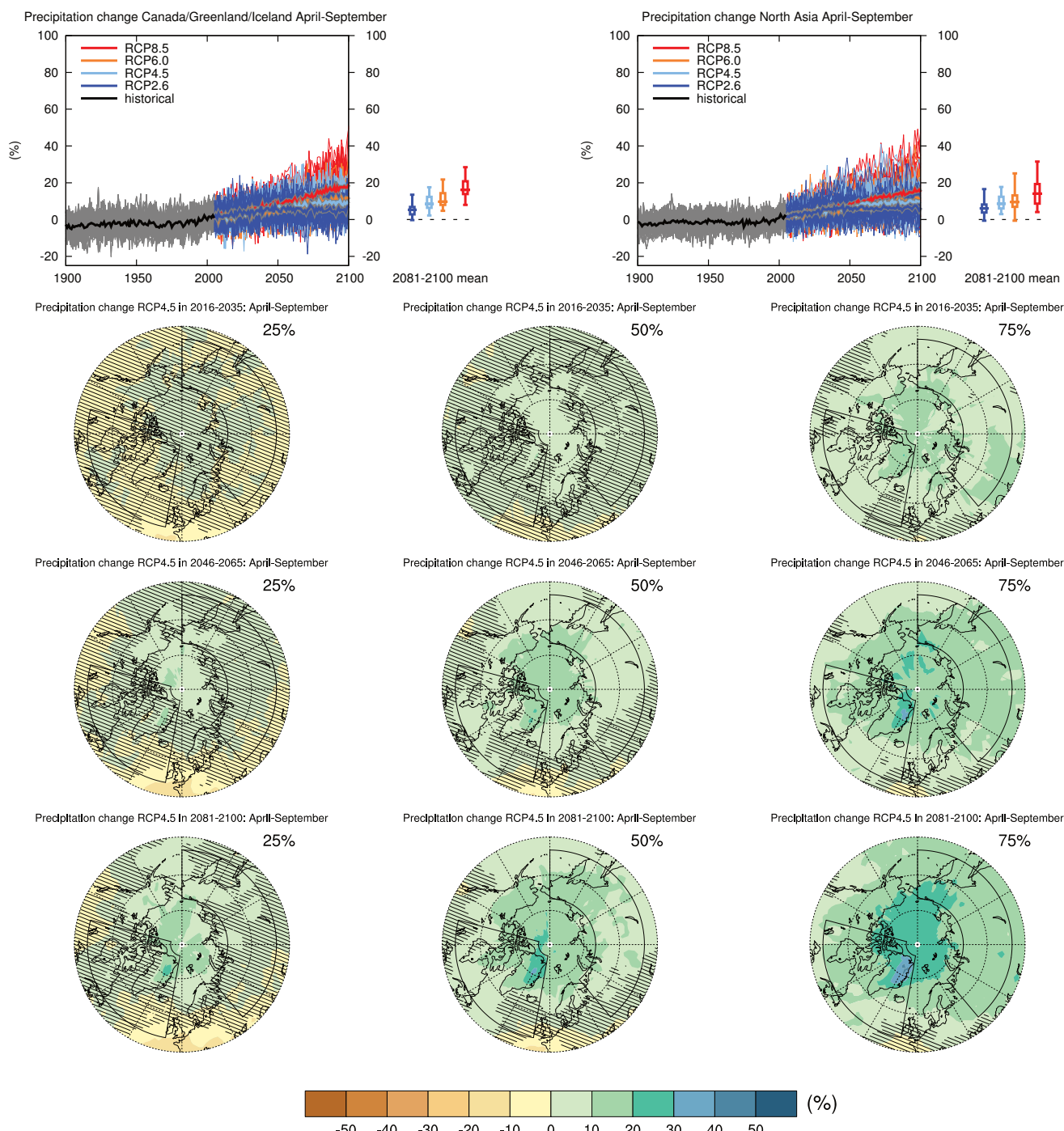


Figure AI.15 | (Top left) Time series of relative change relative to 1986–2005 in precipitation averaged over land grid points in Canada/Greenland/Iceland (50°N to 85°N , 105°W to 10°W) in April to September. (Top right) Same for land grid points in North Asia (50°N to 70°N , 40°E to 180°). Thin lines denote one ensemble member per model, thick lines the CMIP5 multi-model mean. On the right-hand side the 5th, 25th, 50th (median), 75th and 95th percentiles of the distribution of 20-year mean changes are given for 2081–2100 in the four RCP scenarios.

(Below) Maps of precipitation changes in 2016–2035, 2046–2065 and 2081–2100 with respect to 1986–2005 in the RCP4.5 scenario. For each point, the 25th, 50th and 75th percentiles of the distribution of the CMIP5 ensemble are shown; this includes both natural variability and inter-model spread. Hatching denotes areas where the 20-year mean differences of the percentiles are less than the standard deviation of model-estimated present-day natural variability of 20-year mean differences.

Sections 9.4.1.1, 9.6.1.1, 10.3.2.2, 11.3.2.3.1, Box 11.2, 12.4.5.2, 14.8.2, 14.8.8 contain relevant information regarding the evaluation of models in this region, the model spread in the context of other methods of projecting changes and the role of modes of variability and other climate phenomena.

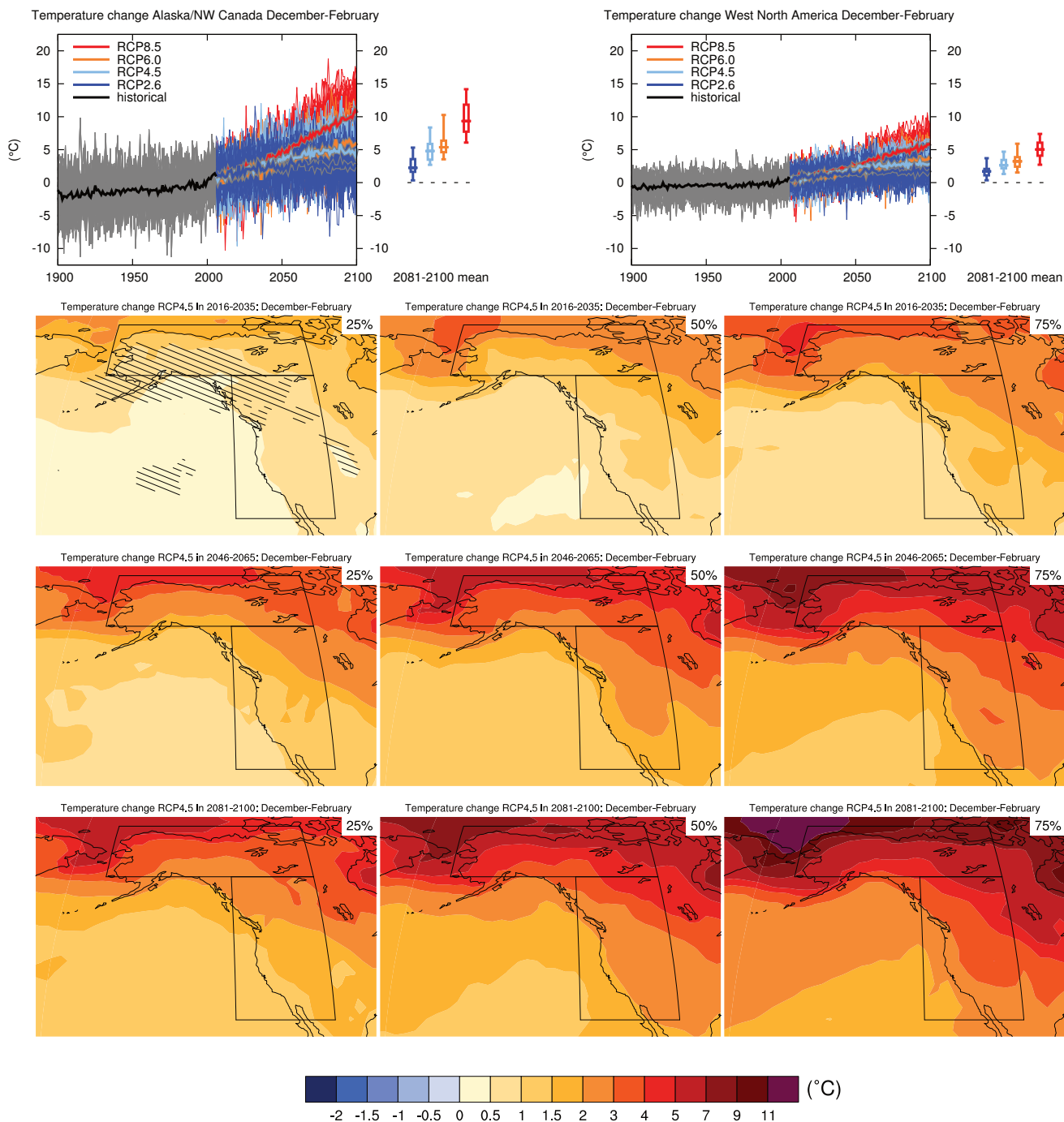


Figure AI.16 | (Top left) Time series of temperature change relative to 1986–2005 averaged over land grid points in Alaska/NW Canada (60°N to 72.6°N , 168°W to 105°W) in December to February. (Top right) Same for land grid points in West North America (28.6°N to 60°N , 130°W to 105°W). Thin lines denote one ensemble member per model, thick lines the CMIP5 multi-model mean. On the right-hand side the 5th, 25th, 50th (median), 75th and 95th percentiles of the distribution of 20-year mean changes are given for 2081–2100 in the four RCP scenarios.

(Below) Maps of temperature changes in 2016–2035, 2046–2065 and 2081–2100 with respect to 1986–2005 in the RCP4.5 scenario. For each point, the 25th, 50th and 75th percentiles of the distribution of the CMIP5 ensemble are shown; this includes both natural variability and inter-model spread. Hatching denotes areas where the 20-year mean differences of the percentiles are less than the standard deviation of model-estimated present-day natural variability of 20-year mean differences.

Sections 9.4.1.1, 9.6.1.1, 10.3.1.1.4, Box 11.2, 14.8.3 contain relevant information regarding the evaluation of models in this region, the model spread in the context of other methods of projecting changes and the role of modes of variability and other climate phenomena.

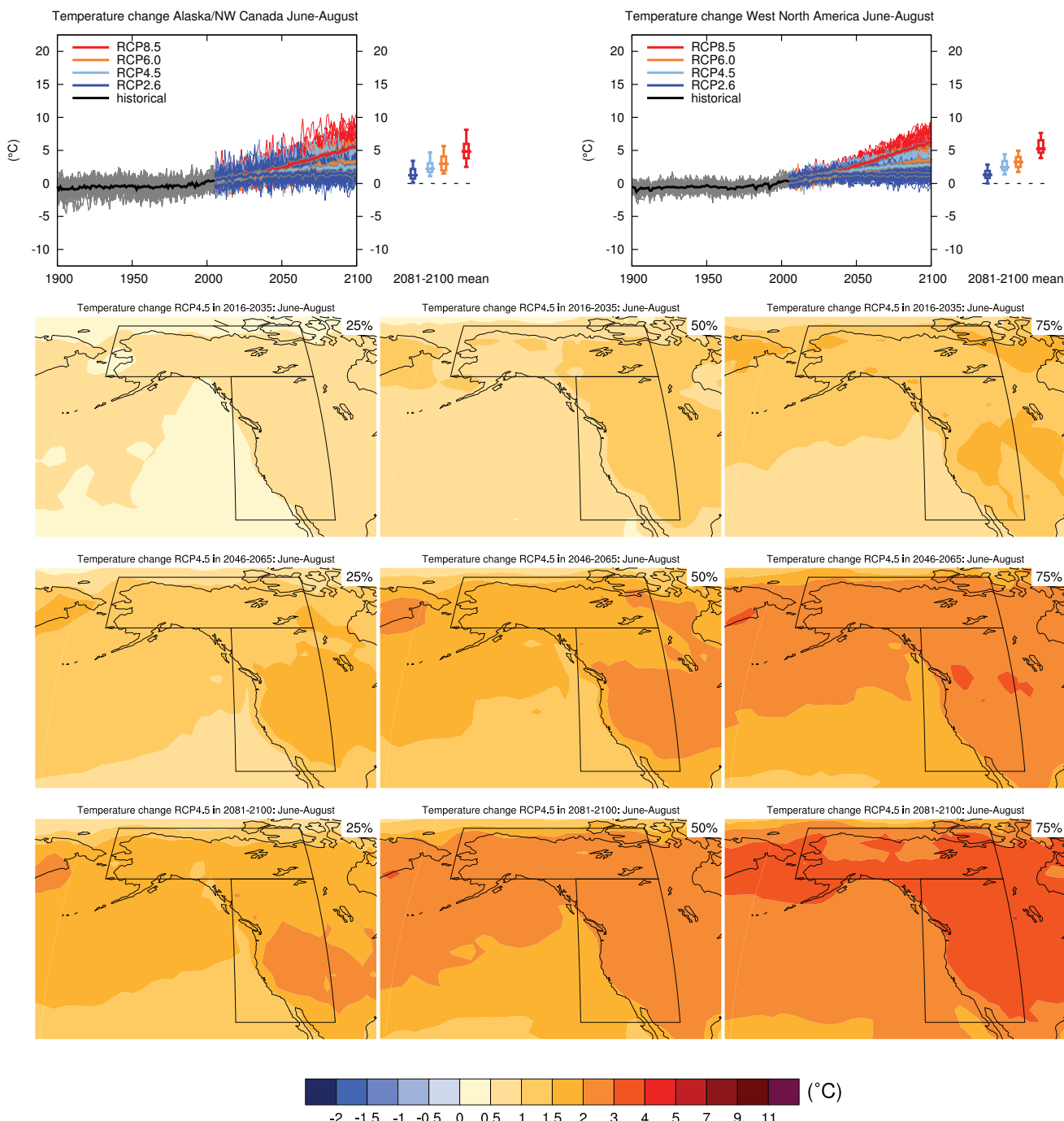


Figure AI.17 | (Top left) Time series of temperature change relative to 1986–2005 averaged over land grid points in Alaska/NW Canada (60°N to 72.6°N , 168°W to 105°W) in June to August. (Top right) Same for land grid points in West North America (28.6°N to 60°N , 130°W to 105°W). Thin lines denote one ensemble member per model, thick lines the CMIP5 multi-model mean. On the right-hand side the 5th, 25th, 50th (median), 75th and 95th percentiles of the distribution of 20-year mean changes are given for 2081–2100 in the four RCP scenarios.

(Below) Maps of temperature changes in 2016–2035, 2046–2065 and 2081–2100 with respect to 1986–2005 in the RCP4.5 scenario. For each point, the 25th, 50th and 75th percentiles of the distribution of the CMIP5 ensemble are shown; this includes both natural variability and inter-model spread. Hatching denotes areas where the 20-year mean differences of the percentiles are less than the standard deviation of model-estimated present-day natural variability of 20-year mean differences.

Sections 9.4.1.1, 9.6.1.1, 10.3.1.1.4, Box 11.2, 14.8.3 contain relevant information regarding the evaluation of models in this region, the model spread in the context of other methods of projecting changes and the role of modes of variability and other climate phenomena.

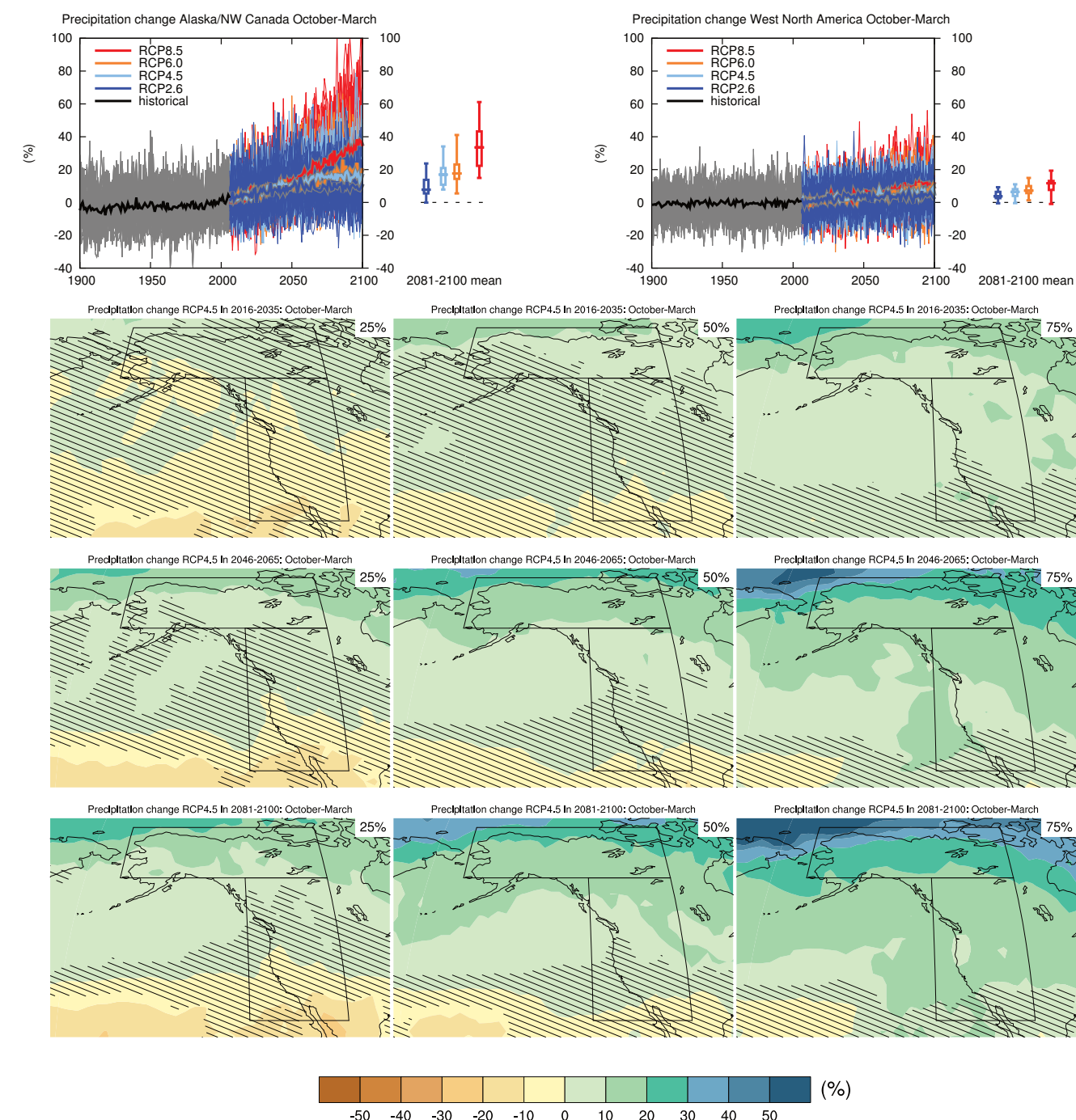


Figure AI.18 | (Top left) Time series of relative change relative to 1986–2005 in precipitation averaged over land grid points in Alaska/NW Canada (60°N to 72.6°N , 168°W to 105°W) in October to March. (Top right) Same for land grid points in West North America (28.6°N to 60°N , 130°W to 105°W). Thin lines denote one ensemble member per model, thick lines the CMIP5 multi-model mean. On the right-hand side the 5th, 25th, 50th (median), 75th and 95th percentiles of the distribution of 20-year mean changes are given for 2081–2100 in the four RCP scenarios.

(Below) Maps of precipitation changes in 2016–2035, 2046–2065 and 2081–2100 with respect to 1986–2005 in the RCP4.5 scenario. For each point, the 25th, 50th and 75th percentiles of the distribution of the CMIP5 ensemble are shown; this includes both natural variability and inter-model spread. Hatching denotes areas where the 20-year mean differences of the percentiles are less than the standard deviation of model-estimated present-day natural variability of 20-year mean differences.

Sections 9.4.1.1, 9.6.1.1, Box 11.2, 12.4.5.2, 14.2.3.1, 14.8.3 contain relevant information regarding the evaluation of models in this region, the model spread in the context of other methods of projecting changes and the role of modes of variability and other climate phenomena.

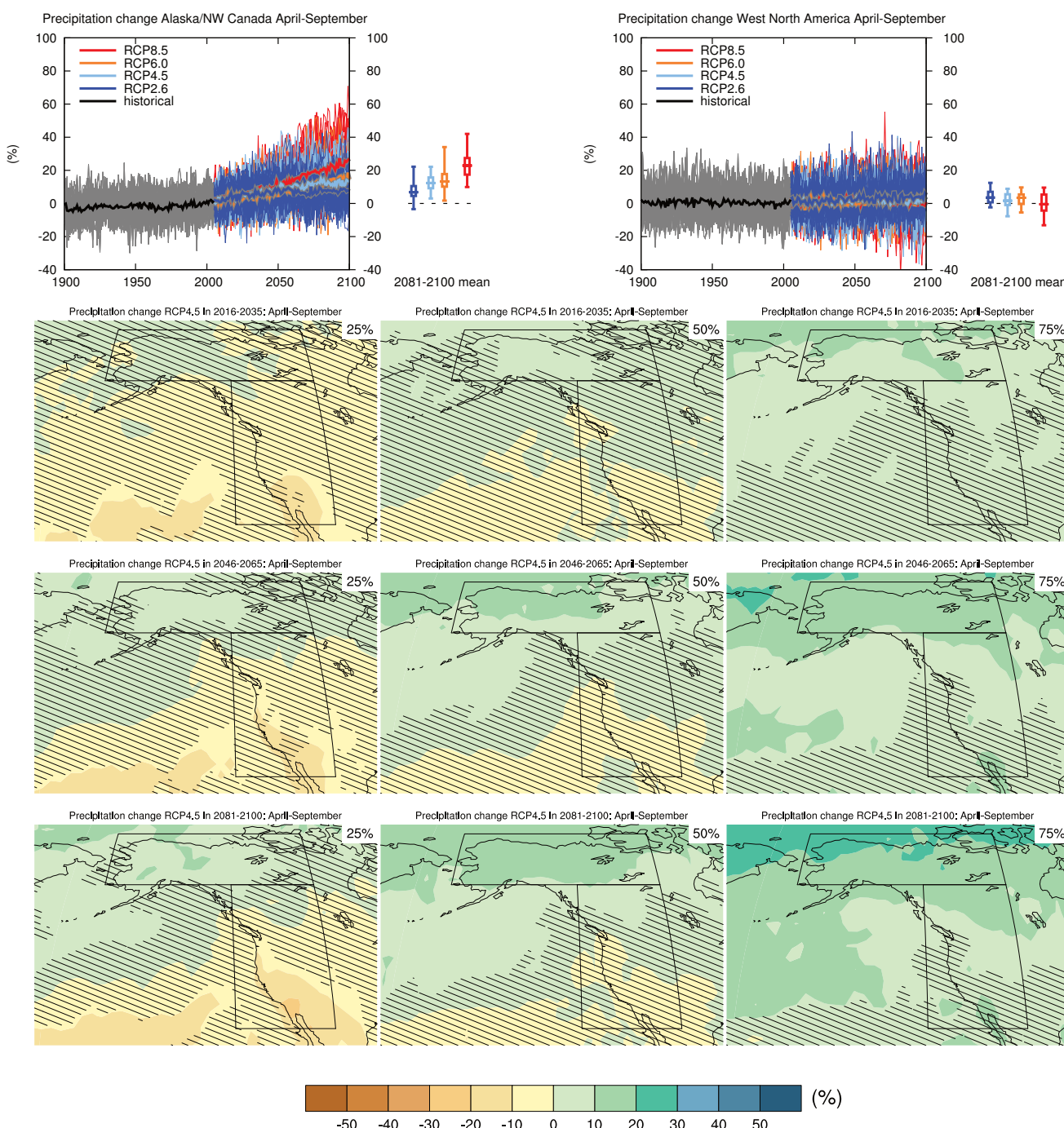


Figure AI.19 | (Top left) Time series of relative change relative to 1986–2005 in precipitation averaged over land grid points in Alaska/NW Canada (60°N to 72.6°N , 168°W to 105°W) in April to September. (Top right) Same for land grid points in West North America (28.6°N to 60°N , 130°W to 105°W). Thin lines denote one ensemble member per model, thick lines the CMIP5 multi-model mean. On the right-hand side the 5th, 25th, 50th (median), 75th and 95th percentiles of the distribution of 20-year mean changes are given for 2081–2100 in the four RCP scenarios.

(Below) Maps of precipitation changes in 2016–2035, 2046–2065 and 2081–2100 with respect to 1986–2005 in the RCP4.5 scenario. For each point, the 25th, 50th and 75th percentiles of the distribution of the CMIP5 ensemble are shown; this includes both natural variability and inter-model spread. Hatching denotes areas where the 20-year mean differences of the percentiles are less than the standard deviation of model-estimated present-day natural variability of 20-year mean differences.

Sections 9.4.1.1, 9.6.1.1, Box 11.2, 12.4.5.2, 14.2.3.1, 14.8.3 contain relevant information regarding the evaluation of models in this region, the model spread in the context of other methods of projecting changes and the role of modes of variability and other climate phenomena.

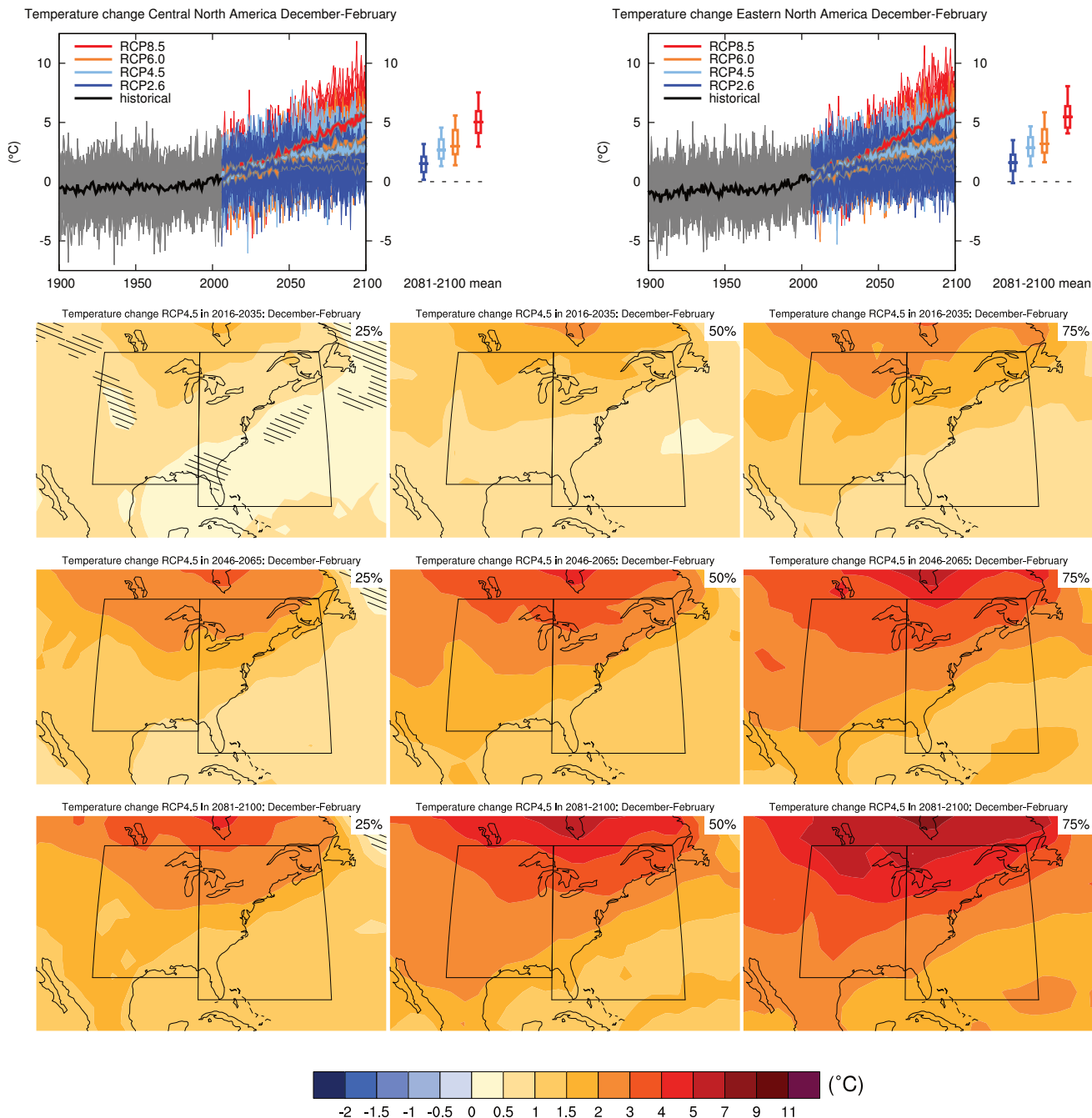


Figure AI.20 | (Top left) Time series of temperature change relative to 1986–2005 averaged over land grid points in Central North America (28.6°N to 50°N , 105°W to 85°W) in December to February. (Top right) Same for land grid points in Eastern North America (25°N to 50°N , 85°W to 60°W). Thin lines denote one ensemble member per model, thick lines the CMIP5 multi-model mean. On the right-hand side the 5th, 25th, 50th (median), 75th and 95th percentiles of the distribution of 20-year mean changes are given for 2081–2100 in the four RCP scenarios.

(Below) Maps of temperature changes in 2016–2035, 2046–2065 and 2081–2100 with respect to 1986–2005 in the RCP4.5 scenario. For each point, the 25th, 50th and 75th percentiles of the distribution of the CMIP5 ensemble are shown; this includes both natural variability and inter-model spread. Hatching denotes areas where the 20-year mean differences of the percentiles are less than the standard deviation of model-estimated present-day natural variability of 20-year mean differences.

Sections 9.4.1.1, 9.6.1.1, 10.3.1.1.4, Box 11.2, 14.8.3 contain relevant information regarding the evaluation of models in this region, the model spread in the context of other methods of projecting changes and the role of modes of variability and other climate phenomena.

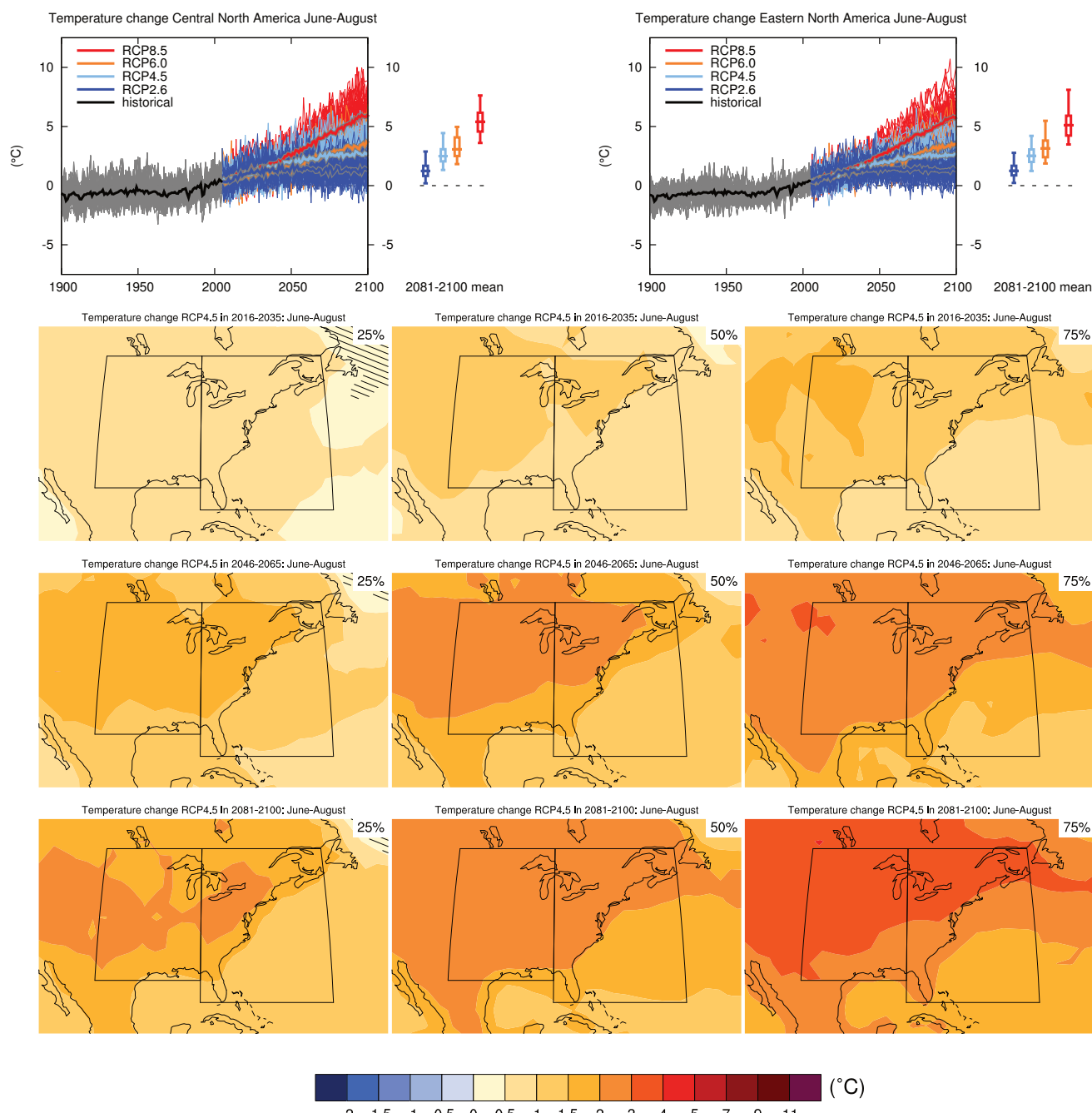


Figure AI.21 | (Top left) Time series of temperature change relative to 1986–2005 averaged over land grid points in Central North America (28.6°N to 50°N , 105°W to 85°W) in June to August. (Top right) Same for land grid points in Eastern North America (25°N to 50°N , 85°W to 60°W). Thin lines denote one ensemble member per model, thick lines the CMIP5 multi-model mean. On the right-hand side the 5th, 25th, 50th (median), 75th and 95th percentiles of the distribution of 20-year mean changes are given for 2081–2100 in the four RCP scenarios.

(Below) Maps of temperature changes in 2016–2035, 2046–2065 and 2081–2100 with respect to 1986–2005

in the RCP4.5 scenario. For each point, the 25th, 50th and 75th percentiles of the distribution of the CMIP5 ensemble are shown; this includes both natural variability and inter-model spread. Hatching denotes areas where the 20-year mean differences of the percentiles are less than the standard deviation of model-estimated present-day natural variability of 20-year mean differences.

Sections 9.4.1.1, 9.6.1.1, 10.3.1.1.4, Box 11.2, 14.8.3 contain relevant information regarding the evaluation of models in this region, the model spread in the context of other methods of projecting changes and the role of modes of variability and other climate phenomena.

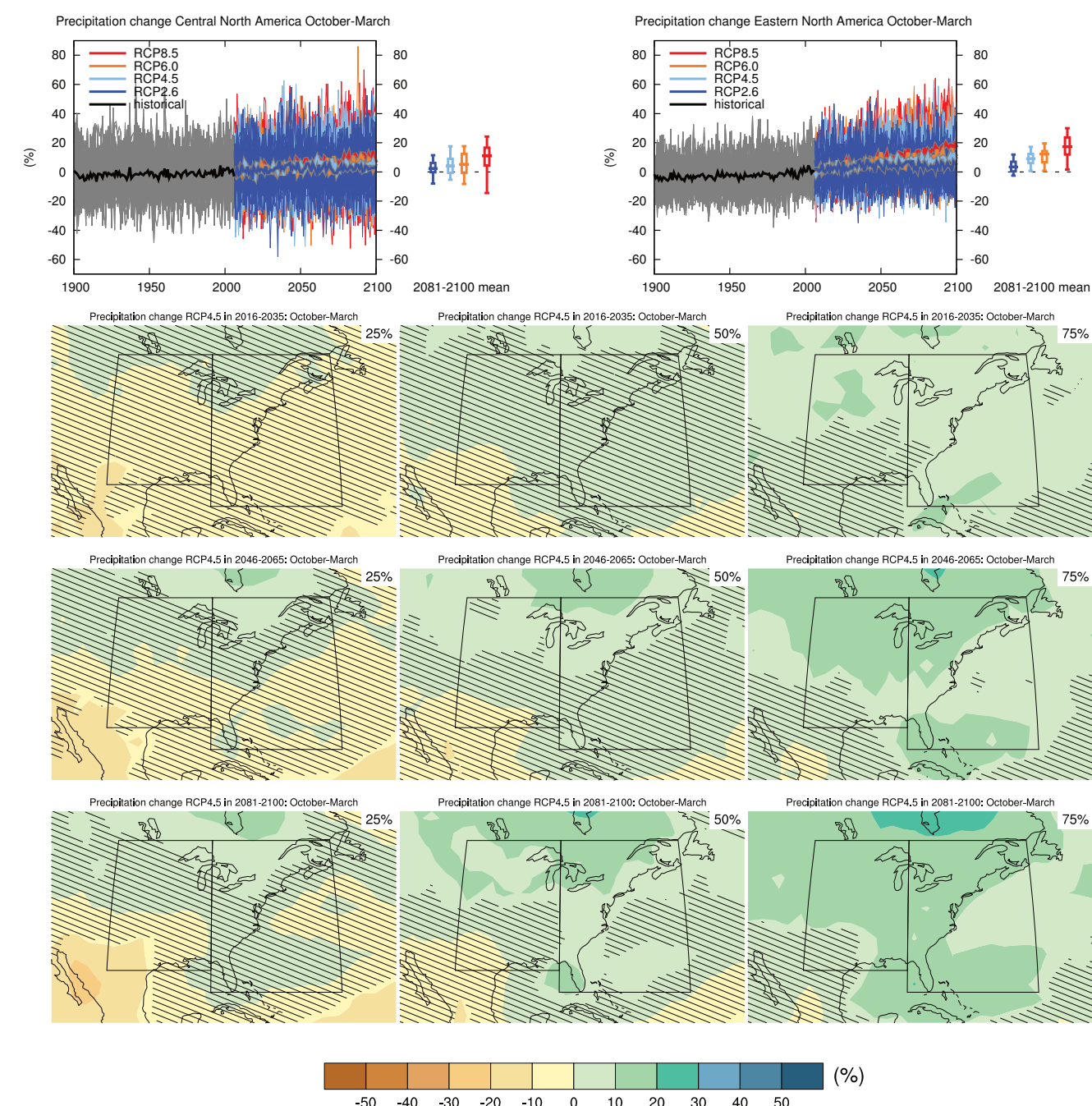


Figure AI.22 | (Top left) Time series of relative change relative to 1986–2005 in precipitation averaged over land grid points in Central North America (28.6°N to 50°N , 105°W to 85°W) in October to March. (Top right) Same for land grid points in Eastern North America (25°N to 50°N , 85°W to 60°W). Thin lines denote one ensemble member per model, thick lines the CMIP5 multi-model mean. On the right-hand side the 5th, 25th, 50th (median), 75th and 95th percentiles of the distribution of 20-year mean changes are given for 2081–2100 in the four RCP scenarios.

(Below) Maps of precipitation changes in 2016–2035, 2046–2065 and 2081–2100 with respect to 1986–2005 in the RCP4.5 scenario. For each point, the 25th, 50th and 75th percentiles of the distribution of the CMIP5 ensemble are shown; this includes both natural variability and inter-model spread. Hatching denotes areas where the 20-year mean differences of the percentiles are less than the standard deviation of model-estimated present-day natural variability of 20-year mean differences.

Sections 9.4.1.1, 9.6.1.1, Box 11.2, 14.8.3 contain relevant information regarding the evaluation of models in this region, the model spread in the context of other methods of projecting changes and the role of modes of variability and other climate phenomena.

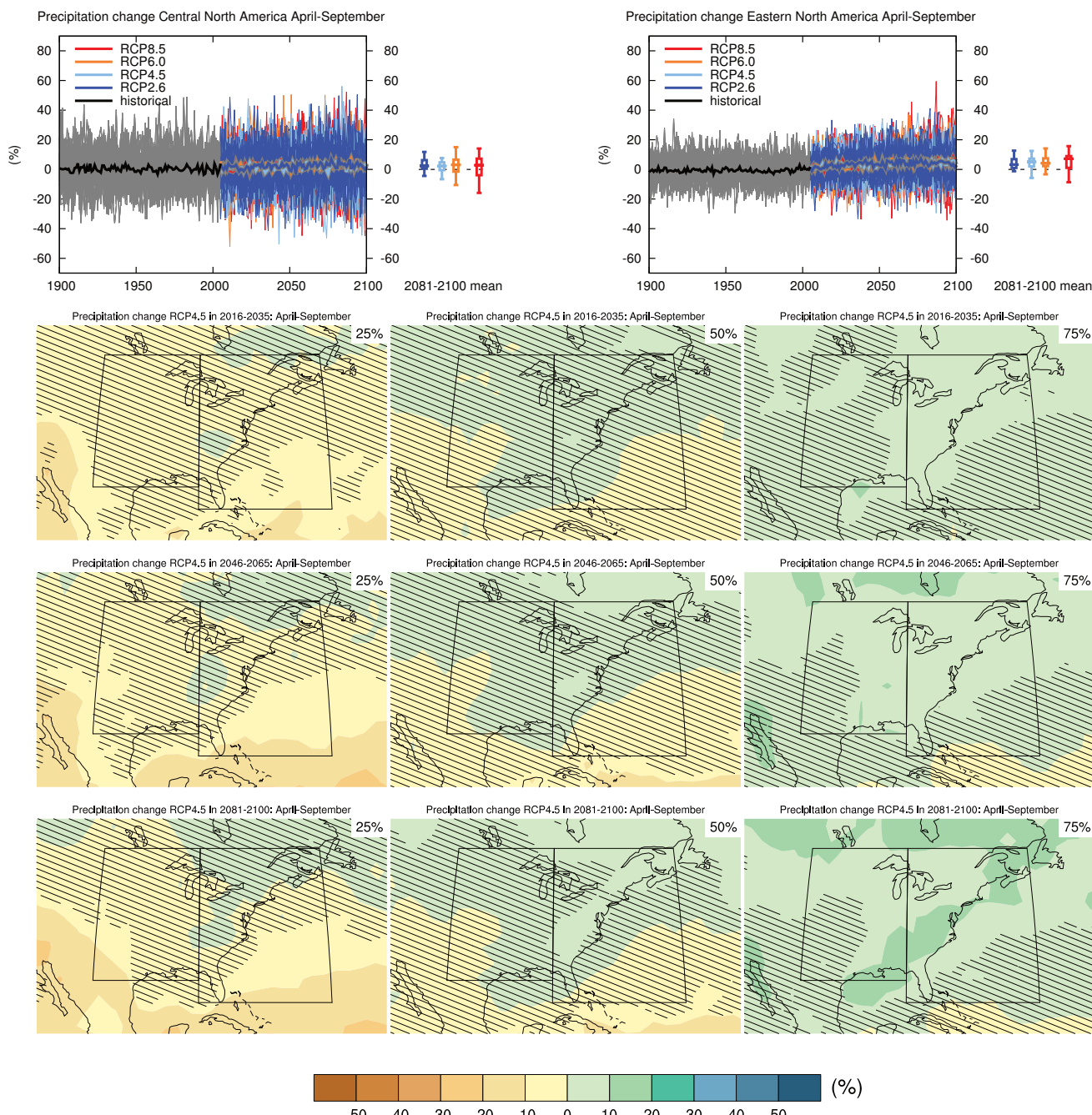


Figure AI.23 | (Top left) Time series of relative change relative to 1986–2005 in precipitation averaged over land grid points in Central North America (28.6°N to 50°N , 105°W to 85°W) in April to September. (Top right) Same for land grid points in Eastern North America (25°N to 50°N , 85°W to 60°W). Thin lines denote one ensemble member per model, thick lines the CMIP5 multi-model mean. On the right-hand side the 5th, 25th, 50th (median), 75th and 95th percentiles of the distribution of 20-year mean changes are given for 2081–2100 in the four RCP scenarios.

(Below) Maps of precipitation changes in 2016–2035, 2046–2065 and 2081–2100 with respect to 1986–2005 in the RCP4.5 scenario. For each point, the 25th, 50th and 75th percentiles of the distribution of the CMIP5 ensemble are shown; this includes both natural variability and inter-model spread. Hatching denotes areas where the 20-year mean differences of the percentiles are less than the standard deviation of model-estimated present-day natural variability of 20-year mean differences.

Sections 9.4.1.1, 9.6.1.1, Box 11.2, 14.8.3 contain relevant information regarding the evaluation of models in this region, the model spread in the context of other methods of projecting changes and the role of modes of variability and other climate phenomena.

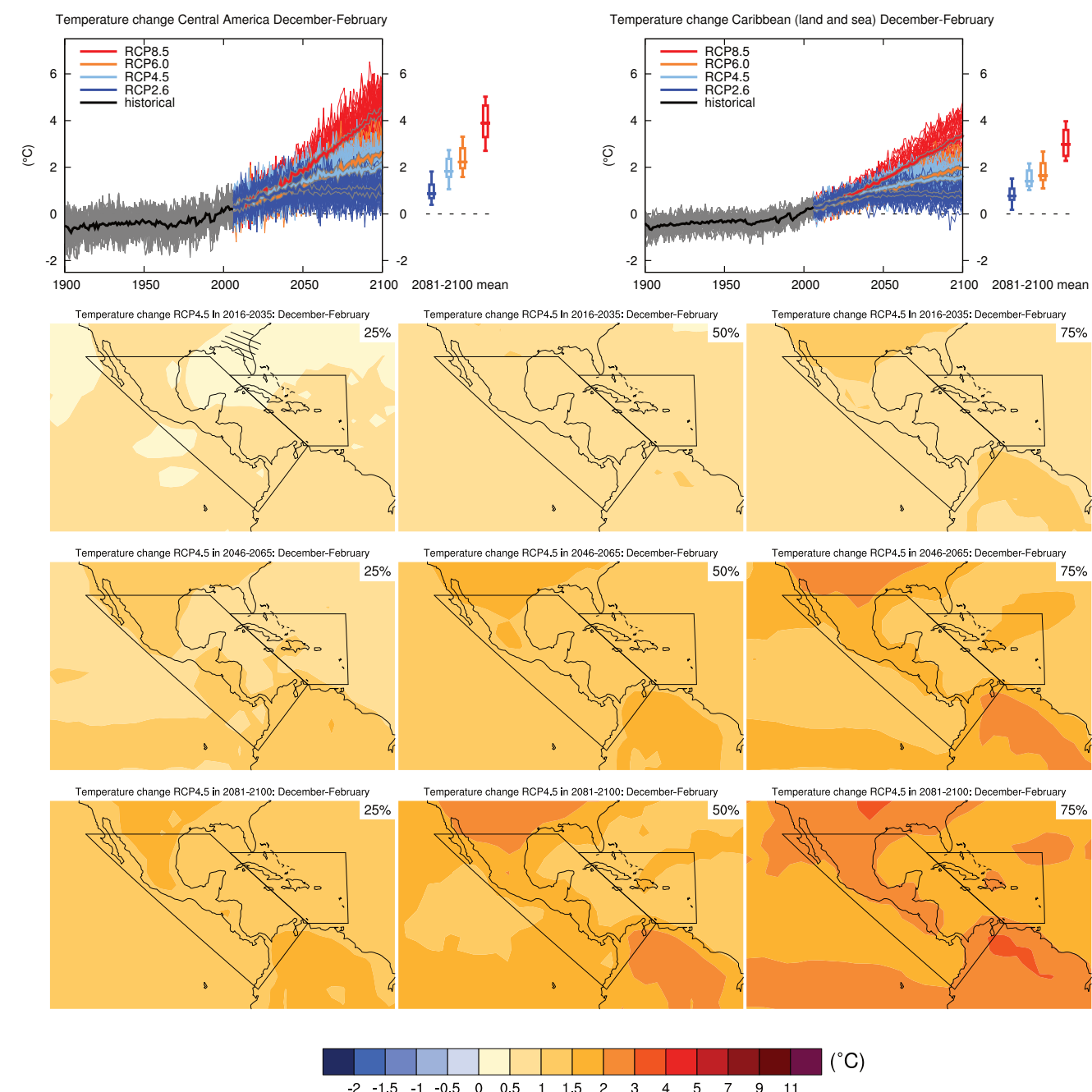


Figure AI.24 | (Top left) Time series of temperature change relative to 1986–2005 averaged over land grid points in Central America ($68.8^{\circ}\text{W}, 11.4^{\circ}\text{N}; 79.7^{\circ}\text{W}, 1.2^{\circ}\text{S}; 116.3^{\circ}\text{W}, 28.6^{\circ}\text{N}; 90.3^{\circ}\text{W}, 28.6^{\circ}\text{N}$) in December to February. (Top right) Same for all grid points in Caribbean (land and sea) ($68.8^{\circ}\text{W}, 11.4^{\circ}\text{N}; 85.8^{\circ}\text{W}, 25^{\circ}\text{N}, 60^{\circ}\text{W}, 25^{\circ}\text{N}, 60^{\circ}\text{W}, 11.44^{\circ}\text{N}$). Thin lines denote one ensemble member per model, thick lines the CMIP5 multi-model mean. On the right-hand side the 5th, 25th, 50th (median), 75th and 95th percentiles of the distribution of 20-year mean changes are given for 2081–2100 in the four RCP scenarios.

(Below) Maps of temperature changes in 2016–2035, 2046–2065 and 2081–2100 with respect to 1986–2005 in the RCP4.5 scenario. For each point, the 25th, 50th and 75th percentiles of the distribution of the CMIP5 ensemble are shown; this includes both natural variability and inter-model spread. Hatching denotes areas where the 20-year mean differences of the percentiles are less than the standard deviation of model-estimated present-day natural variability of 20-year mean differences.

Sections 9.4.1.1, 9.6.1.1, 10.3.1.1.4, Box 11.2, 14.8.4 contain relevant information regarding the evaluation of models in this region, the model spread in the context of other methods of projecting changes and the role of modes of variability and other climate phenomena.

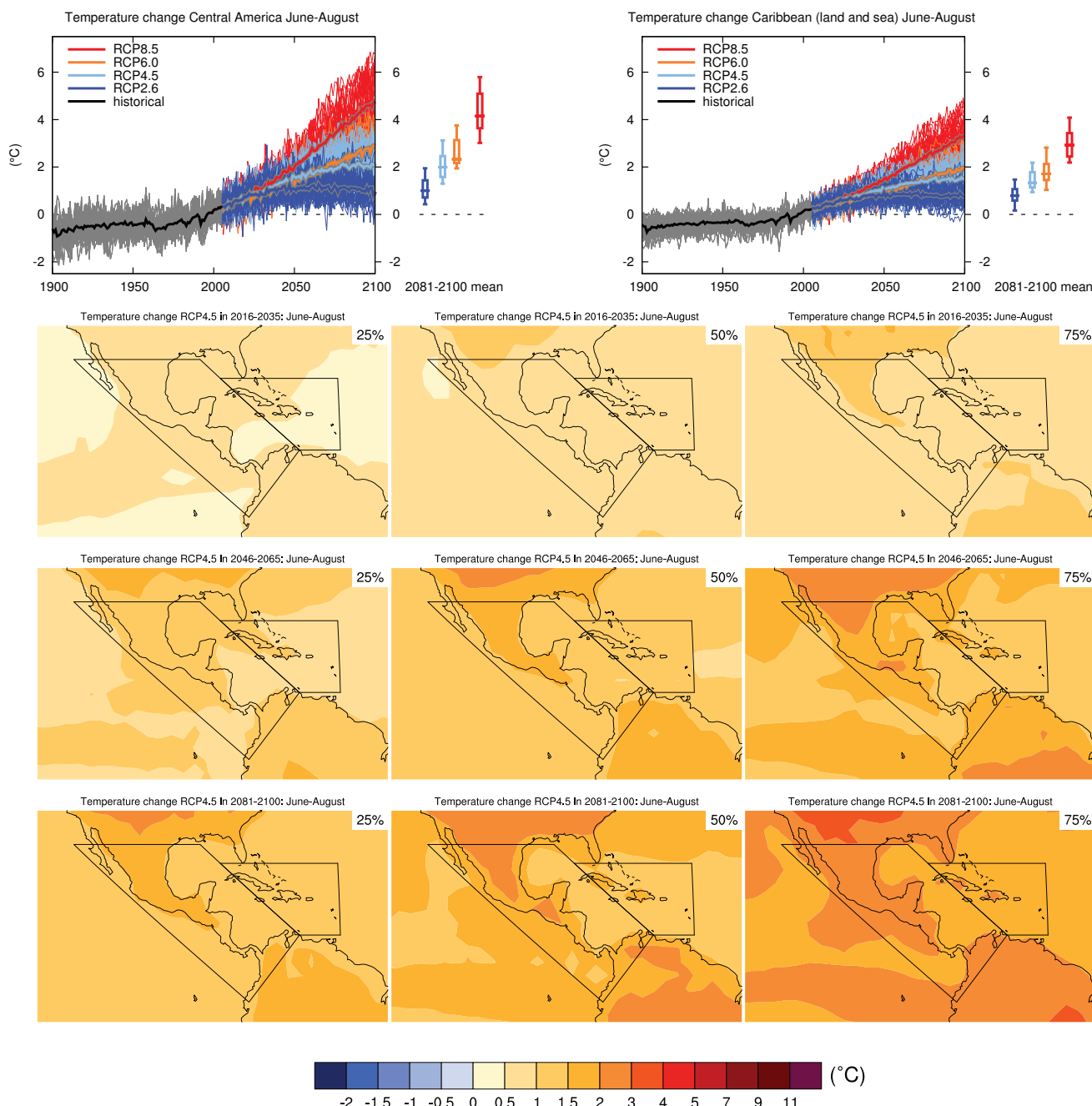


Figure AI.25 | (Top left) Time series of temperature change relative to 1986–2005 averaged over land grid points in Central America (68.8°W , 11.4°N ; 79.7°W , 1.2°S ; 116.3°W , 28.6°N ; 90.3°W , 28.6°N) in June to August. (Top right) Same for all grid points in Caribbean (land and sea) (68.8°W , 11.4°N ; 85.8°W , 25°N , 60°W , 25°N , 60°W , 11.44°N). Thin lines denote one ensemble member per model, thick lines the CMIP5 multi-model mean. On the right-hand side the 5th, 25th, 50th (median), 75th and 95th percentiles of the distribution of 20-year mean changes are given for 2081–2100 in the four RCP scenarios.

(Below) Maps of temperature changes in 2016–2035, 2046–2065 and 2081–2100 with respect to 1986–2005 in the RCP4.5 scenario. For each point, the 25th, 50th and 75th percentiles of the distribution of the CMIP5 ensemble are shown; this includes both natural variability and inter-model spread. Hatching denotes areas where the 20-year mean differences of the percentiles are less than the standard deviation of model-estimated present-day natural variability of 20-year mean differences.

Sections 9.4.1.1, 9.6.1.1, 10.3.1.1.4, Box 11.2, 14.8.4 contain relevant information regarding the evaluation of models in this region, the model spread in the context of other methods of projecting changes and the role of modes of variability and other climate phenomena.

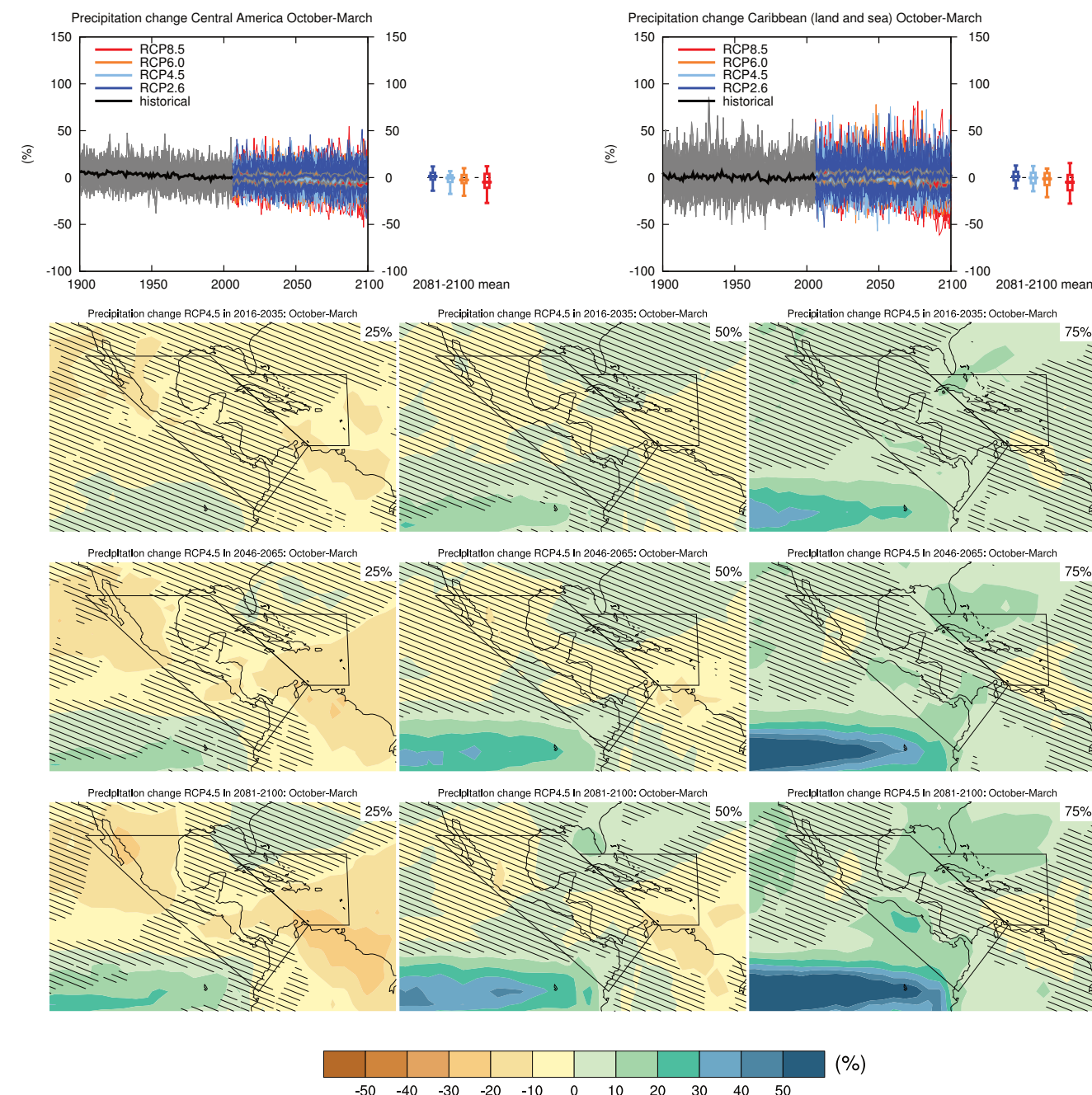


Figure AI.26 | (Top left) Time series of relative change relative to 1986–2005 in precipitation averaged over land grid points in Central America ($68.8^{\circ}\text{W}, 11.4^{\circ}\text{N}; 79.7^{\circ}\text{W}, 1.2^{\circ}\text{S}; 116.3^{\circ}\text{W}, 28.6^{\circ}\text{N}; 90.3^{\circ}\text{W}, 28.6^{\circ}\text{N}$) in October to March. (Top right) Same for all grid points in Caribbean (land and sea) ($68.8^{\circ}\text{W}, 11.4^{\circ}\text{N}; 85.8^{\circ}\text{W}, 25^{\circ}\text{N}, 60^{\circ}\text{W}, 25^{\circ}\text{N}, 60^{\circ}\text{W}, 11.44^{\circ}\text{N}$). Thin lines denote one ensemble member per model, thick lines the CMIP5 multi-model mean. On the right-hand side the 5th, 25th, 50th (median), 75th and 95th percentiles of the distribution of 20-year mean changes are given for 2081–2100 in the four RCP scenarios.

(Below) Maps of precipitation changes in 2016–2035, 2046–2065 and 2081–2100 with respect to 1986–2005 in the RCP4.5 scenario. For each point, the 25th, 50th and 75th percentiles of the distribution of the CMIP5 ensemble are shown; this includes both natural variability and inter-model spread. Hatching denotes areas where the 20-year mean differences of the percentiles are less than the standard deviation of model-estimated present-day natural variability of 20-year mean differences.

Sections 9.4.1.1, 9.6.1.1, Box 11.2, 12.4.5.2, 14.2.3.1, 14.8.4 contain relevant information regarding the evaluation of models in this region, the model spread in the context of other methods of projecting changes and the role of modes of variability and other climate phenomena.

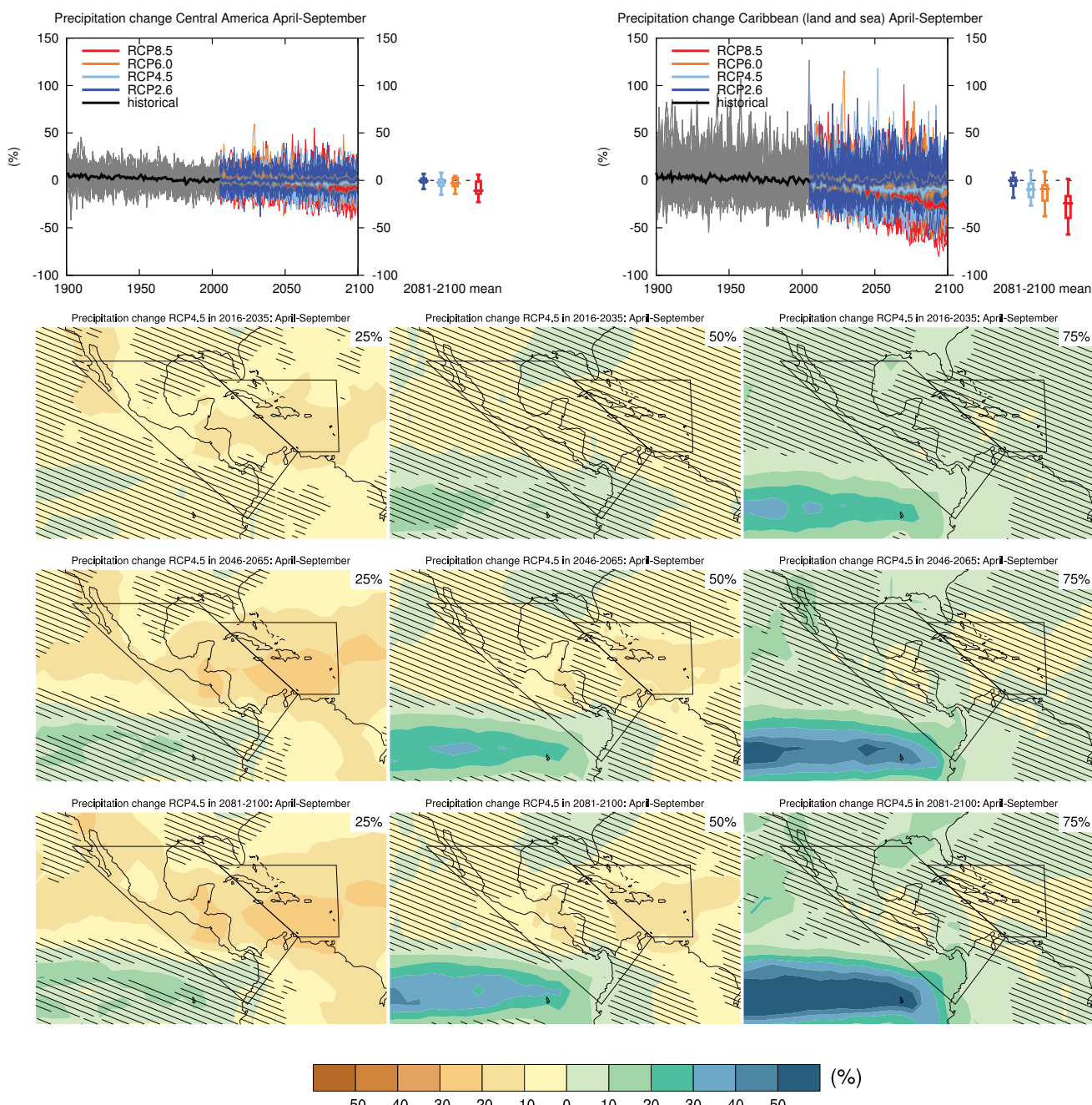


Figure Al.27 | (Top left) Time series of relative change relative to 1986–2005 in precipitation averaged over land grid points in Central America (68.8°W , 11.4°N ; 79.7°W , 1.2°S ; 116.3°W , 28.6°N ; 90.3°W , 28.6°N) in April to September. (Top right) Same for all grid points in Caribbean (land and sea) (68.8°W , 11.4°N ; 85.8°W , 25°N , 60°W , 25°N , 60°W , 11.44°N). Thin lines denote one ensemble member per model, thick lines the CMIP5 multi-model mean. On the right-hand side the 5th, 25th, 50th (median), 75th and 95th percentiles of the distribution of 20-year mean changes are given for 2081–2100 in the four RCP scenarios.

(Below) Maps of precipitation changes in 2016–2035, 2046–2065 and 2081–2100 with respect to 1986–2005 in the RCP4.5 scenario. For each point, the 25th, 50th and 75th percentiles of the distribution of the CMIP5 ensemble are shown; this includes both natural variability and inter-model spread. Hatching denotes areas where the 20-year mean differences of the percentiles are less than the standard deviation of model-estimated present-day natural variability of 20-year mean differences.

Sections 9.4.1.1, 9.6.1.1, Box 11.2, 12.4.5.2, 14.2.3.1, 14.8.4 contain relevant information regarding the evaluation of models in this region, the model spread in the context of other methods of projecting changes and the role of modes of variability and other climate phenomena.

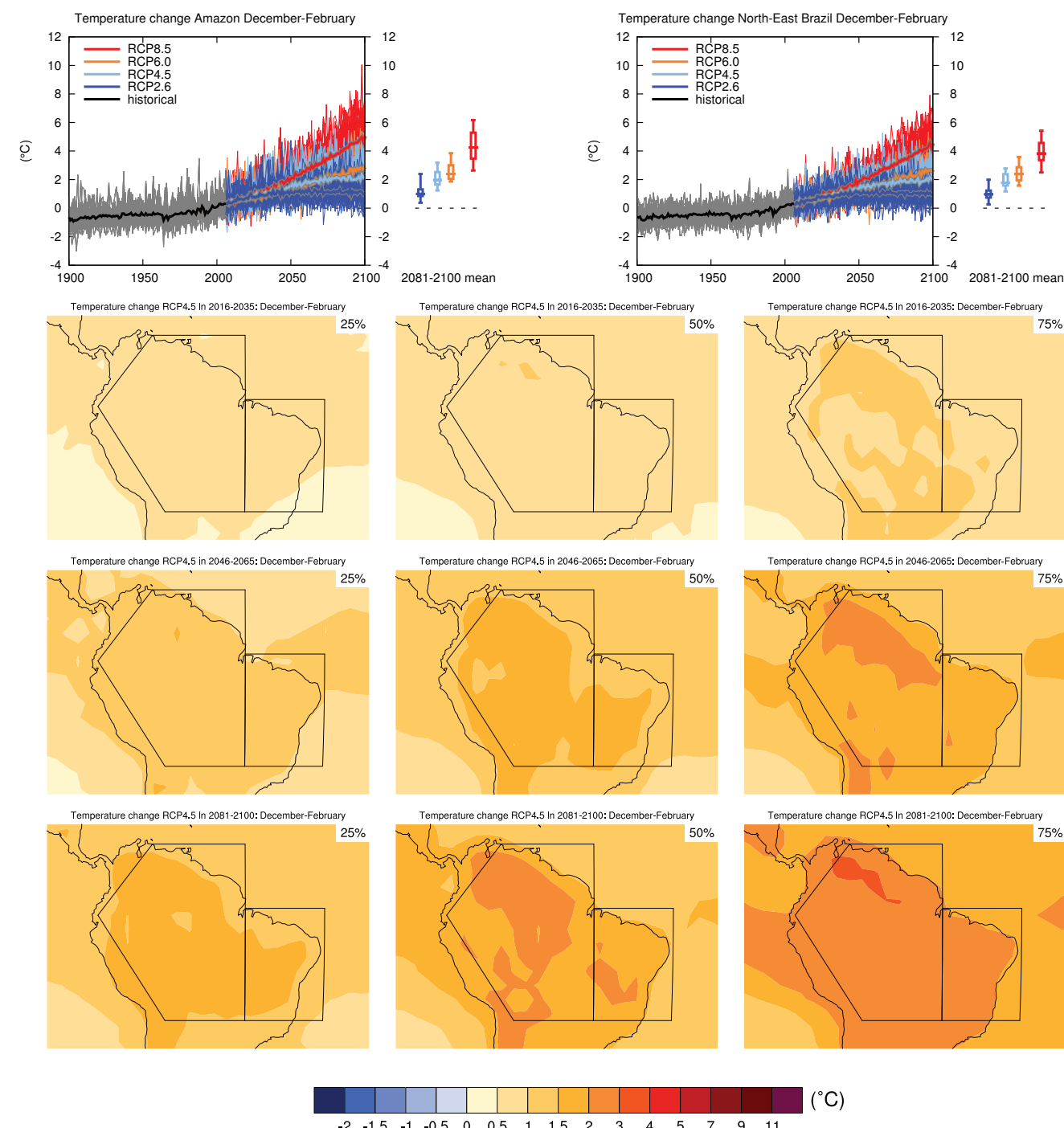


Figure AI.28 | (Top left) Time series of temperature change relative to 1986–2005 averaged over land grid points in the Amazon (20°S , 66.4°W ; 1.24°S , 79.7°W ; 11.44°N , 68.8°W ; 11.44°N , 50°W ; 20°S , 50°W) in December-February. (Top right) Same for land grid points in northeast Brazil (20°S to EQ, 50°W to 34°W). Thin lines denote one ensemble member per model, thick lines the CMIP5 multi-model mean. On the right-hand side the 5th, 25th, 50th (median), 75th and 95th percentiles of the distribution of 20-year mean changes are given for 2081–2100 in the four RCP scenarios.

(Below) Maps of temperature changes in 2016–2035, 2046–2065 and 2081–2100 with respect to 1986–2005 in the RCP4.5 scenario. For each point, the 25th, 50th and 75th percentiles of the distribution of the CMIP5 ensemble are shown; this includes both natural variability and inter-model spread. Hatching denotes areas where the 20-year mean differences of the percentiles are less than the standard deviation of model-estimated present-day natural variability of 20-year mean differences.

Sections 9.4.1.1, 9.6.1.1, 10.3.1.1.4, Box 11.2, 14.8.5 contain relevant information regarding the evaluation of models in this region, the model spread in the context of other methods of projecting changes and the role of modes of variability and other climate phenomena.

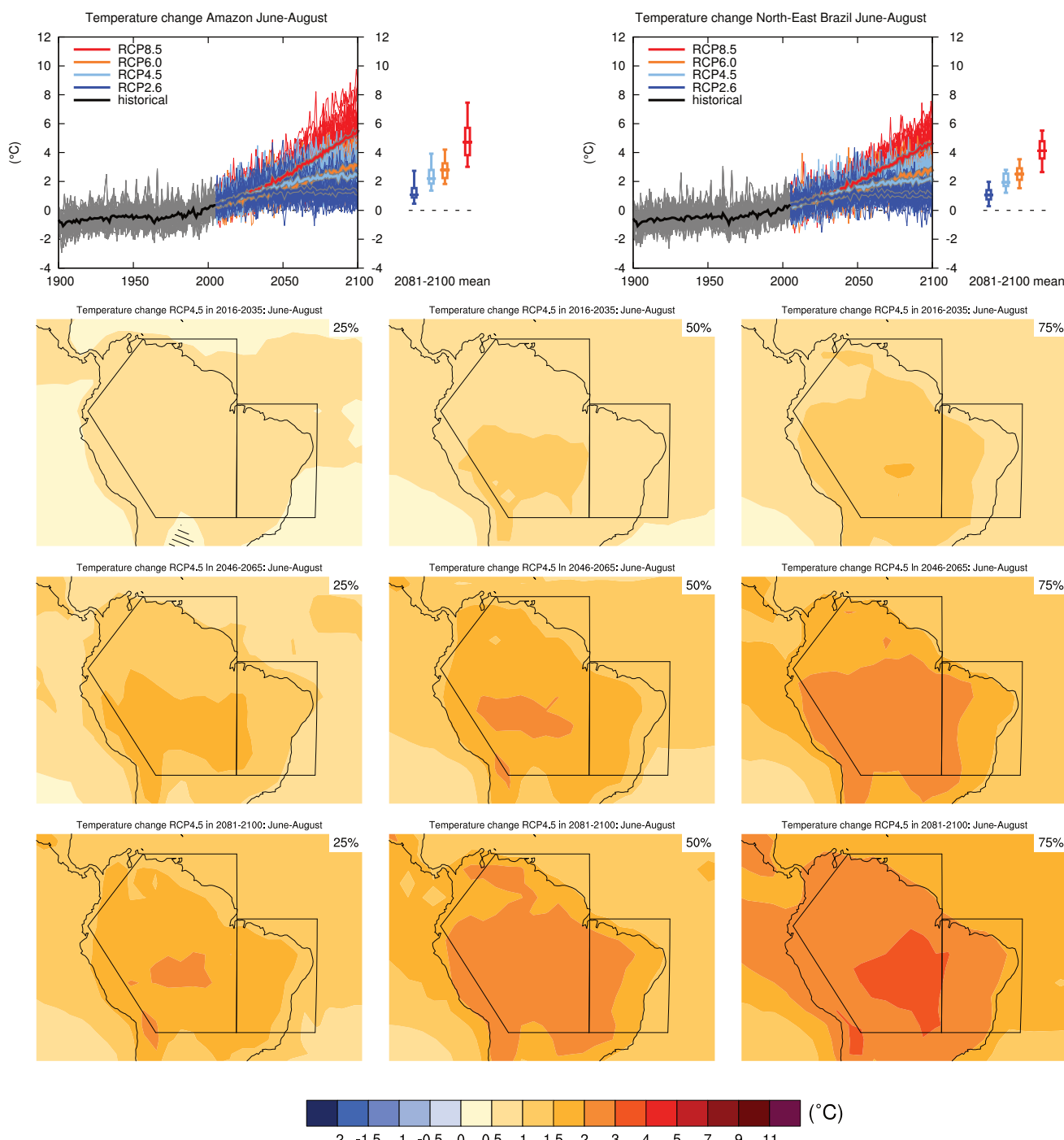


Figure AI.29 | (Top left) Time series of temperature change relative to 1986–2005 averaged over land grid points in the Amazon (20°S , 66.4°W ; 1.24°S , 79.7°W ; 11.44°N , 68.8°W ; 11.44°N , 50°W ; 20°S , 50°W) in June to August. (Top right) Same for land grid points in northeast Brazil (20°S to EQ, 50°W to 34°W). Thin lines denote one ensemble member per model, thick lines the CMIP5 multi-model mean. On the right-hand side the 5th, 25th, 50th (median), 75th and 95th percentiles of the distribution of 20-year mean changes are given for 2081–2100 in the four RCP scenarios.

(Below) Maps of temperature changes in 2016–2035, 2046–2065 and 2081–2100 with respect to 1986–2005 in the RCP4.5 scenario. For each point, the 25th, 50th and 75th percentiles of the distribution of the CMIP5 ensemble are shown; this includes both natural variability and inter-model spread. Hatching denotes areas where the 20-year mean differences of the percentiles are less than the standard deviation of model-estimated present-day natural variability of 20-year mean differences.

Sections 9.4.1.1, 9.6.1.1, 10.3.1.1.4, Box 11.2, 14.8.5 contain relevant information regarding the evaluation of models in this region, the model spread in the context of other methods of projecting changes and the role of modes of variability and other climate phenomena.

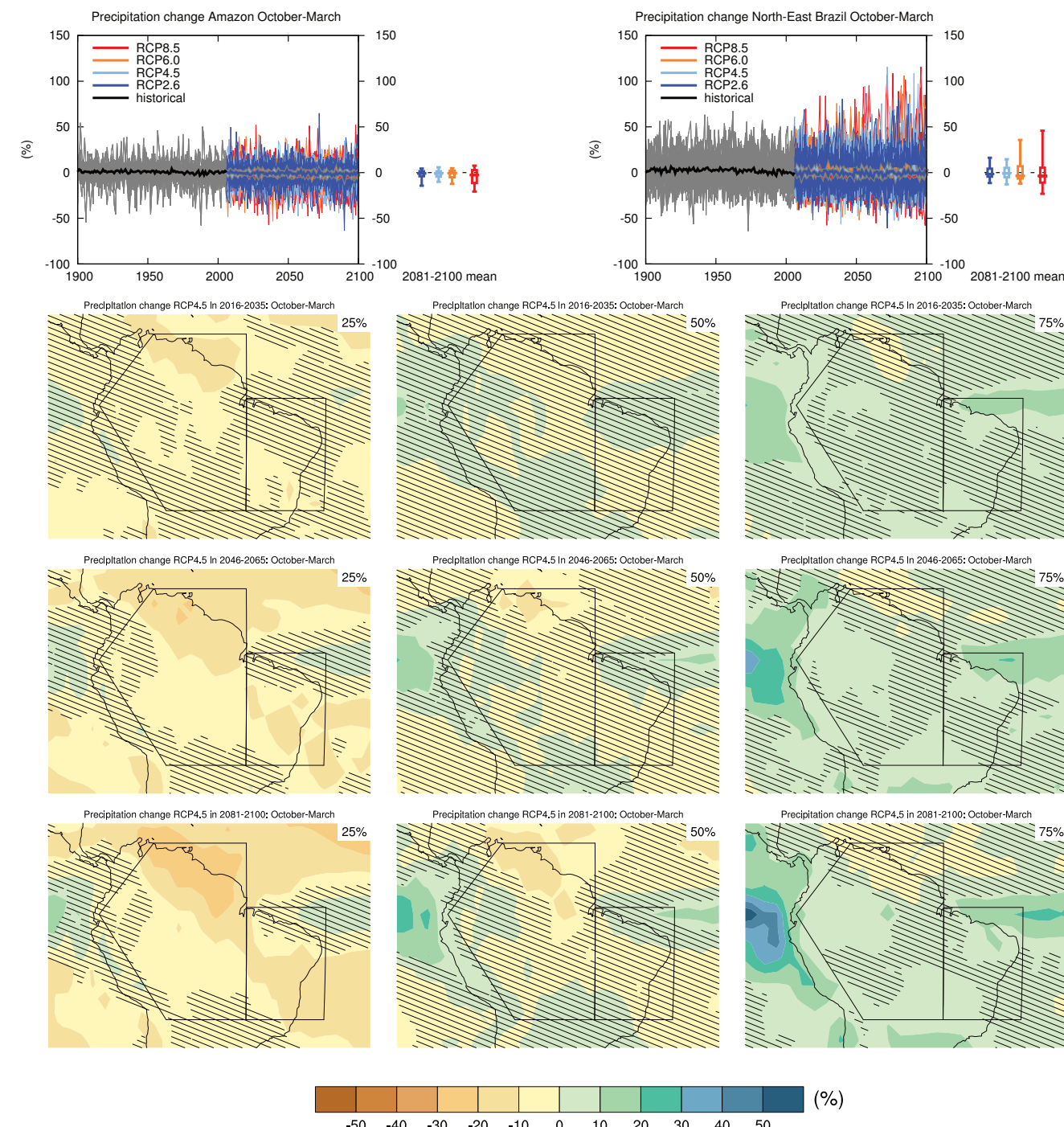


Figure AI.30 | (Top left) Time series of relative change relative to 1986–2005 in precipitation averaged over land grid points in the Amazon (20°S , 66.4°W ; 1.24°S , 79.7°W ; 11.44°N , 68.8°W ; 11.44°N , 50°W ; 20°S , 50°W) in October to March. (Top right) Same for land grid points in northeast Brazil (20°S to EQ, 50°W to 34°W). Thin lines denote one ensemble member per model, thick lines the CMIP5 multi-model mean. On the right-hand side the 5th, 25th, 50th (median), 75th and 95th percentiles of the distribution of 20-year mean changes are given for 2081–2100 in the four RCP scenarios.

(Below) Maps of precipitation changes in 2016–2035, 2046–2065 and 2081–2100 with respect to 1986–2005 in the RCP4.5 scenario. For each point, the 25th, 50th and 75th percentiles of the distribution of the CMIP5 ensemble are shown; this includes both natural variability and inter-model spread. Hatching denotes areas where the 20-year mean differences of the percentiles are less than the standard deviation of model-estimated present-day natural variability of 20-year mean differences.

Sections 9.4.1.1, 9.6.1.1, 11.3.2.1.2, Box 11.2, 14.2.3.2, 14.8.5 contain relevant information regarding the evaluation of models in this region, the model spread in the context of other methods of projecting changes and the role of modes of variability and other climate phenomena.

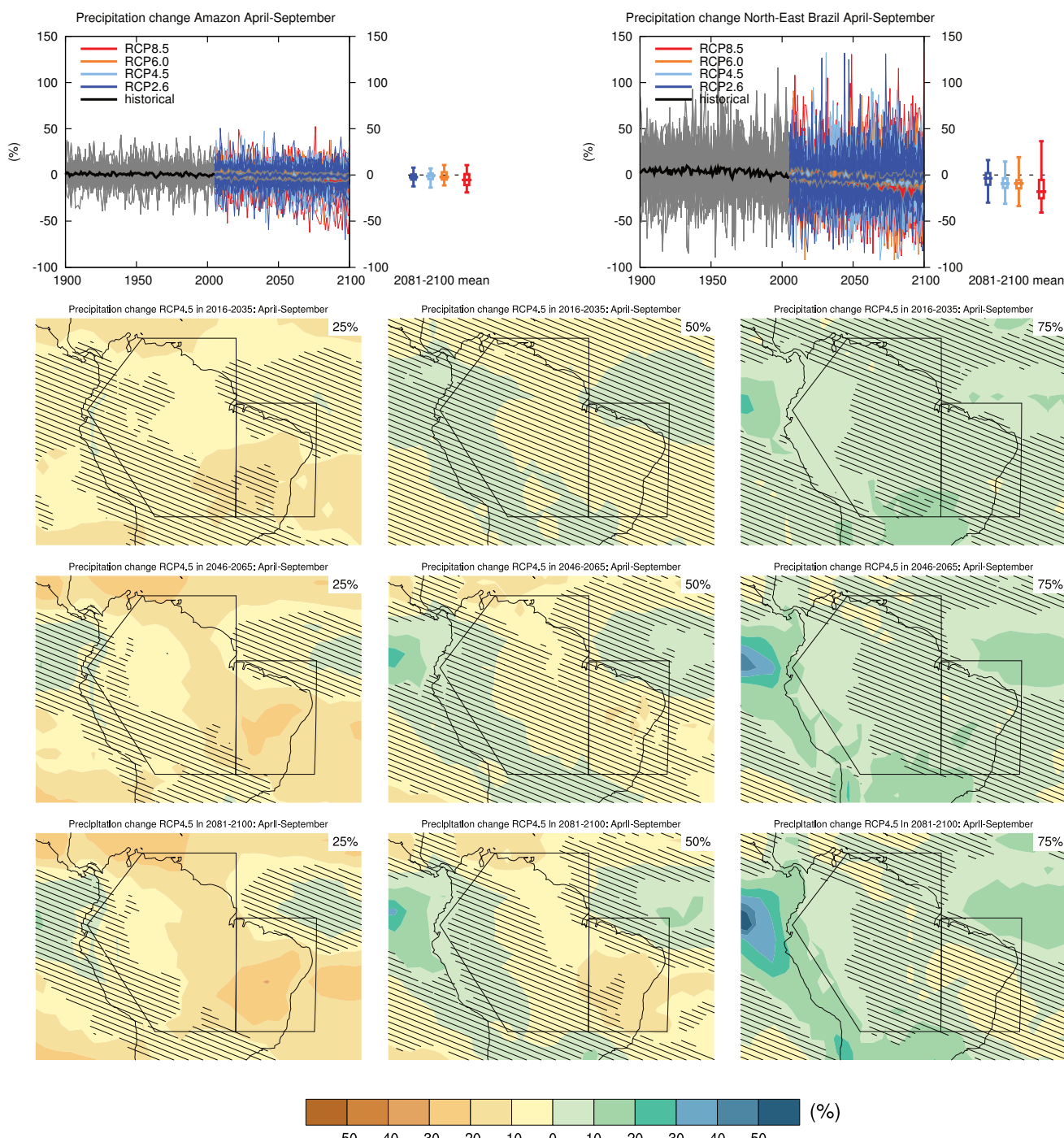


Figure AI.31 | (Top left) Time series of relative change relative to 1986–2005 in precipitation averaged over land grid points in the Amazon (20°S , 66.4°W ; 1.24°S , 79.7°W ; 11.44°N , 68.8°W ; 11.44°N , 50°W ; 20°S , 50°W) in April to September. (Top right) Same for land grid points in northeast Brazil (20°S to EQ , 50°W to 34°W). Thin lines denote one ensemble member per model, thick lines the CMIP5 multi-model mean. On the right-hand side the 5th, 25th, 50th (median), 75th and 95th percentiles of the distribution of 20-year mean changes are given for 2081–2100 in the four RCP scenarios.

(Below) Maps of precipitation changes in 2016–2035, 2046–2065 and 2081–2100 with respect to 1986–2005 in the RCP4.5 scenario. For each point, the 25th, 50th and 75th percentiles of the distribution of the CMIP5 ensemble are shown; this includes both natural variability and inter-model spread. Hatching denotes areas where the 20-year mean differences of the percentiles are less than the standard deviation of model-estimated present-day natural variability of 20-year mean differences.

Sections 9.4.1.1, 9.6.1.1, 11.3.2.1.2, Box 11.2, 14.2.3.2, 14.8.5 contain relevant information regarding the evaluation of models in this region, the model spread in the context of other methods of projecting changes and the role of modes of variability and other climate phenomena.

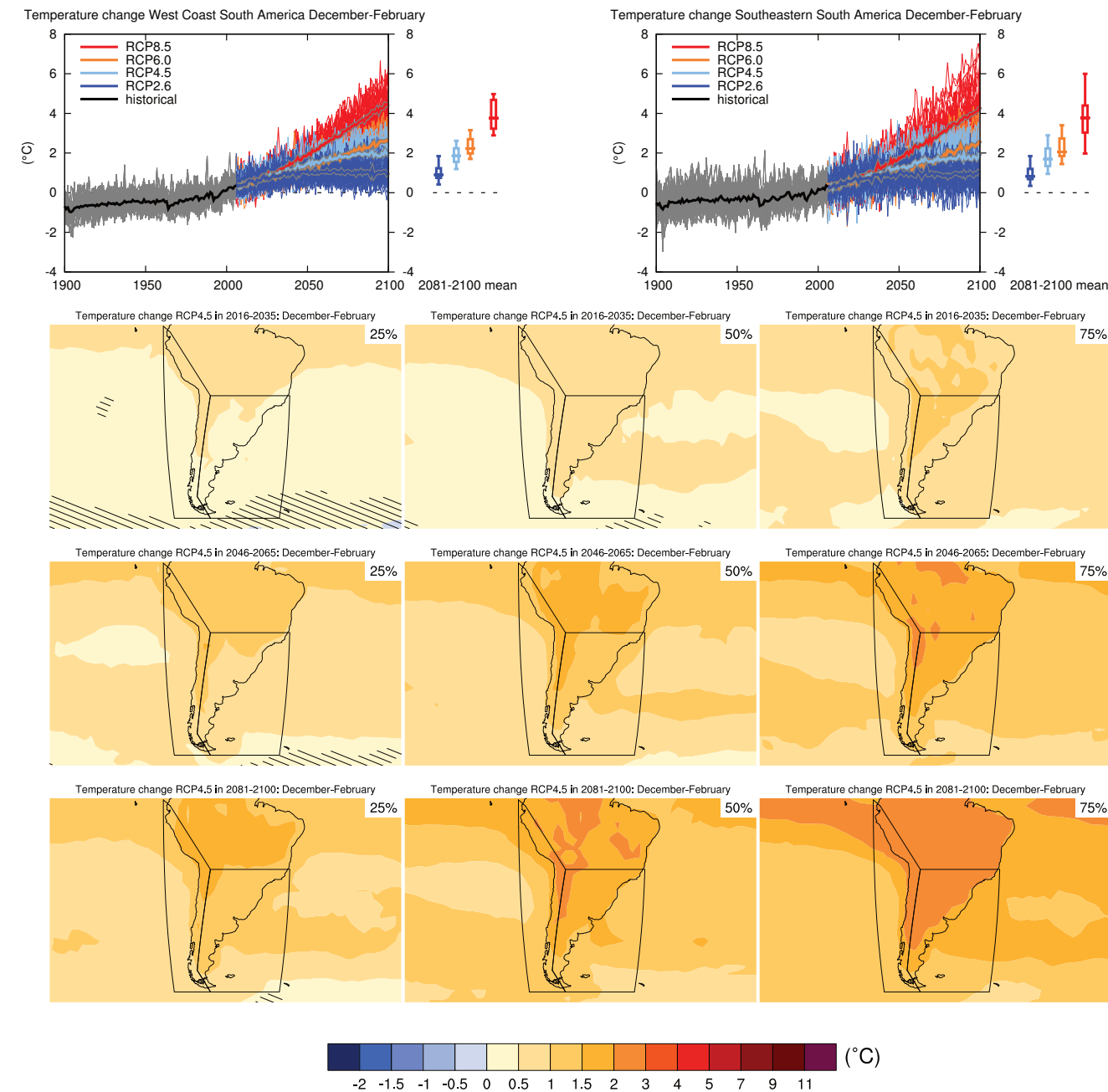


Figure AI.32 | (Top left) Time series of temperature change relative to 1986–2005 averaged over land grid points in the west coast of South America (79.7°W , 1.2°S ; 66.4°W , 20°S ; 72.1°W , 50°S ; 67.3°W , 56.7°S ; 82.0°W , 56.7°S ; 82.2°W , 0.5°N) in December to February. (Top right) Same for land grid points in southeastern South America (39.4°W , 20°S ; 39.4°W , 56.6°S ; 67.3°W , 56.7°S ; 72.1°W , 50°S ; 66°W , 20°S). Thin lines denote one ensemble member per model, thick lines the CMIP5 multi-model mean. On the right-hand side the 5th, 25th, 50th (median), 75th and 95th percentiles of the distribution of 20-year mean changes are given for 2081–2100 in the four RCP scenarios.

(Below) Maps of temperature changes in 2016–2035, 2046–2065 and 2081–2100 with respect to 1986–2005 in the RCP4.5 scenario. For each point, the 25th, 50th and 75th percentiles of the distribution of the CMIP5 ensemble are shown; this includes both natural variability and inter-model spread. Hatching denotes areas where the 20-year mean differences of the percentiles are less than the standard deviation of model-estimated present-day natural variability of 20-year mean differences.

Sections 9.4.1.1, 9.6.1.1, 10.3.1.1.4, Box 11.2, 14.8.5 contain relevant information regarding the evaluation of models in this region, the model spread in the context of other methods of projecting changes and the role of modes of variability and other climate phenomena.

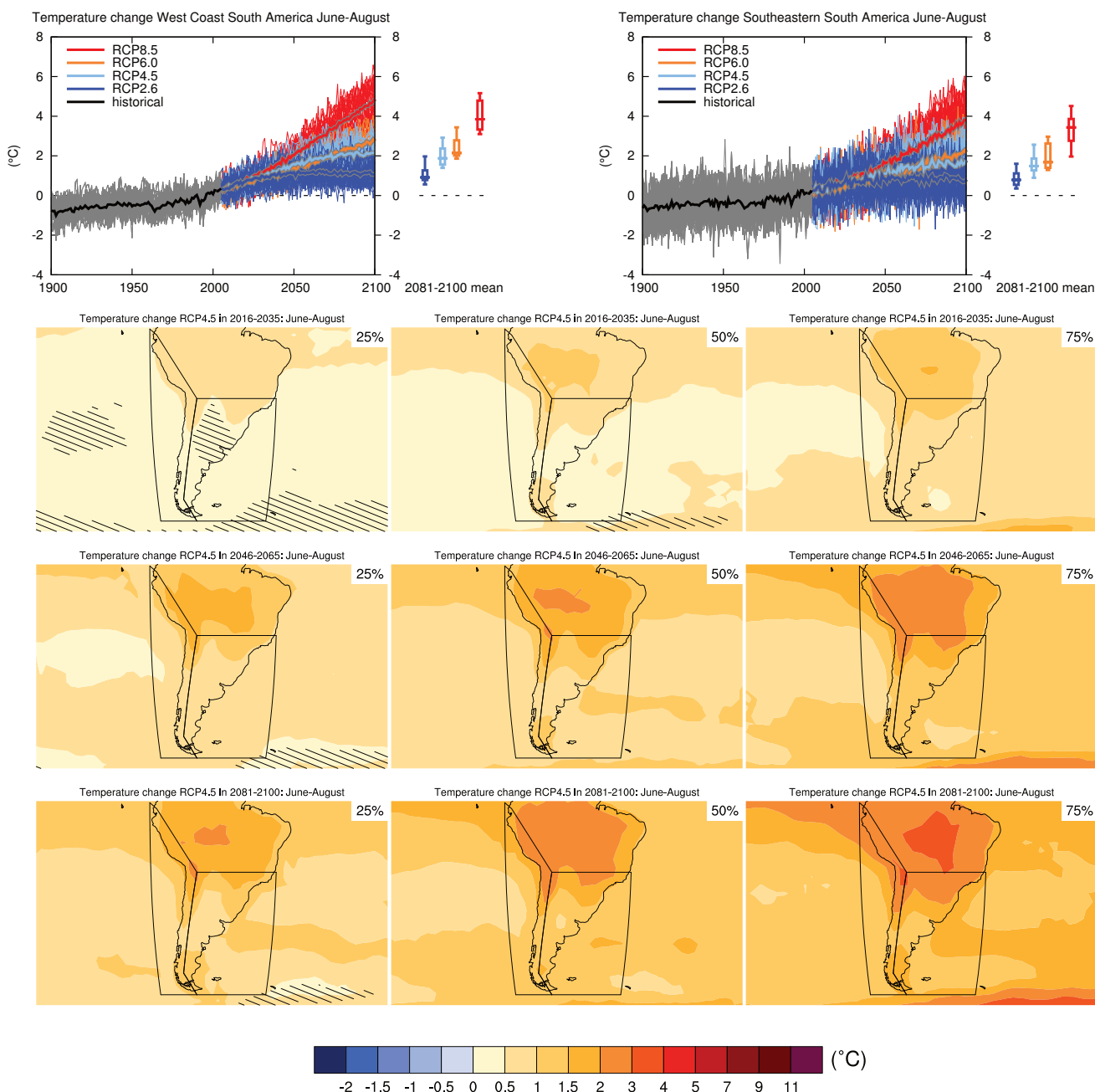


Figure AI.33 | (Top left) Time series of temperature change relative to 1986–2005 averaged over land grid points in the west coast of South America (79.7°W , 1.2°S ; 66.4°W , 20°S ; 72.1°W , 50°S ; 67.3°W , 56.7°S ; 82.0°W , 56.7°S ; 82.2°W , 0.5°N) in June to August. (Top right) Same for land grid points in southeastern South America (39.4°W , 20°S ; 39.4°W , 56.6°S ; 67.3°W , 56.7°S ; 72.1°W , 50°S ; 66°W , 20°S). Thin lines denote one ensemble member per model, thick lines the CMIP5 multi-model mean. On the right-hand side the 5th, 25th, 50th (median), 75th and 95th percentiles of the distribution of 20-year mean changes are given for 2081–2100 in the four RCP scenarios.

(Below) Maps of temperature changes in 2016–2035, 2046–2065 and 2081–2100 with respect to 1986–2005 in the RCP4.5 scenario. For each point, the 25th, 50th and 75th percentiles of the distribution of the CMIP5 ensemble are shown; this includes both natural variability and inter-model spread. Hatching denotes areas where the 20-year mean differences of the percentiles are less than the standard deviation of model-estimated present-day natural variability of 20-year mean differences.

Sections 9.4.1.1, 9.6.1.1, 10.3.1.1.4, Box 11.2, 14.8.5 contain relevant information regarding the evaluation of models in this region, the model spread in the context of other methods of projecting changes and the role of modes of variability and other climate phenomena.

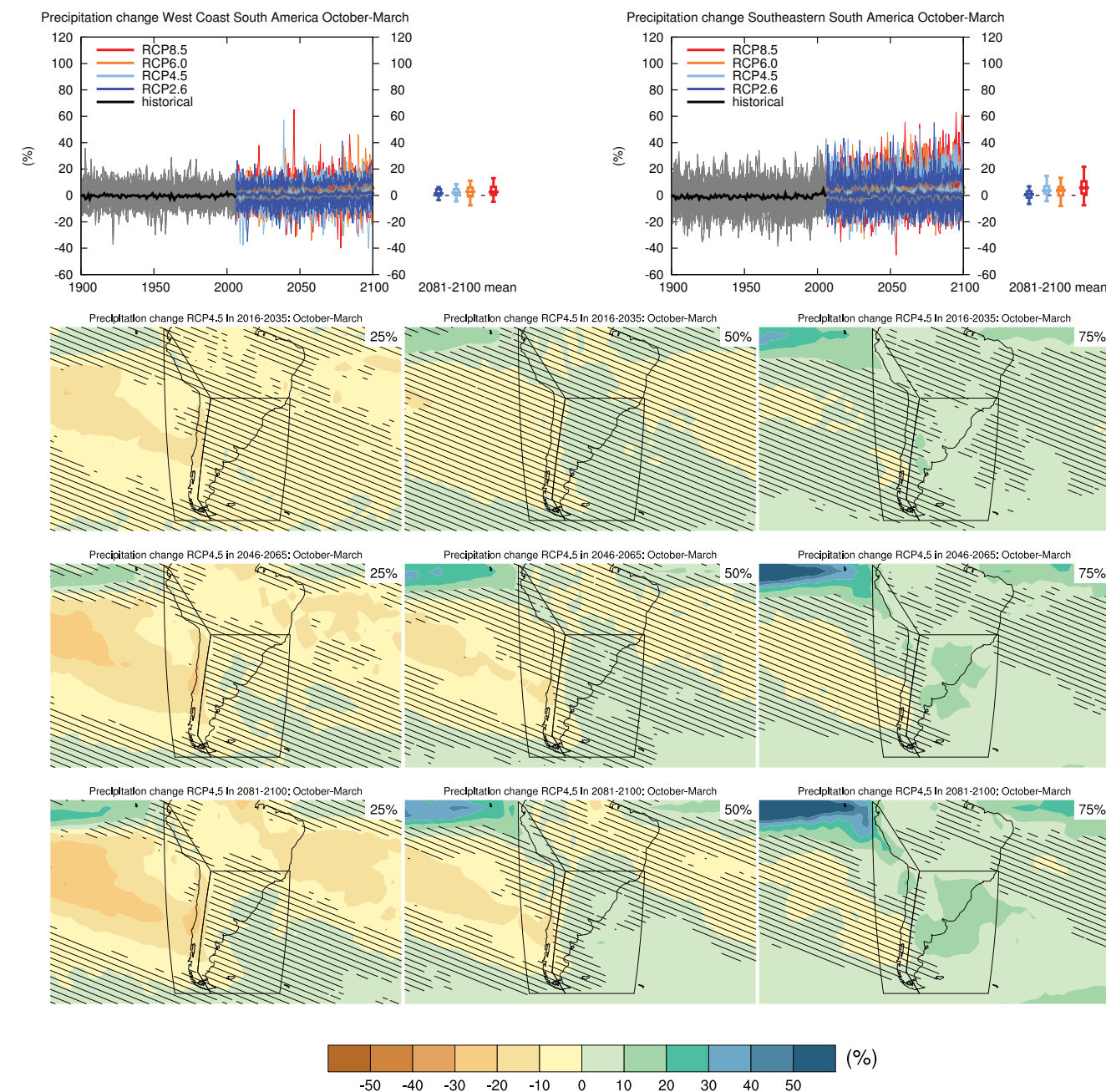


Figure AI.34 | (Top left) Time series of relative change relative to 1986–2005 in precipitation averaged over land grid points in the west coast of South America (79.7°W , 1.2°S ; 66.4°W , 20°S ; 72.1°W , 50°S ; 67.3°W , 56.7°S ; 82.0°W , 56.7°S ; 82.2°W , 0.5°N) in October to March. (Top right) Same for land grid points in southeastern South America (39.4°W , 20°S ; 39.4°W , 56.6°S ; 67.3°W , 56.7°S ; 72.1°W , 50°S ; 66°W , 20°S). Thin lines denote one ensemble member per model, thick lines the CMIP5 multi-model mean. On the right-hand side the 5th, 25th, 50th (median), 75th and 95th percentiles of the distribution of 20-year mean changes are given for 2081–2100 in the four RCP scenarios.

(Below) Maps of precipitation changes in 2016–2035, 2046–2065 and 2081–2100 with respect to 1986–2005 in the RCP4.5 scenario. For each point, the 25th, 50th and 75th percentiles of the distribution of the CMIP5 ensemble are shown; this includes both natural variability and inter-model spread. Hatching denotes areas where the 20-year mean differences of the percentiles are less than the standard deviation of model-estimated present-day natural variability of 20-year mean differences.

Sections 9.4.1.1, 9.6.1.1, Box 11.2, 12.4.5.2, 14.8.5 contain relevant information regarding the evaluation of models in this region, the model spread in the context of other methods of projecting changes and the role of modes of variability and other climate phenomena.

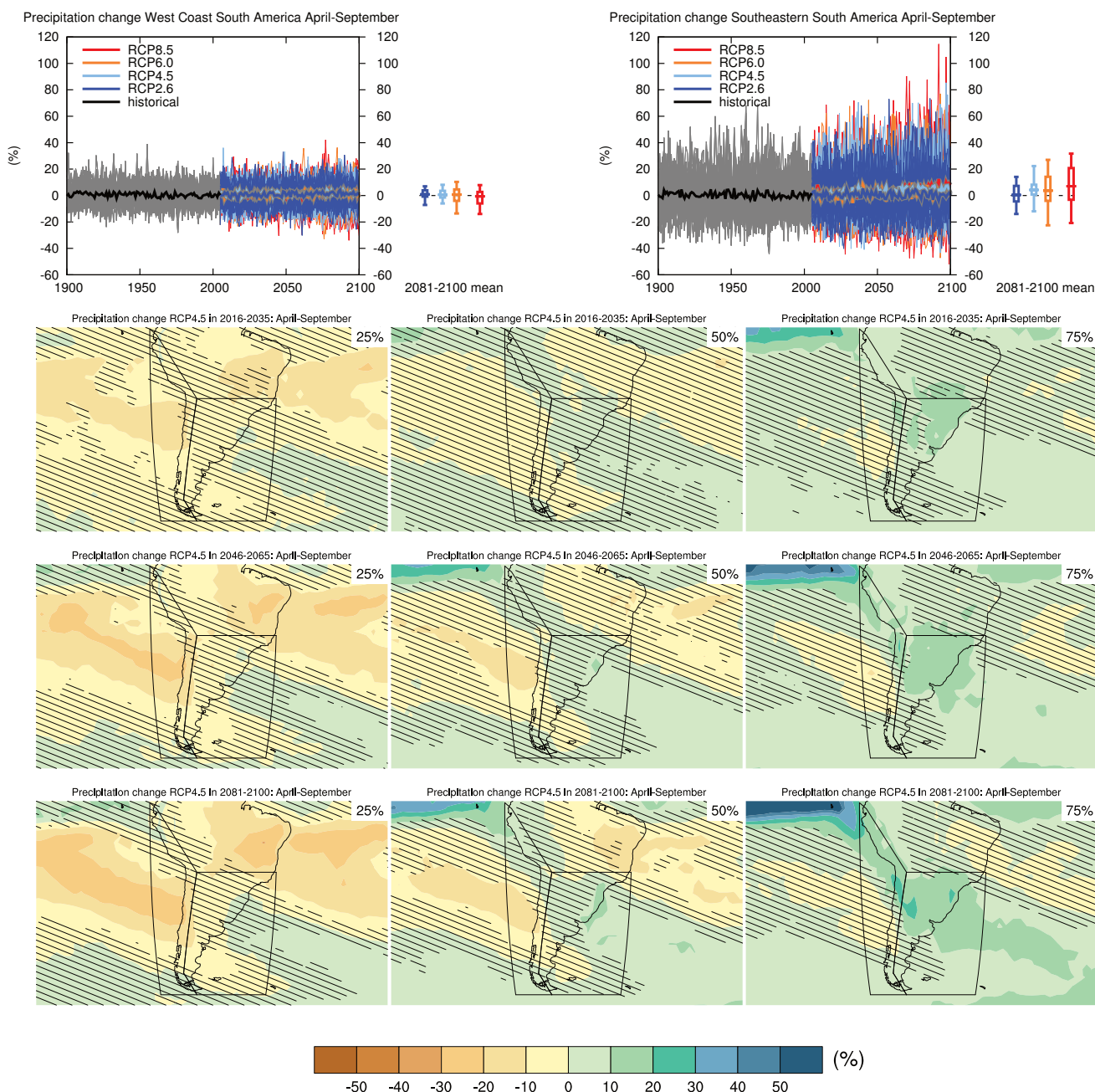


Figure AI.35 | (Top left) Time series of relative change relative to 1986–2005 in precipitation averaged over land grid points in the west coast of South America (79.7°W , 1.2°S ; 66.4°W , 20°S ; 72.1°W , 50°S ; 67.3°W , 56.7°S ; 82.0°W , 56.7°S ; 82.2°W , 0.5°N) in April to September. (Top right) Same for land grid points in southeastern South America (39.4°W , 20°S ; 39.4°W , 56.6°S ; 67.3°W , 56.7°S ; 72.1°W , 50°S ; 66°W , 20°S). Thin lines denote one ensemble member per model, thick lines the CMIP5 multi-model mean. On the right-hand side the 5th, 25th, 50th (median), 75th and 95th percentiles of the distribution of 20-year mean changes are given for 2081–2100 in the four RCP scenarios.

(Below) Maps of precipitation changes in 2016–2035, 2046–2065 and 2081–2100 with respect to 1986–2005 in the RCP4.5 scenario. For each point, the 25th, 50th and 75th percentiles of the distribution of the CMIP5 ensemble are shown; this includes both natural variability and inter-model spread. Hatching denotes areas where the 20-year mean differences of the percentiles are less than the standard deviation of model-estimated present-day natural variability of 20-year mean differences.

Sections 9.4.1.1, 9.6.1.1, Box 11.2, 12.4.5.2, 14.8.5 contain relevant information regarding the evaluation of models in this region, the model spread in the context of other methods of projecting changes and the role of modes of variability and other climate phenomena.

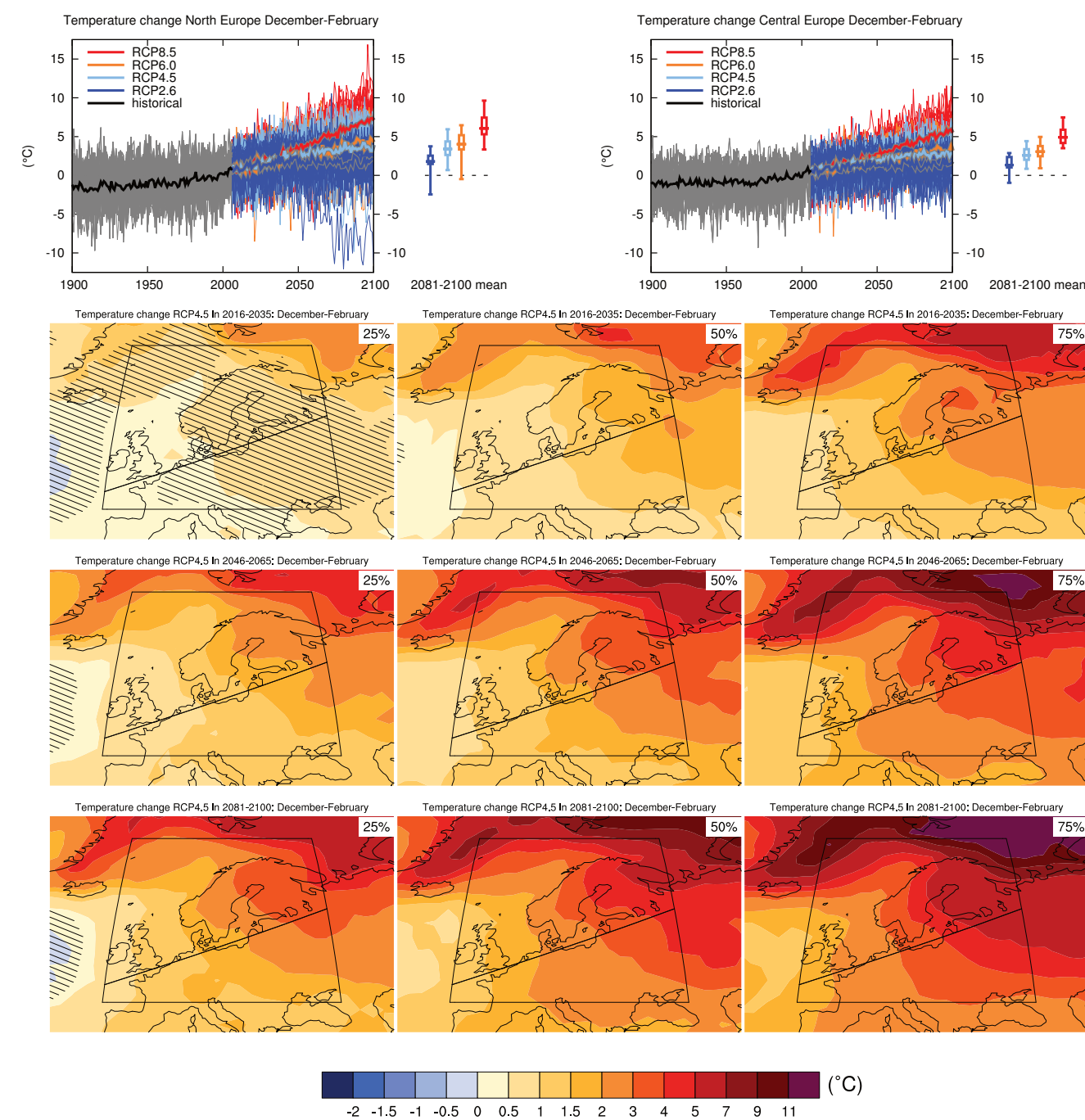


Figure AI.36 | (Top left) Time series of temperature change relative to 1986–2005 averaged over land grid points in North Europe (10°W , 48°N ; 10°W , 75°N ; 40°E , 75°N ; 40°E , 61.3°N) in December to February. (Top right) Same for land grid points in Central Europe (10°W , 45°N ; 10°W , 48°N ; 40°E , 61.3°N ; 40°E , 45°N). Thin lines denote one ensemble member per model, thick lines the CMIP5 multi-model mean. On the right-hand side the 5th, 25th, 50th (median), 75th and 95th percentiles of the distribution of 20-year mean changes are given for 2081–2100 in the four RCP scenarios.

(Below) Maps of temperature changes in 2016–2035, 2046–2065 and 2081–2100 with respect to 1986–2005 in the RCP4.5 scenario. For each point, the 25th, 50th and 75th percentiles of the distribution of the CMIP5 ensemble are shown; this includes both natural variability and inter-model spread. Hatching denotes areas where the 20-year mean differences of the percentiles are less than the standard deviation of model-estimated present-day natural variability of 20-year mean differences.

Sections 9.4.1.1, 9.6.1.1, 10.3.1.1.4, 10.3, Box 11.2, 14.8.6 contain relevant information regarding the evaluation of models in this region, the model spread in the context of other methods of projecting changes and the role of modes of variability and other climate phenomena.

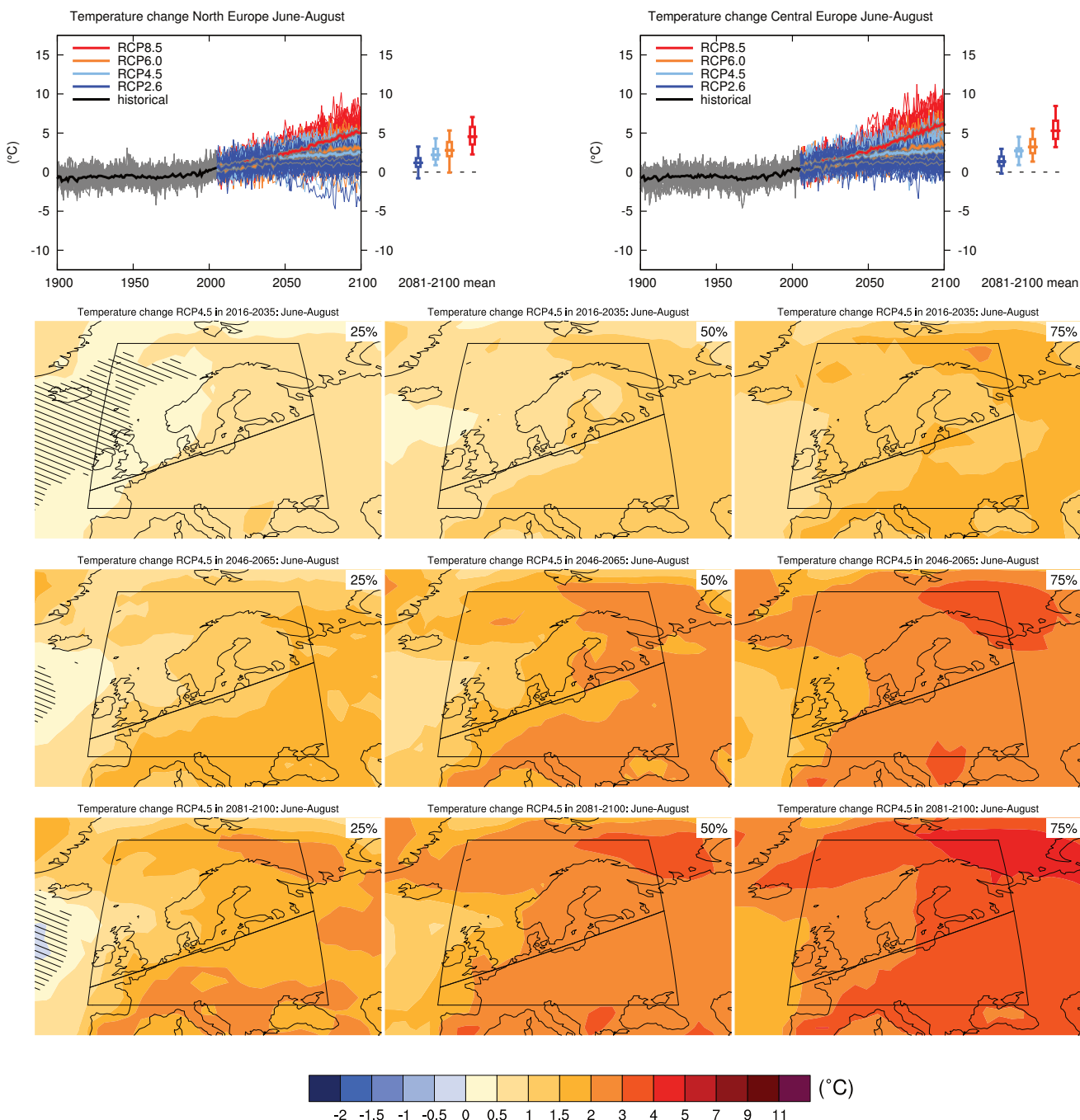


Figure Al.37 | (Top left) Time series of temperature change relative to 1986–2005 averaged over land grid points in North Europe (10°W , 48°N ; 10°W , 75°N ; 40°E , 75°N ; 40°E , 61.3°N) in June to August. (Top right) Same for land grid points in Central Europe (10°W , 45°N ; 10°W , 48°N ; 40°E , 61.3°N ; 40°E , 45°N). Thin lines denote one ensemble member per model, thick lines the CMIP5 multi-model mean. On the right-hand side the 5th, 25th, 50th (median), 75th and 95th percentiles of the distribution of 20-year mean changes are given for 2081–2100 in the four RCP scenarios.

(Below) Maps of temperature changes in 2016–2035, 2046–2065 and 2081–2100 with respect to 1986–2005 in the RCP4.5 scenario. For each point, the 25th, 50th and 75th percentiles of the distribution of the CMIP5 ensemble are shown; this includes both natural variability and inter-model spread. Hatching denotes areas where the 20-year mean differences of the percentiles are less than the standard deviation of model-estimated present-day natural variability of 20-year mean differences.

Sections 9.4.1.1, 9.6.1.1, 10.3.1.1.4, 10.3, Box 11.2, 14.8.6 contain relevant information regarding the evaluation of models in this region, the model spread in the context of other methods of projecting changes and the role of modes of variability and other climate phenomena.

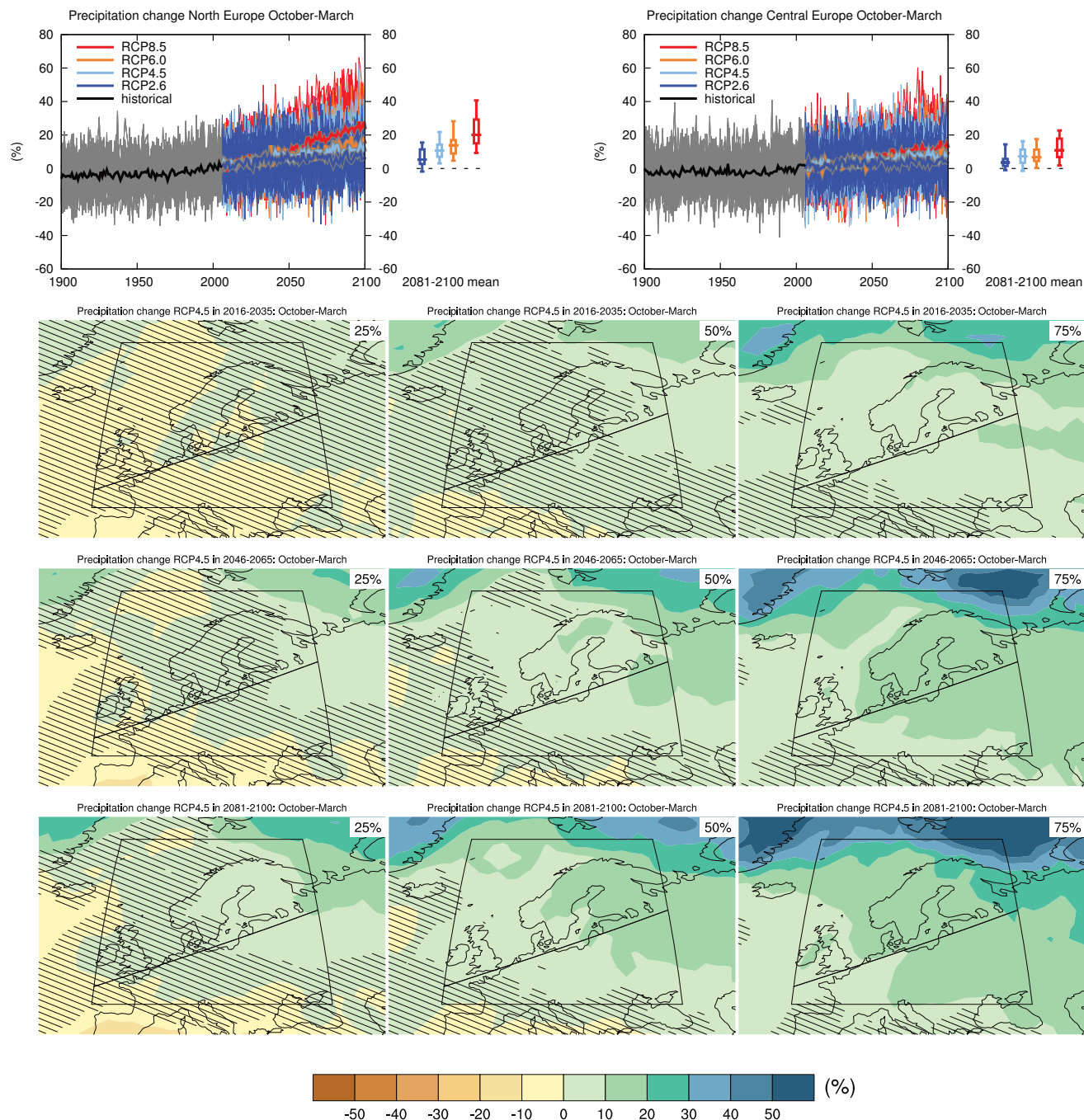


Figure AI.38 | (Top left) Time series of relative change relative to 1986–2005 in precipitation averaged over land grid points in North Europe (10°W , 48°N ; 10°W , 75°N ; 40°E , 75°N ; 40°E , 61.3°N) in October to March. (Top right) Same for land grid points in Central Europe (10°W , 45°N ; 10°W , 48°N ; 40°E , 61.3°N ; 40°E , 45°N). Thin lines denote one ensemble member per model, thick lines the CMIP5 multi-model mean. On the right-hand side the 5th, 25th, 50th (median), 75th and 95th percentiles of the distribution of 20-year mean changes are given for 2081–2100 in the four RCP scenarios.

(Below) Maps of precipitation changes in 2016–2035, 2046–2065 and 2081–2100 with respect to 1986–2005 in the RCP4.5 scenario. For each point, the 25th, 50th and 75th percentiles of the distribution of the CMIP5 ensemble are shown; this includes both natural variability and inter-model spread. Hatching denotes areas where the 20-year mean differences of the percentiles are less than the standard deviation of model-estimated present-day natural variability of 20-year mean differences.

Sections 9.4.1.1, 9.6.1.1, Box 11.2, 12.4.5.2, 14.8.6 contain relevant information regarding the evaluation of models in this region, the model spread in the context of other methods of projecting changes and the role of modes of variability and other climate phenomena.

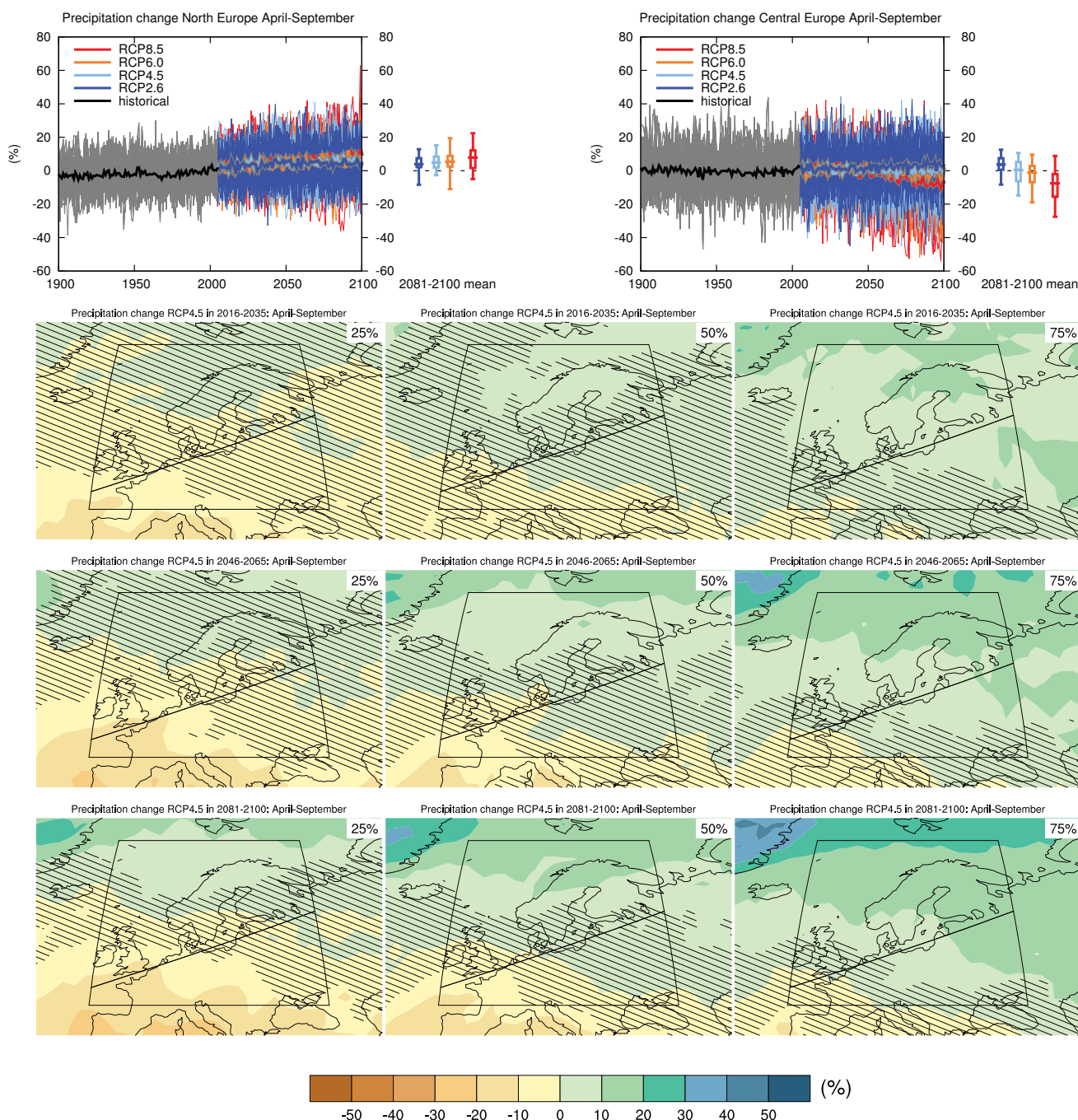


Figure AI.39 | (Top left) Time series of relative change relative to 1986–2005 in precipitation averaged over land grid points in North Europe (10°W , 48°N ; 10°W , 75°N ; 40°E , 75°N ; 40°E , 61.3°N) in April to September. (Top right) Same for land grid points in Central Europe (10°W , 45°N ; 10°W , 48°N ; 40°E , 61.3°N ; 40°E , 45°N). Thin lines denote one ensemble member per model, thick lines the CMIP5 multi-model mean. On the right-hand side the 5th, 25th, 50th (median), 75th and 95th percentiles of the distribution of 20-year mean changes are given for 2081–2100 in the four RCP scenarios.

(Below) Maps of precipitation changes in 2016–2035, 2046–2065 and 2081–2100 with respect to 1986–2005 in the RCP4.5 scenario. For each point, the 25th, 50th and 75th percentiles of the distribution of the CMIP5 ensemble are shown; this includes both natural variability and inter-model spread. Hatching denotes areas where the 20-year mean differences of the percentiles are less than the standard deviation of model-estimated present-day natural variability of 20-year mean differences.

Sections 9.4.1.1, 9.6.1.1, Box 11.2, 12.4.5.2, 14.8.6 contain relevant information regarding the evaluation of models in this region, the model spread in the context of other methods of projecting changes and the role of modes of variability and other climate phenomena.

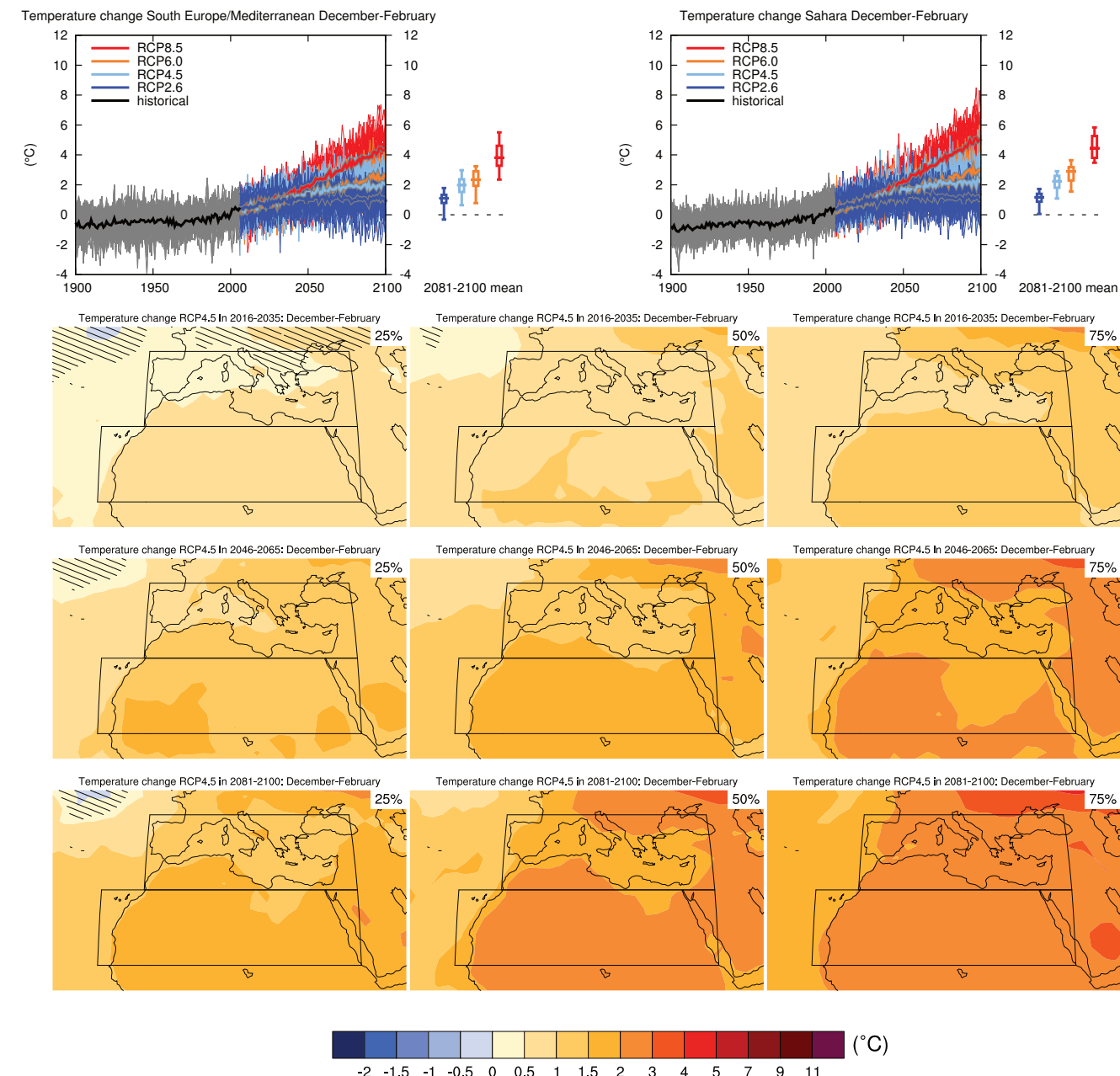


Figure AI.40 | (Top left) Time series of temperature change relative to 1986–2005 averaged over land grid points in the region South Europe/Mediterranean (30°N to 45°N , 10°W to 40°E) in December to February. (Top right) Same for land grid points in the Sahara (15°N to 30°N , 20°W to 40°E). Thin lines denote one ensemble member per model, thick lines the CMIP5 multi-model mean. On the right-hand side the 5th, 25th, 50th (median), 75th and 95th percentiles of the distribution of 20-year mean changes are given for 2081–2100 in the four RCP scenarios.

(Below) Maps of temperature changes in 2016–2035, 2046–2065 and 2081–2100 with respect to 1986–2005 in the RCP4.5 scenario. For each point, the 25th, 50th and 75th percentiles of the distribution of the CMIP5 ensemble are shown; this includes both natural variability and inter-model spread. Hatching denotes areas where the 20-year mean differences of the percentiles are less than the standard deviation of model-estimated present-day natural variability of 20-year mean differences.

Sections 9.4.1.1, 9.6.1.1, 10.3.1.1.4, Box 11.2, 14.8.6, 14.8.7 contain relevant information regarding the evaluation of models in this region, the model spread in the context of other methods of projecting changes and the role of modes of variability and other climate phenomena.

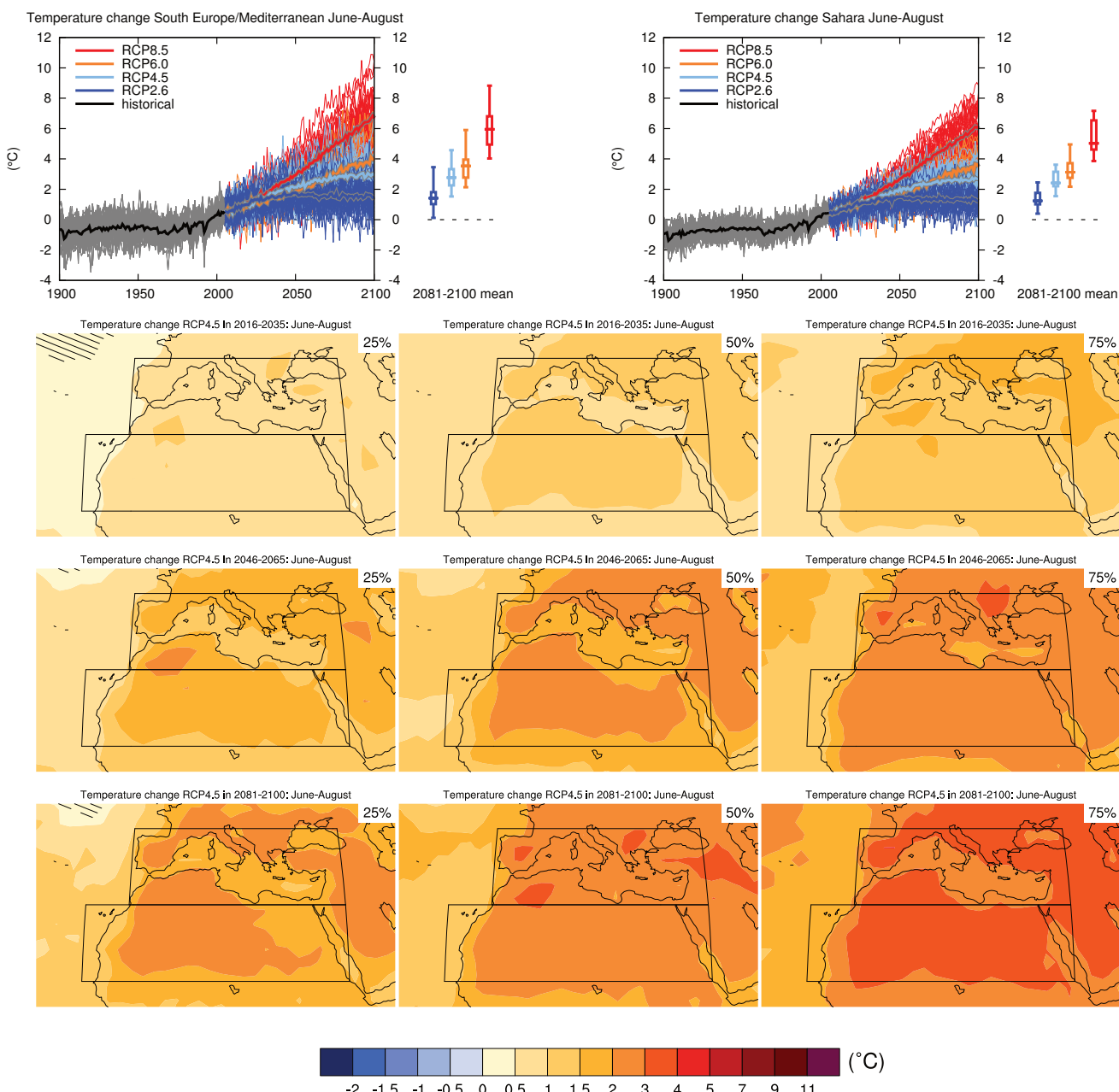


Figure A1.41 | (Top left) Time series of temperature change relative to 1986–2005 averaged over land grid points in the region South Europe/Mediterranean (30°N to 45°N , 10°W to 40°E) in June to August. (Top right) Same for land grid points in the Sahara (15°N to 30°N , 20°W to 40°E). Thin lines denote one ensemble member per model, thick lines the CMIP5 multi-model mean. On the right-hand side the 5th, 25th, 50th (median), 75th and 95th percentiles of the distribution of 20-year mean changes are given for 2081–2100 in the four RCP scenarios.

(Below) Maps of temperature changes in 2016–2035, 2046–2065 and 2081–2100 with respect to 1986–2005 in the RCP4.5 scenario. For each point, the 25th, 50th and 75th percentiles of the distribution of the CMIP5 ensemble are shown; this includes both natural variability and inter-model spread. Hatching denotes areas where the 20-year mean differences of the percentiles are less than the standard deviation of model-estimated present-day natural variability of 20-year mean differences.

Sections 9.4.1.1, 9.6.1.1, 10.3.1.1.4, Box 11.2, 14.8.6, 14.8.7 contain relevant information regarding the evaluation of models in this region, the model spread in the context of other methods of projecting changes and the role of modes of variability and other climate phenomena.

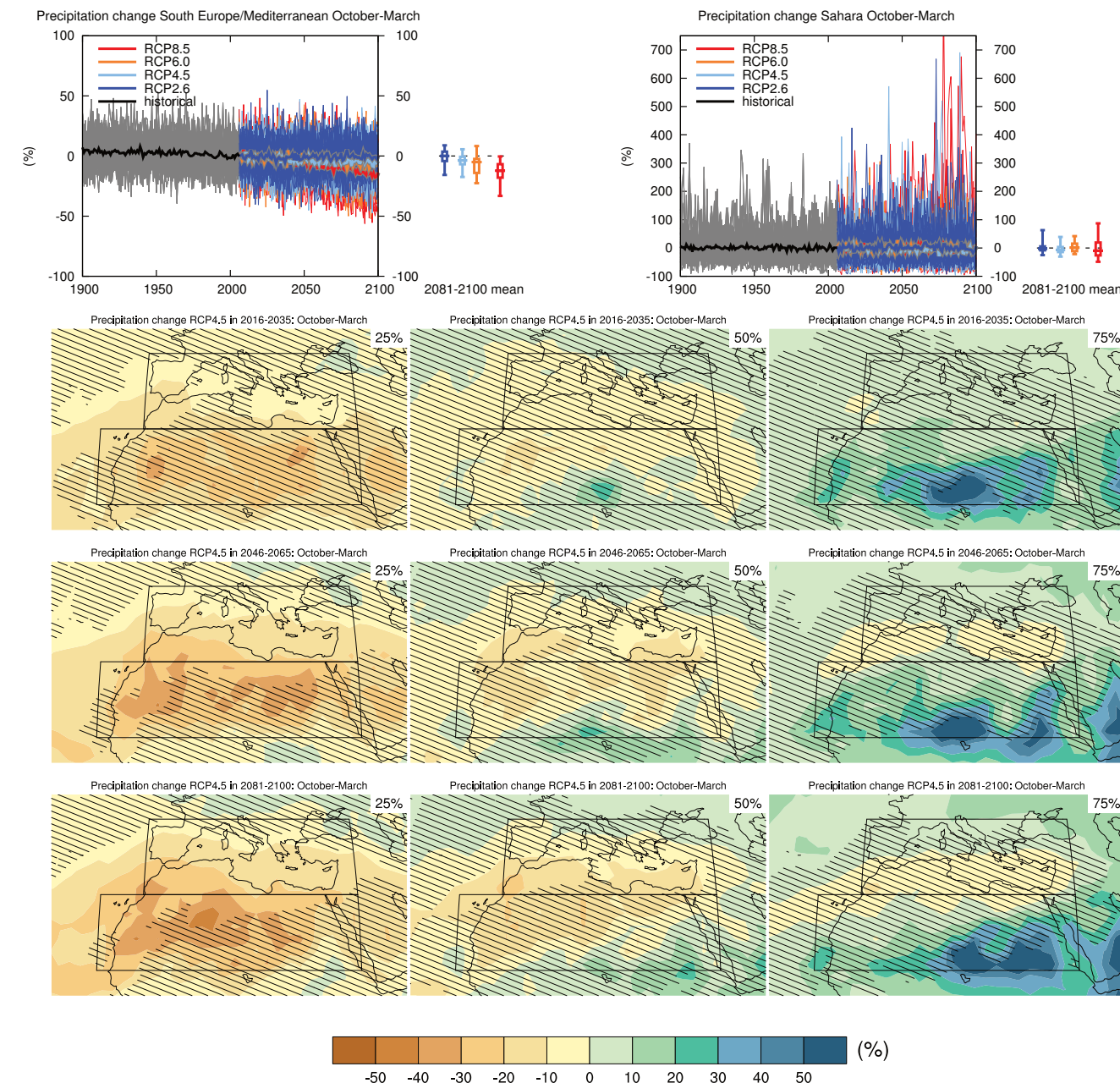


Figure AI.42 | (Top left) Time series of relative change relative to 1986–2005 in precipitation averaged over land grid points in the region South Europe/Mediterranean (30°N to 45°N , 10°W to 40°E) in October to March. (Top right) Same for land grid points in the Sahara (15°N to 30°N , 20°W to 40°E). Thin lines denote one ensemble member per model, thick lines the CMIP5 multi-model mean. On the right-hand side the 5th, 25th, 50th (median), 75th and 95th percentiles of the distribution of 20-year mean changes are given for 2081–2100 in the four RCP scenarios. Note different scales.

(Below) Maps of precipitation changes in 2016–2035, 2046–2065 and 2081–2100 with respect to 1986–2005 in the RCP4.5 scenario. For each point, the 25th, 50th and 75th percentiles of the distribution of the CMIP5 ensemble are shown; this includes both natural variability and inter-model spread. Hatching denotes areas where the 20-year mean differences of the percentiles are less than the standard deviation of model-estimated present-day natural variability of 20-year mean differences.

Sections 9.4.1.1, 9.6.1.1, Box 11.2, 12.4.5.2, 14.8.6, 14.8.7 contain relevant information regarding the evaluation of models in this region, the model spread in the context of other methods of projecting changes and the role of modes of variability and other climate phenomena.

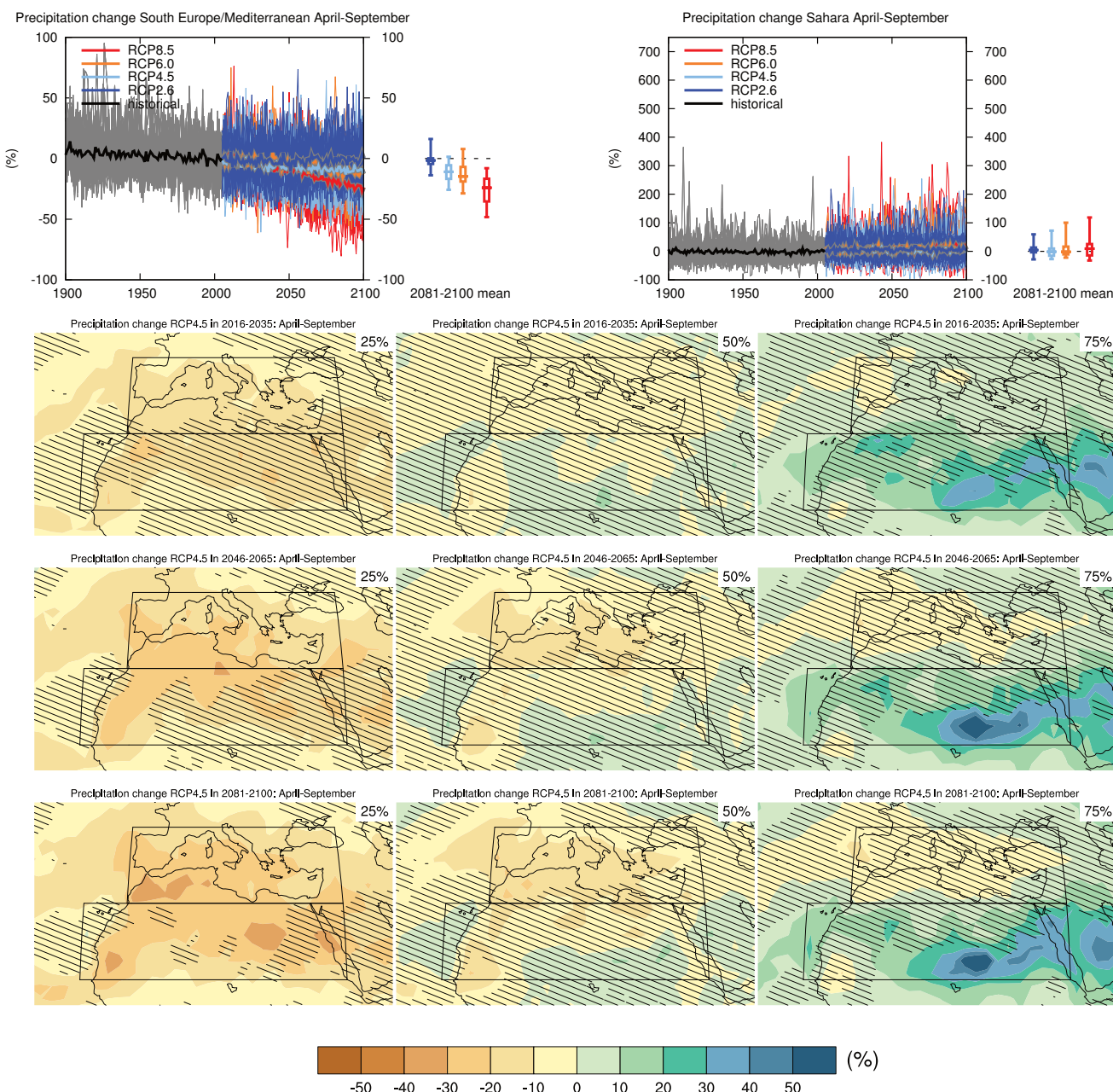


Figure AI.43 | (Top left) Time series of relative change relative to 1986–2005 in precipitation averaged over land grid points in the region South Europe/Mediterranean (30°N to 45°N , 10°W to 40°E) in April to September. (Top right) Same for land grid points in the Sahara (15°N to 30°N , 20°W to 40°E). Thin lines denote one ensemble member per model, thick lines the CMIP5 multi-model mean. On the right-hand side the 5th, 25th, 50th (median), 75th and 95th percentiles of the distribution of 20-year mean changes are given for 2081–2100 in the four RCP scenarios. Note different scales.

(Below) Maps of precipitation changes in 2016–2035, 2046–2065 and 2081–2100 with respect to 1986–2005 in the RCP4.5 scenario. For each point, the 25th, 50th and 75th percentiles of the distribution of the CMIP5 ensemble are shown; this includes both natural variability and inter-model spread. Hatching denotes areas where the 20-year mean differences of the percentiles are less than the standard deviation of model-estimated present-day natural variability of 20-year mean differences.

Sections 9.4.1.1, 9.6.1.1, Box 11.2, 12.4.5.2, 14.8.6, 14.8.7 contain relevant information regarding the evaluation of models in this region, the model spread in the context of other methods of projecting changes and the role of modes of variability and other climate phenomena.

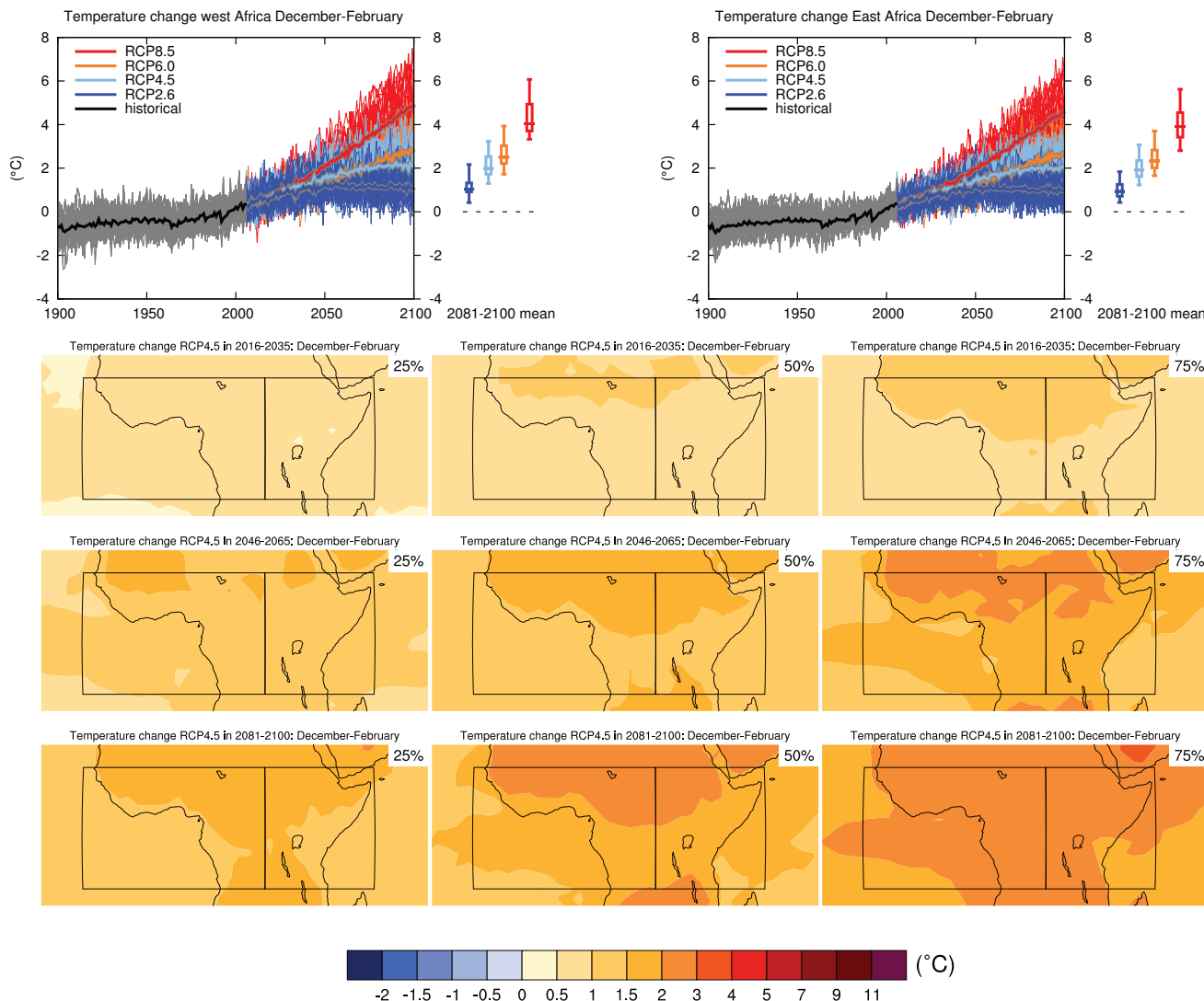


Figure AI.44 | (Top left) Time series of temperature change relative to 1986–2005 averaged over land grid points in West Africa (11.4°S to 15°N , 20°W to 25°E) in December to February. (Top right) Same for land grid points in East Africa (11.3°S to 15°N , 25°E to 52°E). Thin lines denote one ensemble member per model, thick lines the CMIP5 multi-model mean. On the right-hand side the 5th, 25th, 50th (median), 75th and 95th percentiles of the distribution of 20-year mean changes are given for 2081–2100 in the four RCP scenarios.

(Below) Maps of temperature changes in 2016–2035, 2046–2065 and 2081–2100 with respect to 1986–2005 in the RCP4.5 scenario. For each point, the 25th, 50th and 75th percentiles of the distribution of the CMIP5 ensemble are shown; this includes both natural variability and inter-model spread. Hatching denotes areas where the 20-year mean differences of the percentiles are less than the standard deviation of model-estimated present-day natural variability of 20-year mean differences.

Sections 9.4.1.1, 9.6.1.1, 10.3.1.1.4, Box 11.2, 14.8.7 contain relevant information regarding the evaluation of models in this region, the model spread in the context of other methods of projecting changes and the role of modes of variability and other climate phenomena.

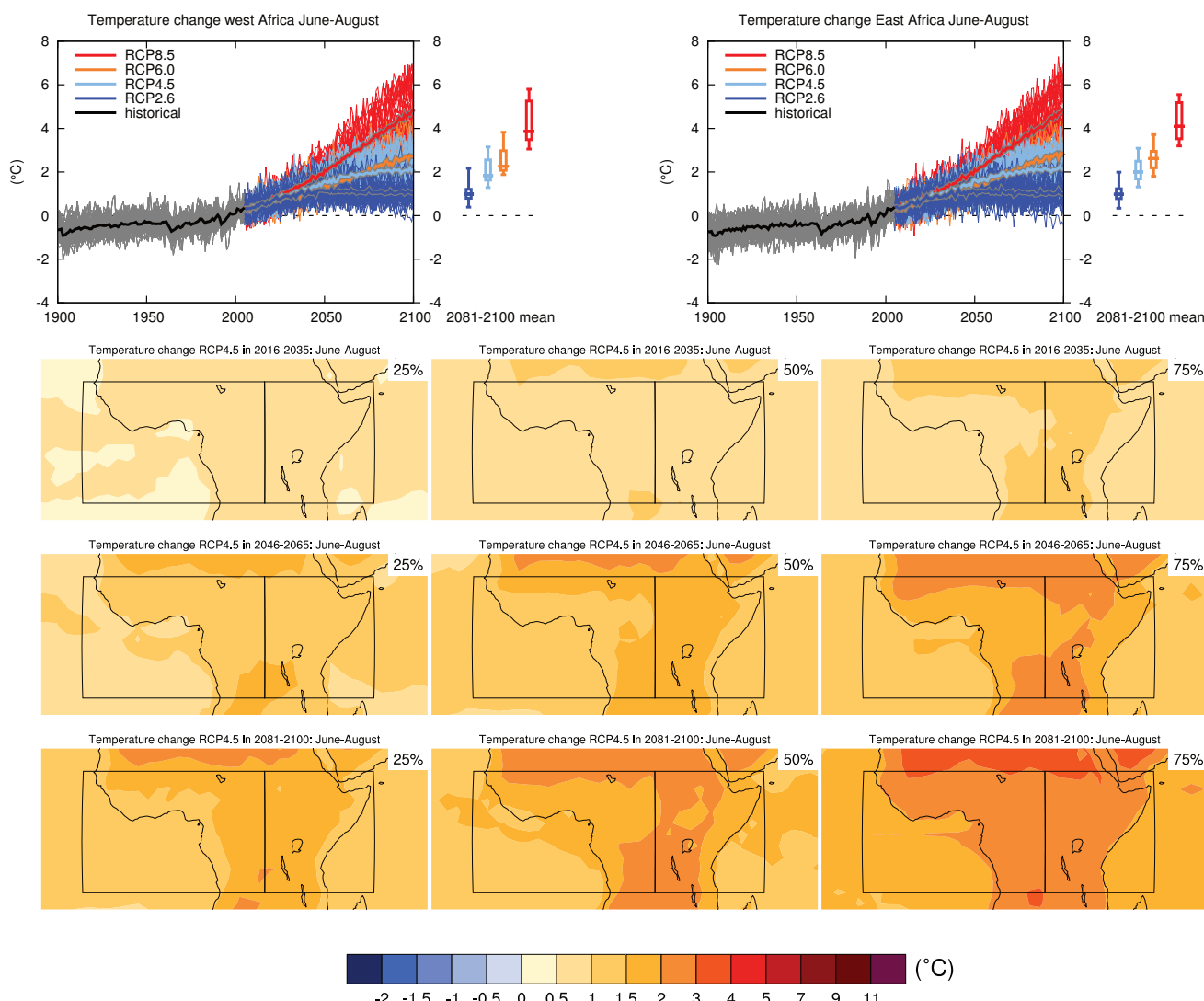


Figure AI.45 | (Top left) Time series of temperature change relative to 1986–2005 averaged over land grid points in West Africa (11.4°S to 15°N , 20°W to 25°E) in June to August. (Top right) Same for land grid points in East Africa (11.3°S to 15°N , 25°E to 52°E). Thin lines denote one ensemble member per model, thick lines the CMIP5 multi-model mean. On the right-hand side the 5th, 25th, 50th (median), 75th and 95th percentiles of the distribution of 20-year mean changes are given for 2081–2100 in the four RCP scenarios.

(Below) Maps of temperature changes in 2016–2035, 2046–2065 and 2081–2100 with respect to 1986–2005 in the RCP4.5 scenario. For each point, the 25th, 50th and 75th percentiles of the distribution of the CMIP5 ensemble are shown; this includes both natural variability and inter-model spread. Hatching denotes areas where the 20-year mean differences of the percentiles are less than the standard deviation of model-estimated present-day natural variability of 20-year mean differences.

Sections 9.4.1.1, 9.6.1.1, 10.3.1.1.4, Box 11.2, 14.8.7 contain relevant information regarding the evaluation of models in this region, the model spread in the context of other methods of projecting changes and the role of modes of variability and other climate phenomena.

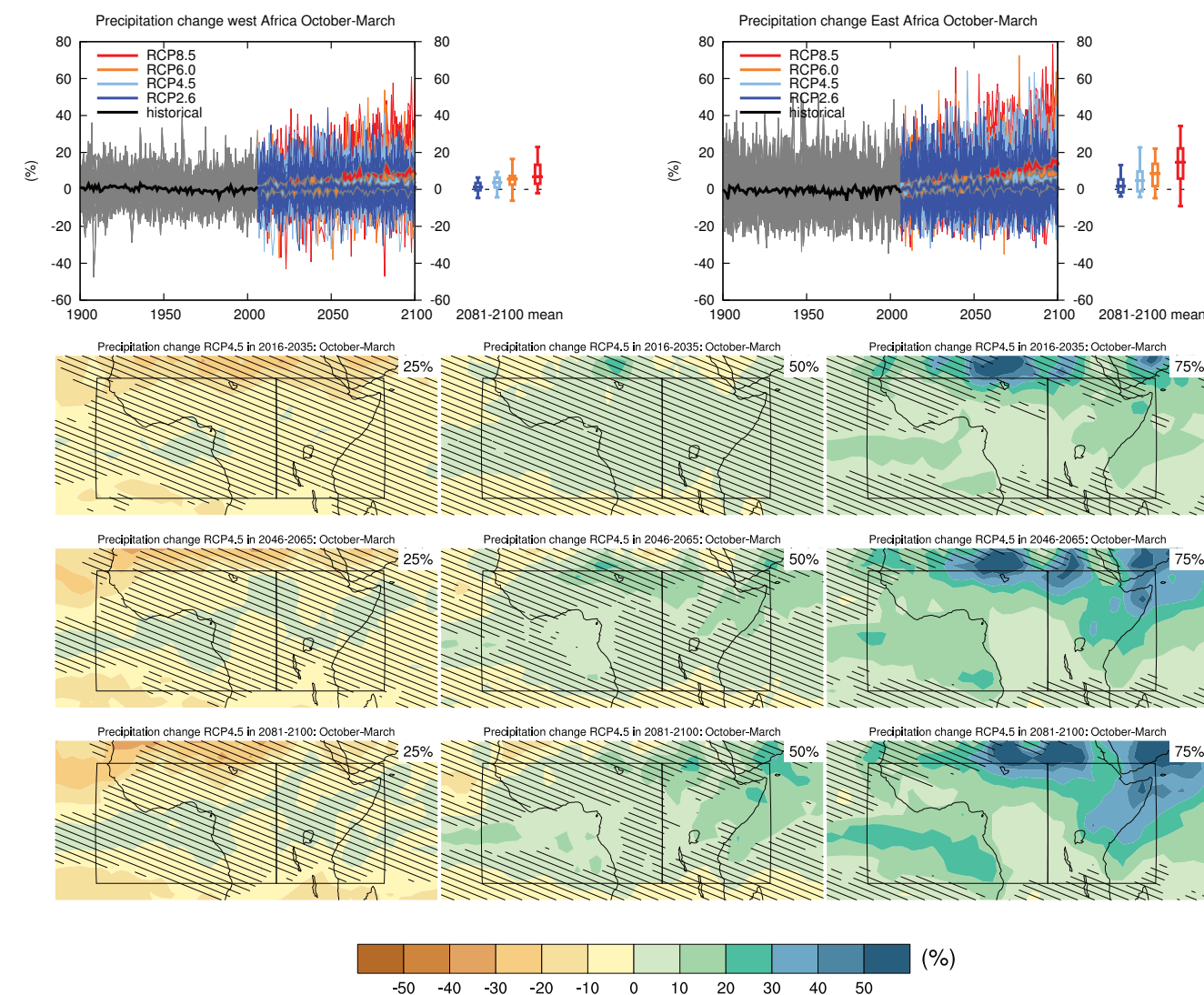


Figure AI.46 | (Top left) Time series of relative change relative to 1986–2005 in precipitation averaged over land grid points in West Africa (11.4°S to 15°N , 20°W to 25°E) in October to March. (Top right) Same for land grid points in East Africa (11.3°S to 15°N , 25°E to 52°E). Thin lines denote one ensemble member per model, thick lines the CMIP5 multi-model mean. On the right-hand side the 5th, 25th, 50th (median), 75th and 95th percentiles of the distribution of 20-year mean changes are given for 2081–2100 in the four RCP scenarios.

(Below) Maps of precipitation changes in 2016–2035, 2046–2065 and 2081–2100 with respect to 1986–2005 in the RCP4.5 scenario. For each point, the 25th, 50th and 75th percentiles of the distribution of the CMIP5 ensemble are shown; this includes both natural variability and inter-model spread. Hatching denotes areas where the 20-year mean differences of the percentiles are less than the standard deviation of model-estimated present-day natural variability of 20-year mean differences.

Sections 9.4.1.1, 9.6.1.1, 11.3.2.1.2, Box 11.2, 12.4.5.2, 14.2.4, 14.8.7 contain relevant information regarding the evaluation of models in this region, the model spread in the context of other methods of projecting changes and the role of modes of variability and other climate phenomena.

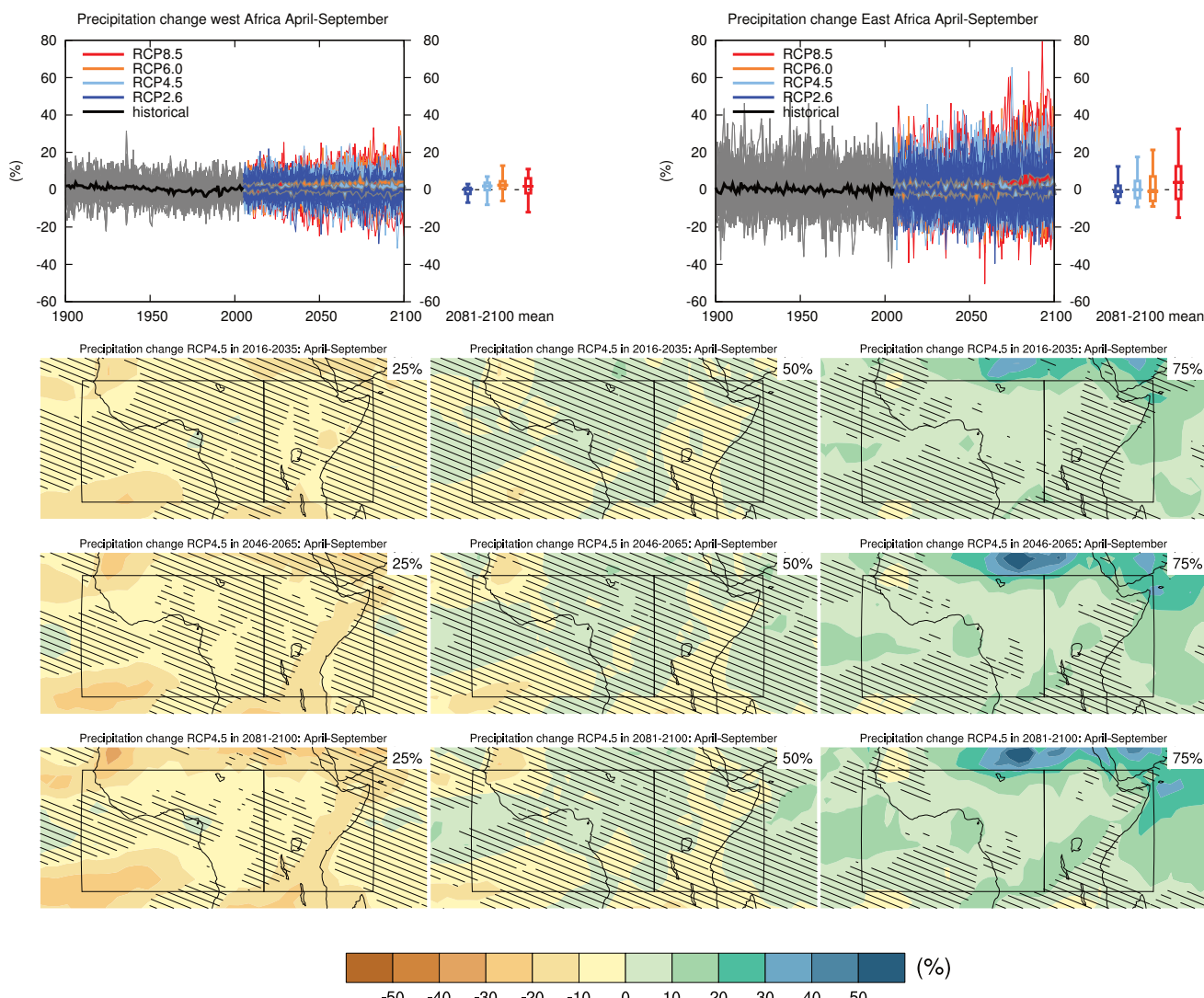


Figure AI.47 | (Top left) Time series of relative change relative to 1986–2005 in precipitation averaged over land grid points in West Africa (11.4°S to 15°N , 20°W to 25°E) in April to September. (Top right) Same for land grid points in East Africa (11.3°S to 15°N , 25°E to 52°E). Thin lines denote one ensemble member per model, thick lines the CMIP5 multi-model mean. On the right-hand side the 5th, 25th, 50th (median), 75th and 95th percentiles of the distribution of 20-year mean changes are given for 2081–2100 in the four RCP scenarios.

(Below) Maps of precipitation changes in 2016–2035, 2046–2065 and 2081–2100 with respect to 1986–2005 in the RCP4.5 scenario. For each point, the 25th, 50th and 75th percentiles of the distribution of the CMIP5 ensemble are shown; this includes both natural variability and inter-model spread. Hatching denotes areas where the 20-year mean differences of the percentiles are less than the standard deviation of model-estimated present-day natural variability of 20-year mean differences.

Sections 9.4.1.1, 9.6.1.1, 11.3.2.1.2, Box 11.2, 12.4.5.2, 14.2.4, 14.8.7 contain relevant information regarding the evaluation of models in this region, the model spread in the context of other methods of projecting changes and the role of modes of variability and other climate phenomena.

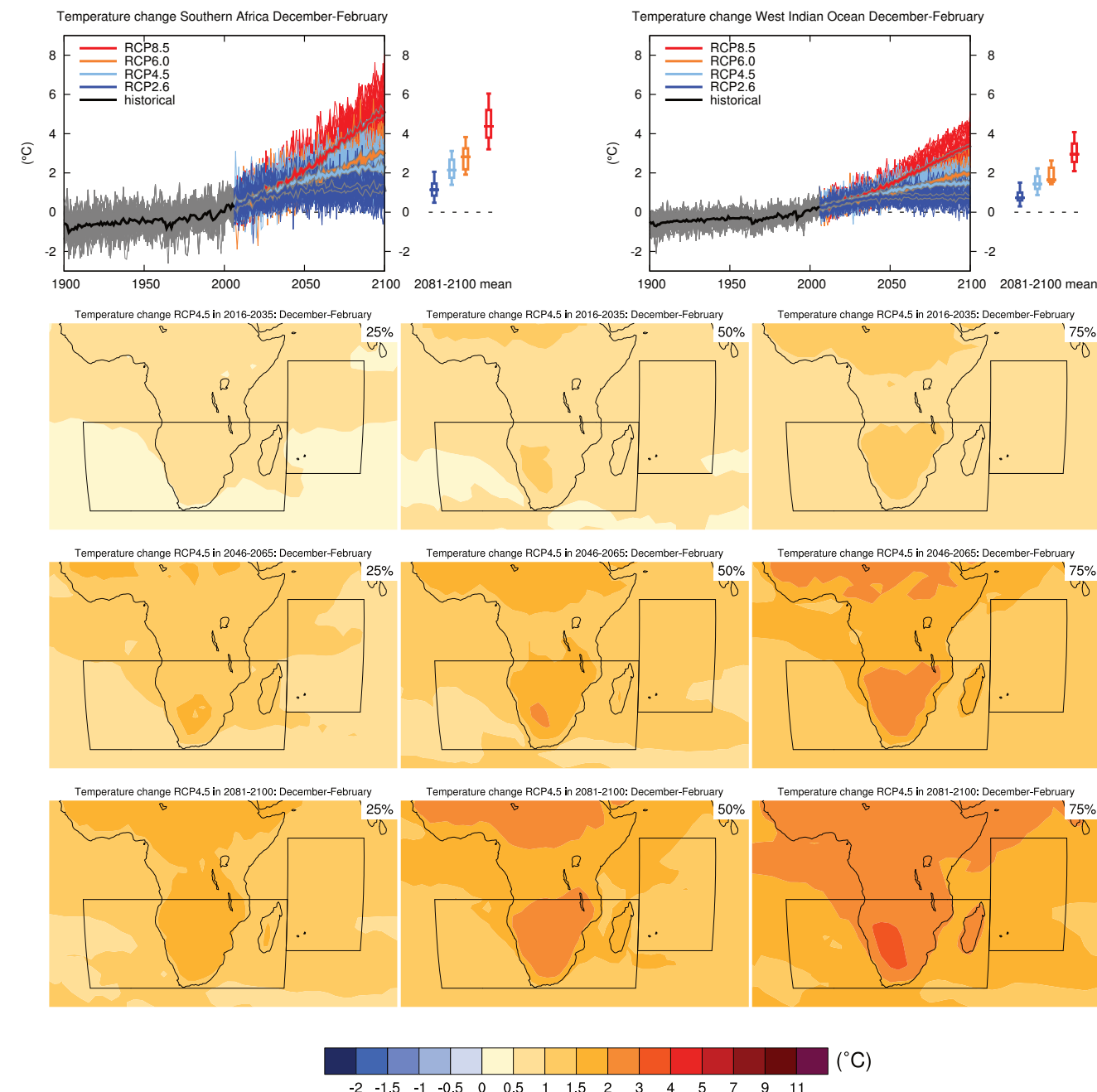


Figure AI.48 | (Top left) Time series of temperature change relative to 1986–2005 averaged over land grid points in Southern Africa (35°S to 11.4°S , 10°W to 52°E) in December to February. (Top right) Same for sea grid points in the West Indian Ocean (25°S to 5°N , 52°E to 75°E). Thin lines denote one ensemble member per model, thick lines the CMIP5 multi-model mean. On the right-hand side the 5th, 25th, 50th (median), 75th and 95th percentiles of the distribution of 20-year mean changes are given for 2081–2100 in the four RCP scenarios.

(Below) Maps of temperature changes in 2016–2035, 2046–2065 and 2081–2100 with respect to 1986–2005 in the RCP4.5 scenario. For each point, the 25th, 50th and 75th percentiles of the distribution of the CMIP5 ensemble are shown; this includes both natural variability and inter-model spread. Hatching denotes areas where the 20-year mean differences of the percentiles are less than the standard deviation of model-estimated present-day natural variability of 20-year mean differences.

Sections 9.4.1.1, 9.6.1.1, 10.3.1.1.4, Box 11.2, 14.8.7 contain relevant information regarding the evaluation of models in this region, the model spread in the context of other methods of projecting changes and the role of modes of variability and other climate phenomena.

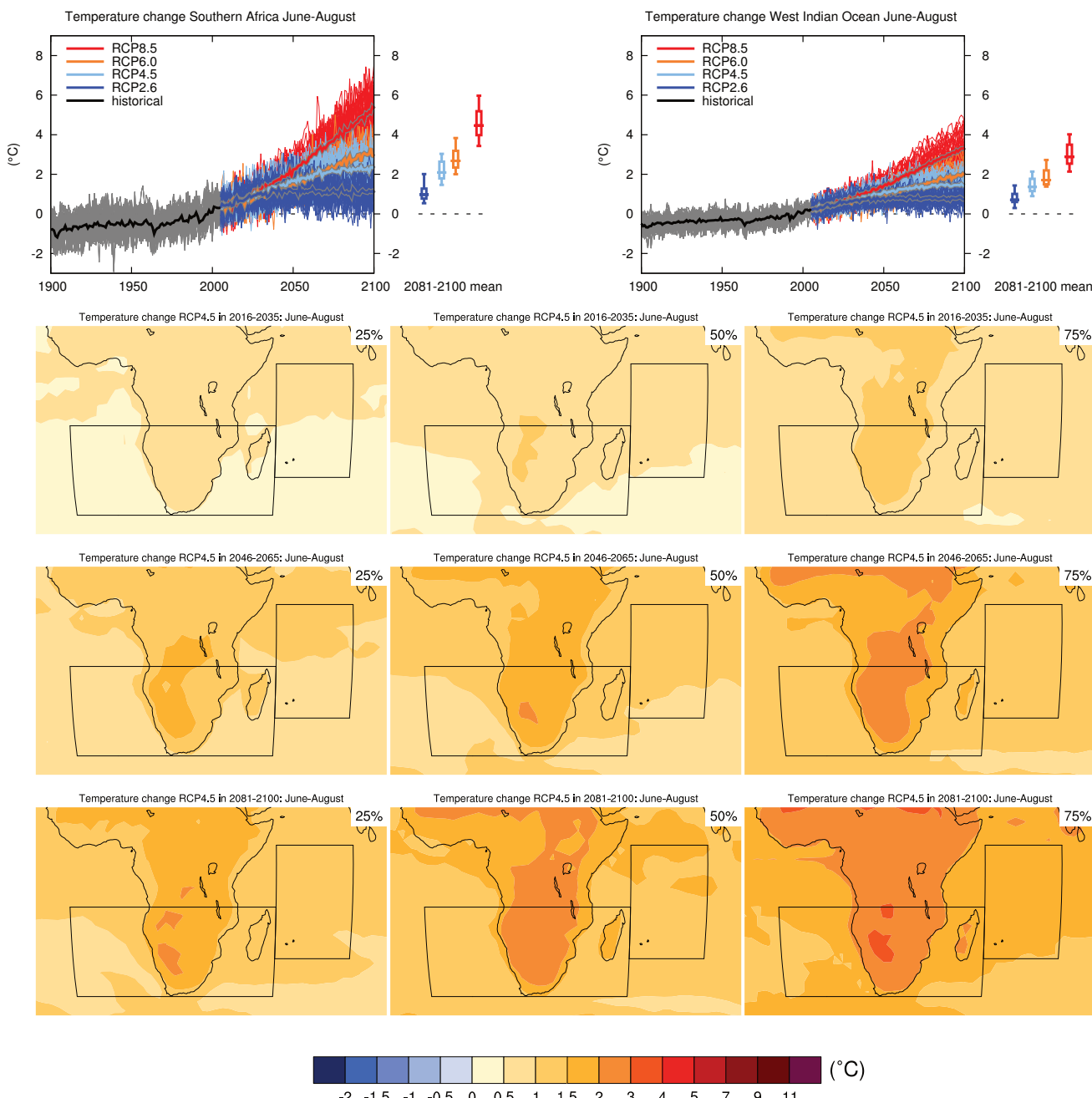


Figure AI.49 | (Top left) Time series of temperature change relative to 1986–2005 averaged over land grid points in Southern Africa (35°S to 11.4°S , 10°W to 52°E) in June to August. (Top right) Same for sea grid points in the West Indian Ocean (25°S to 5°N , 52°E to 75°E). Thin lines denote one ensemble member per model, thick lines the CMIP5 multi-model mean. On the right-hand side the 5th, 25th, 50th (median), 75th and 95th percentiles of the distribution of 20-year mean changes are given for 2081–2100 in the four RCP scenarios.

(Below) Maps of temperature changes in 2016–2035, 2046–2065 and 2081–2100 with respect to 1986–2005 in the RCP4.5 scenario. For each point, the 25th, 50th and 75th percentiles of the distribution of the CMIP5 ensemble are shown; this includes both natural variability and inter-model spread. Hatching denotes areas where the 20-year mean differences of the percentiles are less than the standard deviation of model-estimated present-day natural variability of 20-year mean differences.

Sections 9.4.1.1, 9.6.1.1, 10.3.1.1.4, Box 11.2, 14.8.7 contain relevant information regarding the evaluation of models in this region, the model spread in the context of other methods of projecting changes and the role of modes of variability and other climate phenomena.

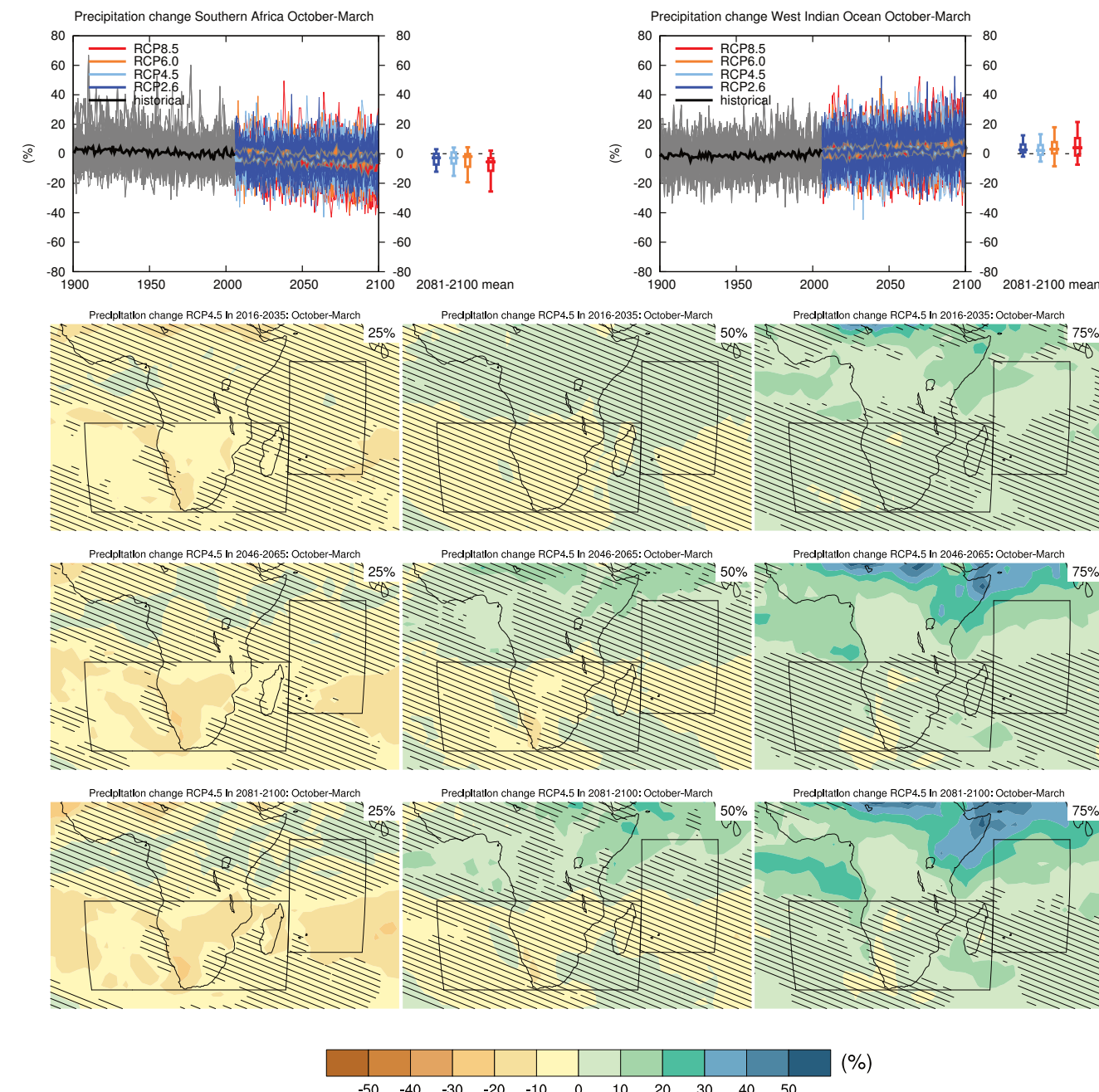


Figure AI.50 | (Top left) Time series of relative change relative to 1986–2005 in precipitation averaged over land grid points in Southern Africa (35°S to 11.4°S , 10°W to 52°E) in October to March. (Top right) Same for sea grid points in the West Indian Ocean (25°S to 5°N , 52°E to 75°E). Thin lines denote one ensemble member per model, thick lines the CMIP5 multi-model mean. On the right-hand side the 5th, 25th, 50th (median), 75th and 95th percentiles of the distribution of 20-year mean changes are given for 2081–2100 in the four RCP scenarios.

(Below) Maps of precipitation changes in 2016–2035, 2046–2065 and 2081–2100 with respect to 1986–2005 in the RCP4.5 scenario. For each point, the 25th, 50th and 75th percentiles of the distribution of the CMIP5 ensemble are shown; this includes both natural variability and inter-model spread. Hatching denotes areas where the 20-year mean differences of the percentiles are less than the standard deviation of model-estimated present-day natural variability of 20-year mean differences.

Sections 9.4.1.1, 9.6.1.1, Box 11.2, 12.4.5.2, 14.8.7 contain relevant information regarding the evaluation of models in this region, the model spread in the context of other methods of projecting changes and the role of modes of variability and other climate phenomena.

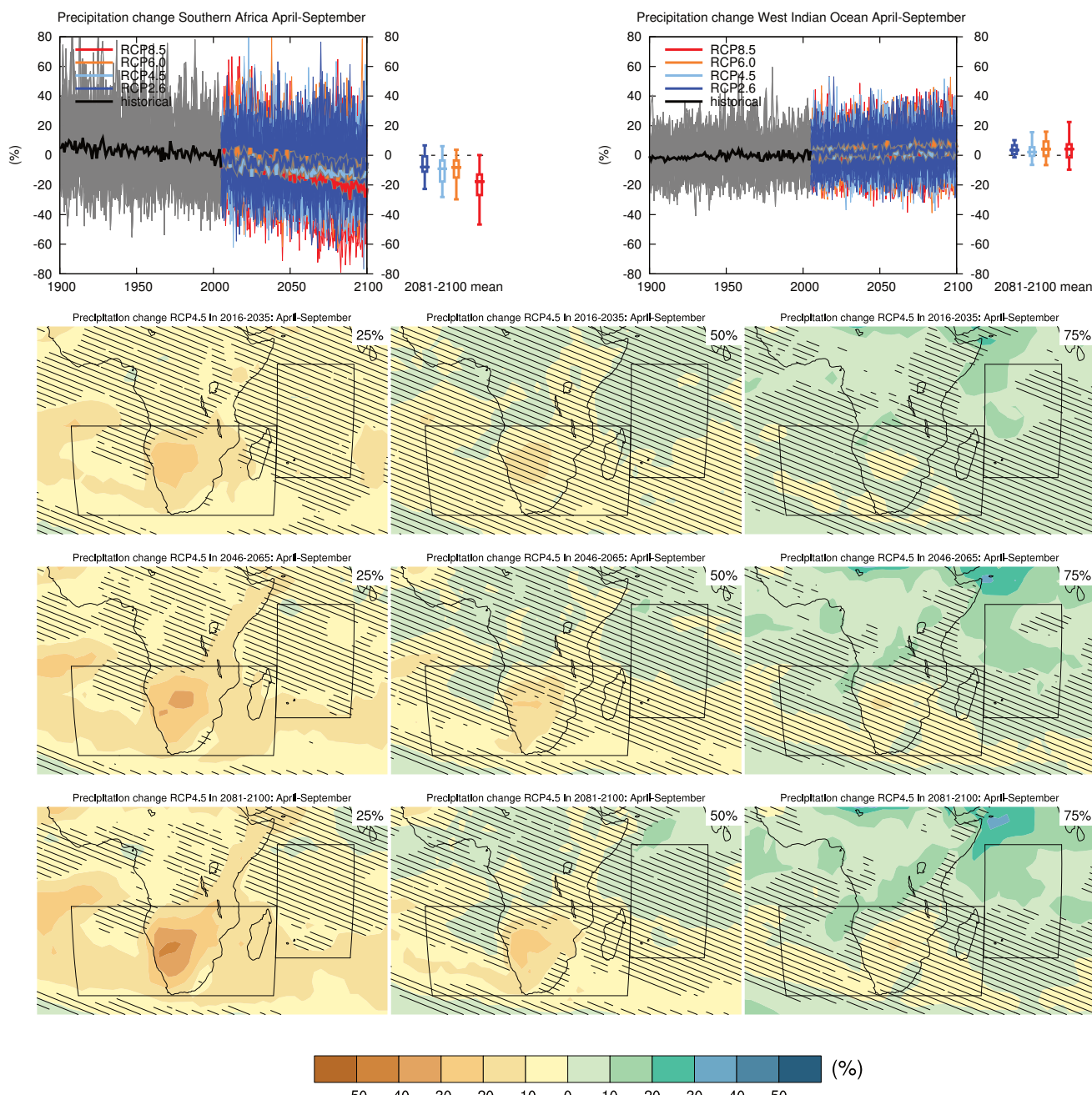


Figure AI.51 | (Top left) Time series of relative change relative to 1986–2005 in precipitation averaged over land grid points in Southern Africa (35°S to 11.4°S , 10°W to 52°E) in April to September. (Top right) Same for sea grid points in the West Indian Ocean (25°S to 5°N , 52°E to 75°E). Thin lines denote one ensemble member per model, thick lines the CMIP5 multi-model mean. On the right-hand side the 5th, 25th, 50th (median), 75th and 95th percentiles of the distribution of 20-year mean changes are given for 2081–2100 in the four RCP scenarios.

(Below) Maps of precipitation changes in 2016–2035, 2046–2065 and 2081–2100 with respect to 1986–2005 in the RCP4.5 scenario. For each point, the 25th, 50th and 75th percentiles of the distribution of the CMIP5 ensemble are shown; this includes both natural variability and inter-model spread. Hatching denotes areas where the 20-year mean differences of the percentiles are less than the standard deviation of model-estimated present-day natural variability of 20-year mean differences.

Sections 9.4.1.1, 9.6.1.1, Box 11.2, 12.4.5.2, 14.8.7 contain relevant information regarding the evaluation of models in this region, the model spread in the context of other methods of projecting changes and the role of modes of variability and other climate phenomena.

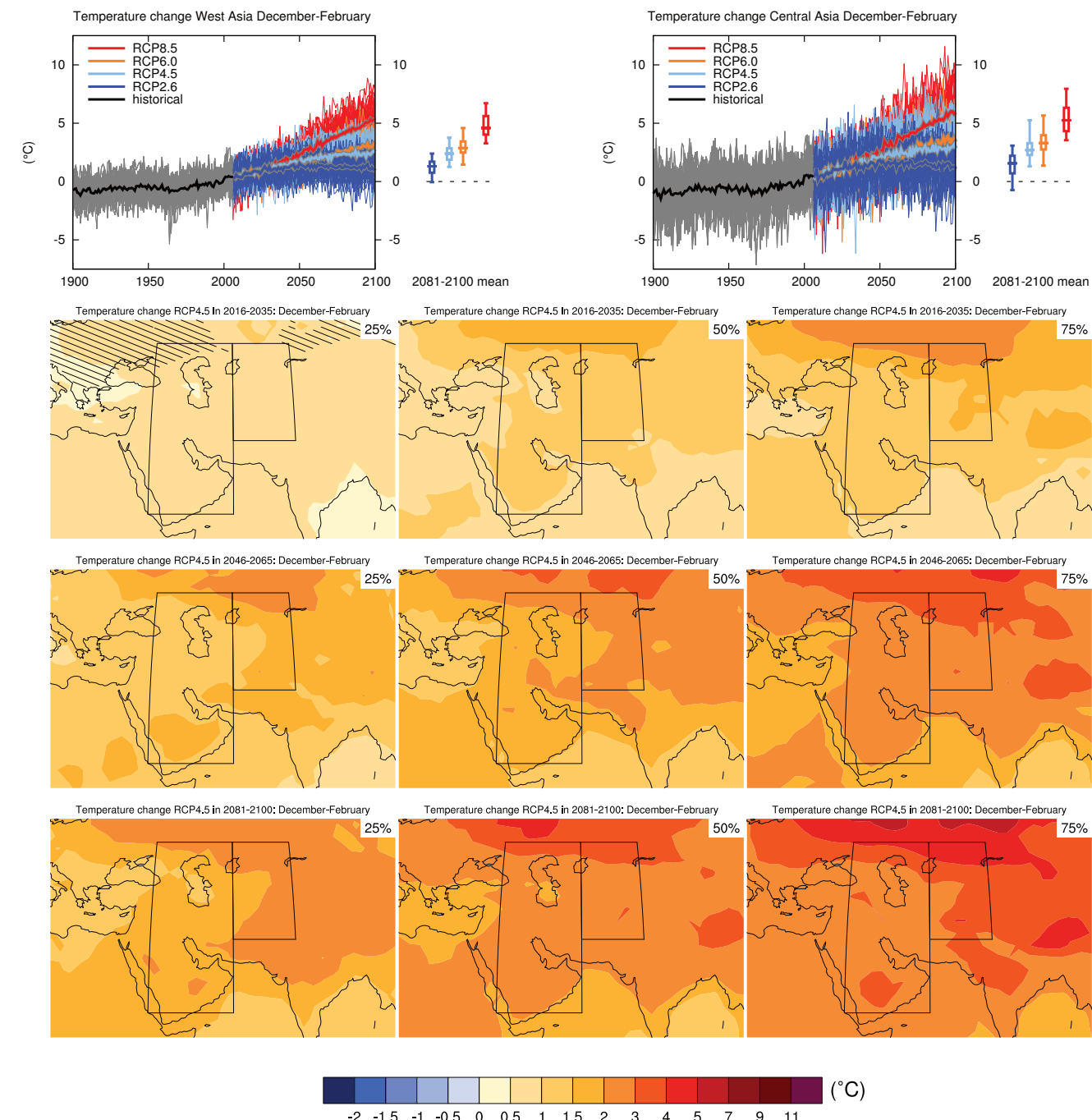


Figure A1.52 | (Top left) Time series of temperature change relative to 1986–2005 averaged over land grid points in West Asia (15°N to 50°N , 40°E to 60°E) in December to February. (Top right) Same for land grid points in Central Asia (30°N to 50°N , 60°E to 75°E). Thin lines denote one ensemble member per model, thick lines the CMIP5 multi-model mean. On the right-hand side the 5th, 25th, 50th (median), 75th and 95th percentiles of the distribution of 20-year mean changes are given for 2081–2100 in the four RCP scenarios.

(Below) Maps of temperature changes in 2016–2035, 2046–2065 and 2081–2100 with respect to 1986–2005 in the RCP4.5 scenario. For each point, the 25th, 50th and 75th percentiles of the distribution of the CMIP5 ensemble are shown; this includes both natural variability and inter-model spread. Hatching denotes areas where the 20-year mean differences of the percentiles are less than the standard deviation of model-estimated present-day natural variability of 20-year mean differences.

Sections 9.4.1.1, 9.6.1.1, 10.3.1.1.4, Box 11.2, 14.8.8, 14.8.10 contain relevant information regarding the evaluation of models in this region, the model spread in the context of other methods of projecting changes and the role of modes of variability and other climate phenomena.

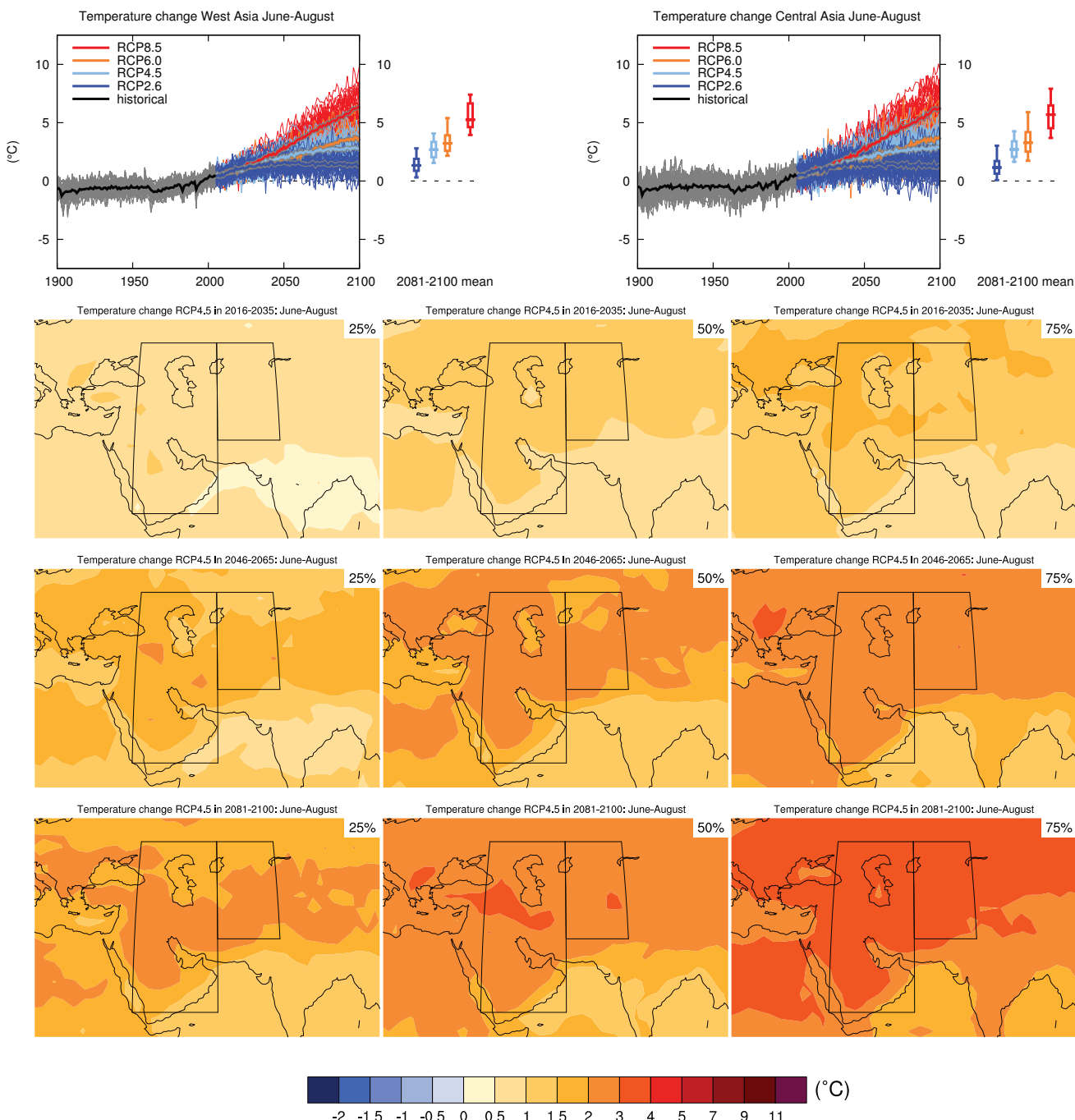


Figure AI.53 | (Top left) Time series of temperature change relative to 1986–2005 averaged over land grid points in West Asia (15°N to 50°N , 40°E to 60°E) in June to August. (Top right) Same for land grid points in Central Asia (30°N to 50°N , 60°E to 75°E). Thin lines denote one ensemble member per model, thick lines the CMIP5 multi-model mean. On the right-hand side the 5th, 25th, 50th (median), 75th and 95th percentiles of the distribution of 20-year mean changes are given for 2081–2100 in the four RCP scenarios.

(Below) Maps of temperature changes in 2016–2035, 2046–2065 and 2081–2100 with respect to 1986–2005 in the RCP4.5 scenario. For each point, the 25th, 50th and 75th percentiles of the distribution of the CMIP5 ensemble are shown; this includes both natural variability and inter-model spread. Hatching denotes areas where the 20-year mean differences of the percentiles are less than the standard deviation of model-estimated present-day natural variability of 20-year mean differences.

Sections 9.4.1.1, 9.6.1.1, 10.3.1.1.4, Box 11.2, 14.8.8, 14.8.10 contain relevant information regarding the evaluation of models in this region, the model spread in the context of other methods of projecting changes and the role of modes of variability and other climate phenomena.

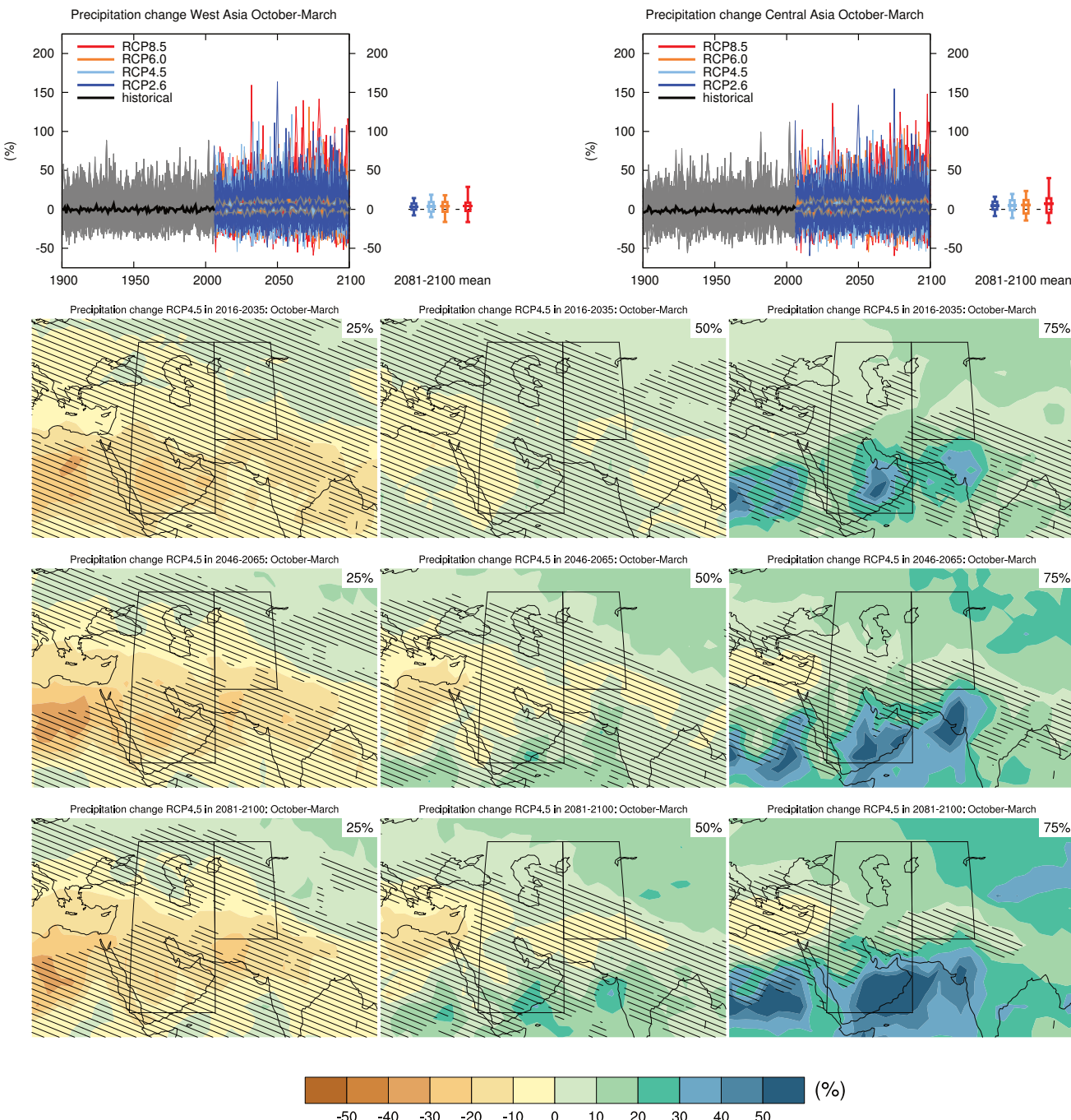


Figure AI.54 | (Top left) Time series of relative change relative to 1986–2005 in precipitation averaged over land grid points in West Asia (15°N to 50°N , 40°E to 60°E) in October to March. (Top right) Same for land grid points in Central Asia (30°N to 50°N , 60°E to 75°E). Thin lines denote one ensemble member per model, thick lines the CMIP5 multi-model mean. On the right-hand side the 5th, 25th, 50th (median), 75th and 95th percentiles of the distribution of 20-year mean changes are given for 2081–2100 in the four RCP scenarios.

(Below) Maps of precipitation changes in 2016–2035, 2046–2065 and 2081–2100 with respect to 1986–2005 in the RCP4.5 scenario. For each point, the 25th, 50th and 75th percentiles of the distribution of the CMIP5 ensemble are shown; this includes both natural variability and inter-model spread. Hatching denotes areas where the 20-year mean differences of the percentiles are less than the standard deviation of model-estimated present-day natural variability of 20-year mean differences.

Sections 9.4.1.1, 9.6.1.1, Box 11.2, 12.4.5.2, 14.8.8, 14.8.10 contain relevant information regarding the evaluation of models in this region, the model spread in the context of other methods of projecting changes and the role of modes of variability and other climate phenomena.

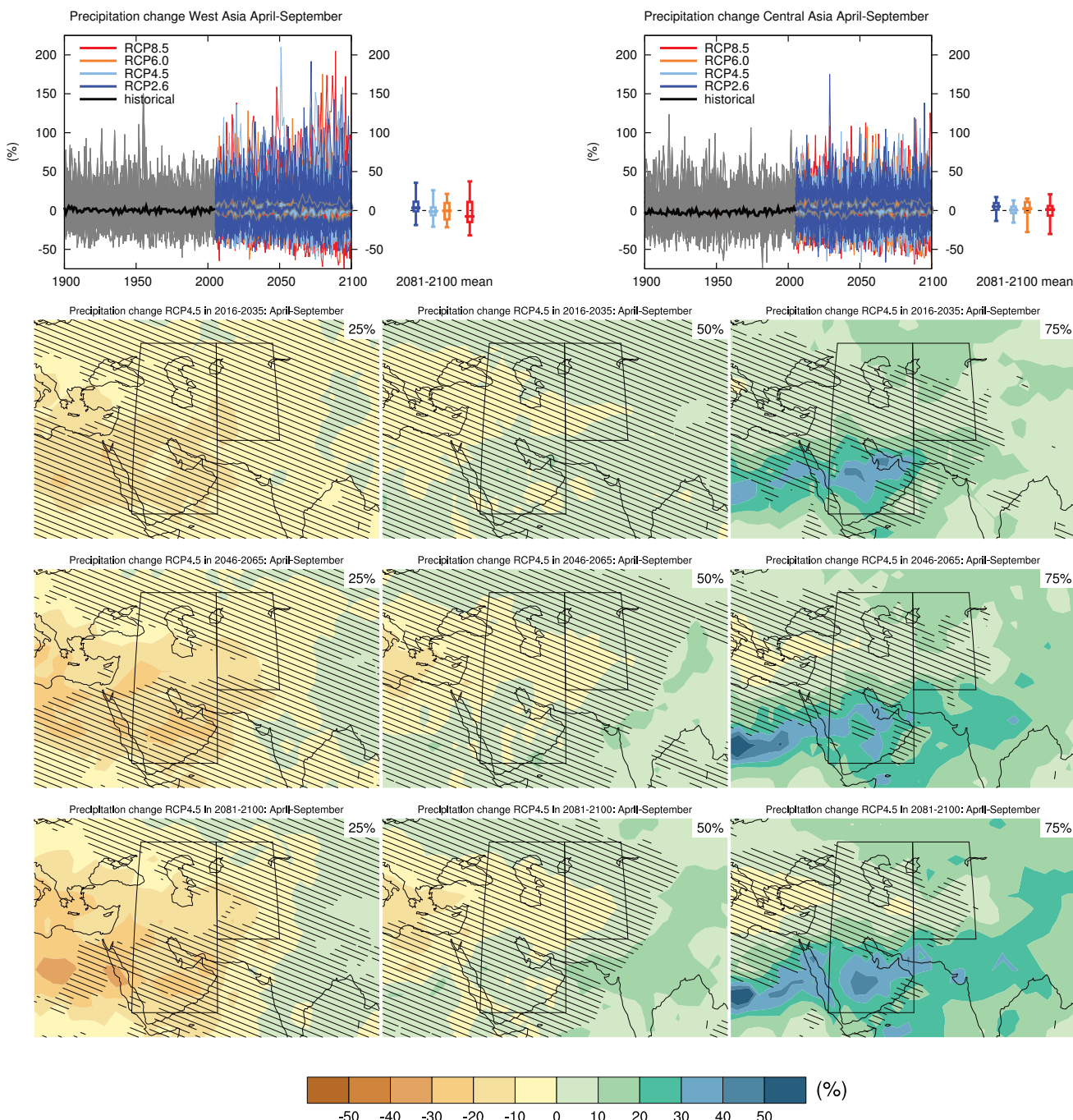


Figure A1.55 | (Top left) Time series of relative change relative to 1986–2005 in precipitation averaged over land grid points in West Asia (15°N to 50°N , 40°E to 60°E) in April to September. (Top right) Same for land grid points in Central Asia (30°N to 50°N , 60°E to 75°E). Thin lines denote one ensemble member per model, thick lines the CMIP5 multi-model mean. On the right-hand side the 5th, 25th, 50th (median), 75th and 95th percentiles of the distribution of 20-year mean changes are given for 2081–2100 in the four RCP scenarios.

(Below) Maps of precipitation changes in 2016–2035, 2046–2065 and 2081–2100 with respect to 1986–2005 in the RCP4.5 scenario. For each point, the 25th, 50th and 75th percentiles of the distribution of the CMIP5 ensemble are shown; this includes both natural variability and inter-model spread. Hatching denotes areas where the 20-year mean differences of the percentiles are less than the standard deviation of model-estimated present-day natural variability of 20-year mean differences.

Sections 9.4.1.1, 9.6.1.1, Box 11.2, 12.4.5.2, 14.8.8, 14.8.10 contain relevant information regarding the evaluation of models in this region, the model spread in the context of other methods of projecting changes and the role of modes of variability and other climate phenomena.

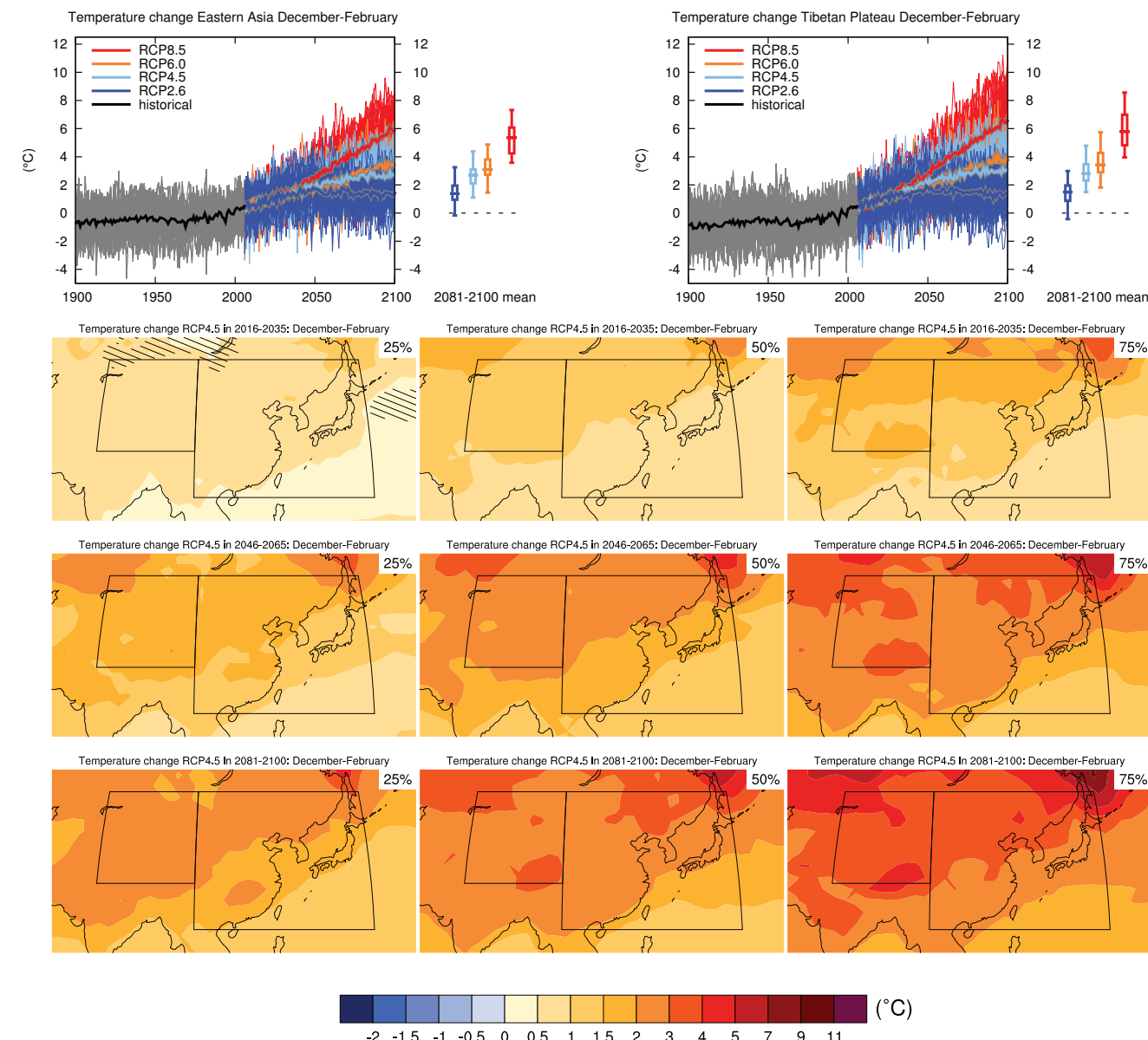


Figure AI.56 | (Top left) Time series of temperature change relative to 1986–2005 averaged over land grid points in Eastern Asia (20°N to 50°N , 100°E to 145°E) in December to February. (Top right) Same for land grid points on the Tibetan Plateau (30°N to 50°N , 75°E to 100°E). Thin lines denote one ensemble member per model, thick lines the CMIP5 multi-model mean. On the right-hand side the 5th, 25th, 50th (median), 75th and 95th percentiles of the distribution of 20-year mean changes are given for 2081–2100 in the four RCP scenarios.

(Below) Maps of temperature changes in 2016–2035, 2046–2065 and 2081–2100 with respect to 1986–2005 in the RCP4.5 scenario. For each point, the 25th, 50th and 75th percentiles of the distribution of the CMIP5 ensemble are shown; this includes both natural variability and inter-model spread. Hatching denotes areas where the 20-year mean differences of the percentiles are less than the standard deviation of model-estimated present-day natural variability of 20-year mean differences.

Sections 9.4.1.1, 9.6.1.1, 10.3.1.1.4, Box 11.2, 14.8.8, 14.8.9 contain relevant information regarding the evaluation of models in this region, the model spread in the context of other methods of projecting changes and the role of modes of variability and other climate phenomena.

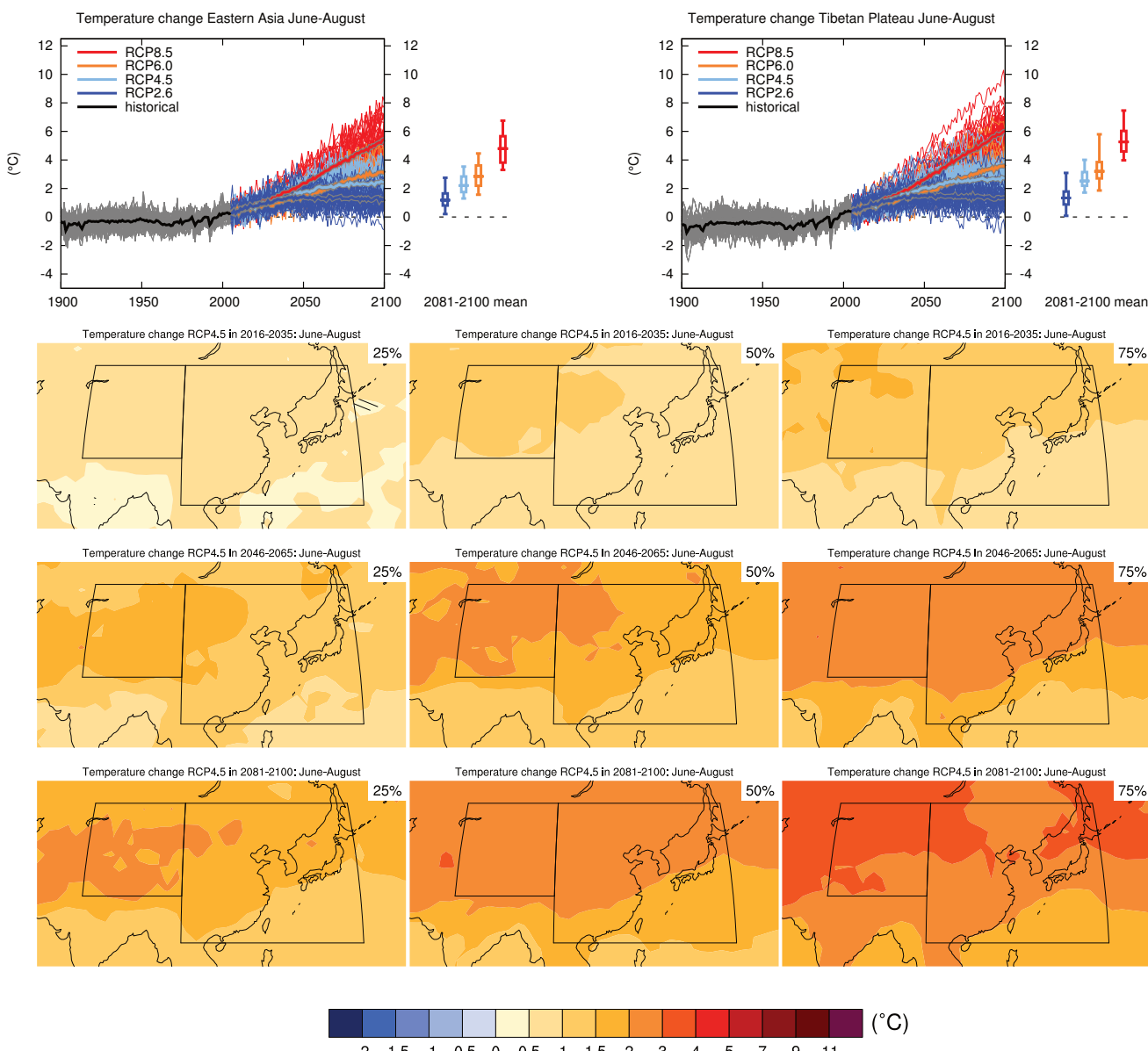


Figure AI.57 | (Top left) Time series of temperature change relative to 1986–2005 averaged over land grid points in Eastern Asia (20°N to 50°N , 100°E to 145°E) in June to August. (Top right) Same for land grid points on the Tibetan Plateau (30°N to 50°N , 75°E to 100°E). Thin lines denote one ensemble member per model, thick lines the CMIP5 multi-model mean. On the right-hand side the 5th, 25th, 50th (median), 75th and 95th percentiles of the distribution of 20-year mean changes are given for 2081–2100 in the four RCP scenarios.

(Below) Maps of temperature changes in 2016–2035, 2046–2065 and 2081–2100 with respect to 1986–2005 in the RCP4.5 scenario. For each point, the 25th, 50th and 75th percentiles of the distribution of the CMIP5 ensemble are shown; this includes both natural variability and inter-model spread. Hatching denotes areas where the 20-year mean differences of the percentiles are less than the standard deviation of model-estimated present-day natural variability of 20-year mean differences.

Sections 9.4.1.1, 9.6.1.1, 10.3.1.1.4, Box 11.2, 14.8.8, 14.8.9 contain relevant information regarding the evaluation of models in this region, the model spread in the context of other methods of projecting changes and the role of modes of variability and other climate phenomena.

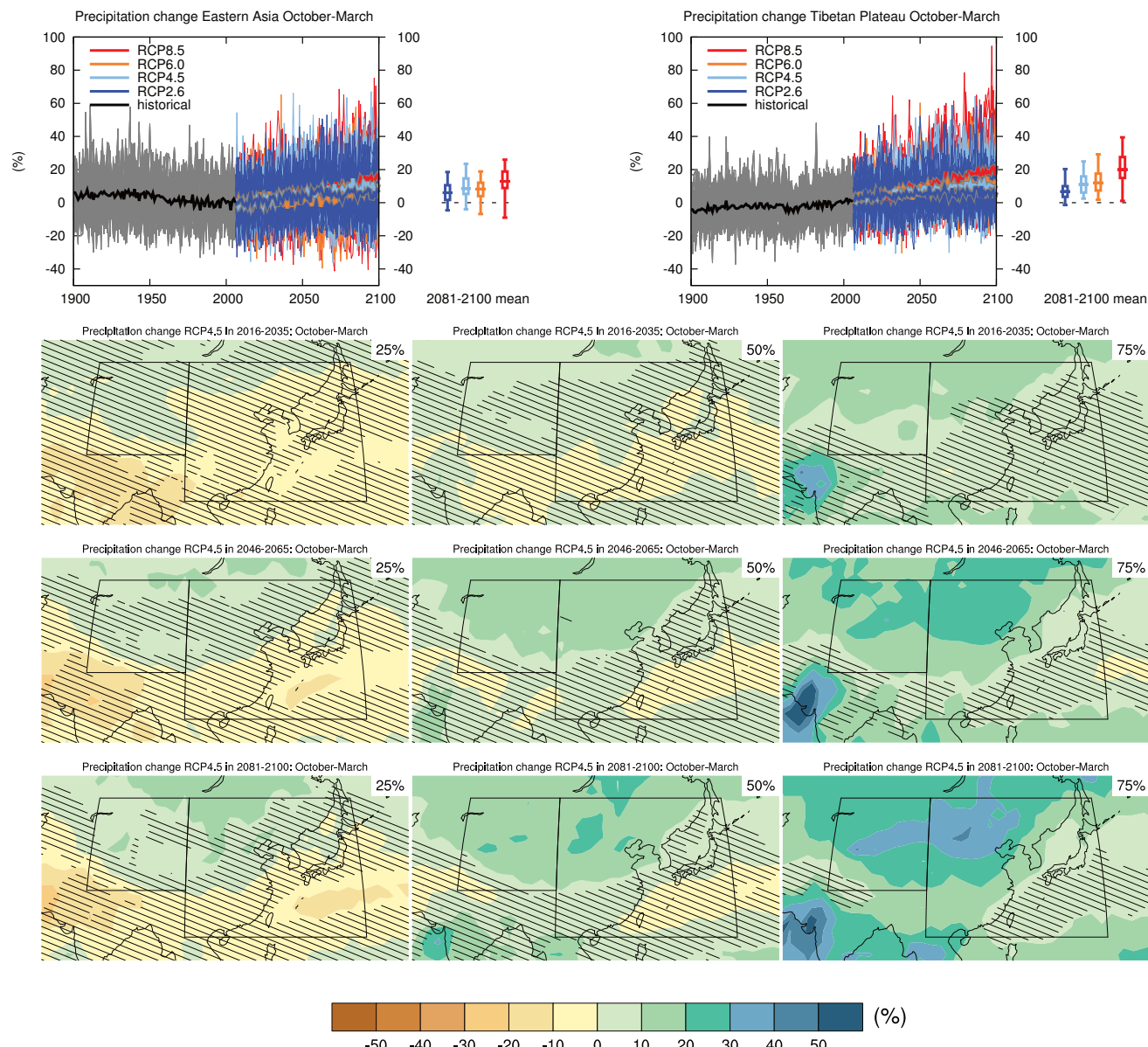


Figure AI.58 | (Top left) Time series of relative change relative to 1986–2005 in precipitation averaged over land grid points in Eastern Asia (20°N to 50°N , 100°E to 145°E) in October to March. (Top right) Same for land grid points on the Tibetan Plateau (30°N to 50°N , 75°E to 100°E). Thin lines denote one ensemble member per model, thick lines the CMIP5 multi-model mean. On the right-hand side the 5th, 25th, 50th (median), 75th and 95th percentiles of the distribution of 20-year mean changes are given for 2081–2100 in the four RCP scenarios.

(Below) Maps of precipitation changes in 2016–2035, 2046–2065 and 2081–2100 with respect to 1986–2005 in the RCP4.5 scenario. For each point, the 25th, 50th and 75th percentiles of the distribution of the CMIP5 ensemble are shown; this includes both natural variability and inter-model spread. Hatching denotes areas where the 20-year mean differences of the percentiles are less than the standard deviation of model-estimated present-day natural variability of 20-year mean differences.

Sections 9.4.1.1, 9.6.1.1, Box 11.2, 14.2.2.2, 14.8.8, 14.8.9 contain relevant information regarding the evaluation of models in this region, the model spread in the context of other methods of projecting changes and the role of modes of variability and other climate phenomena.

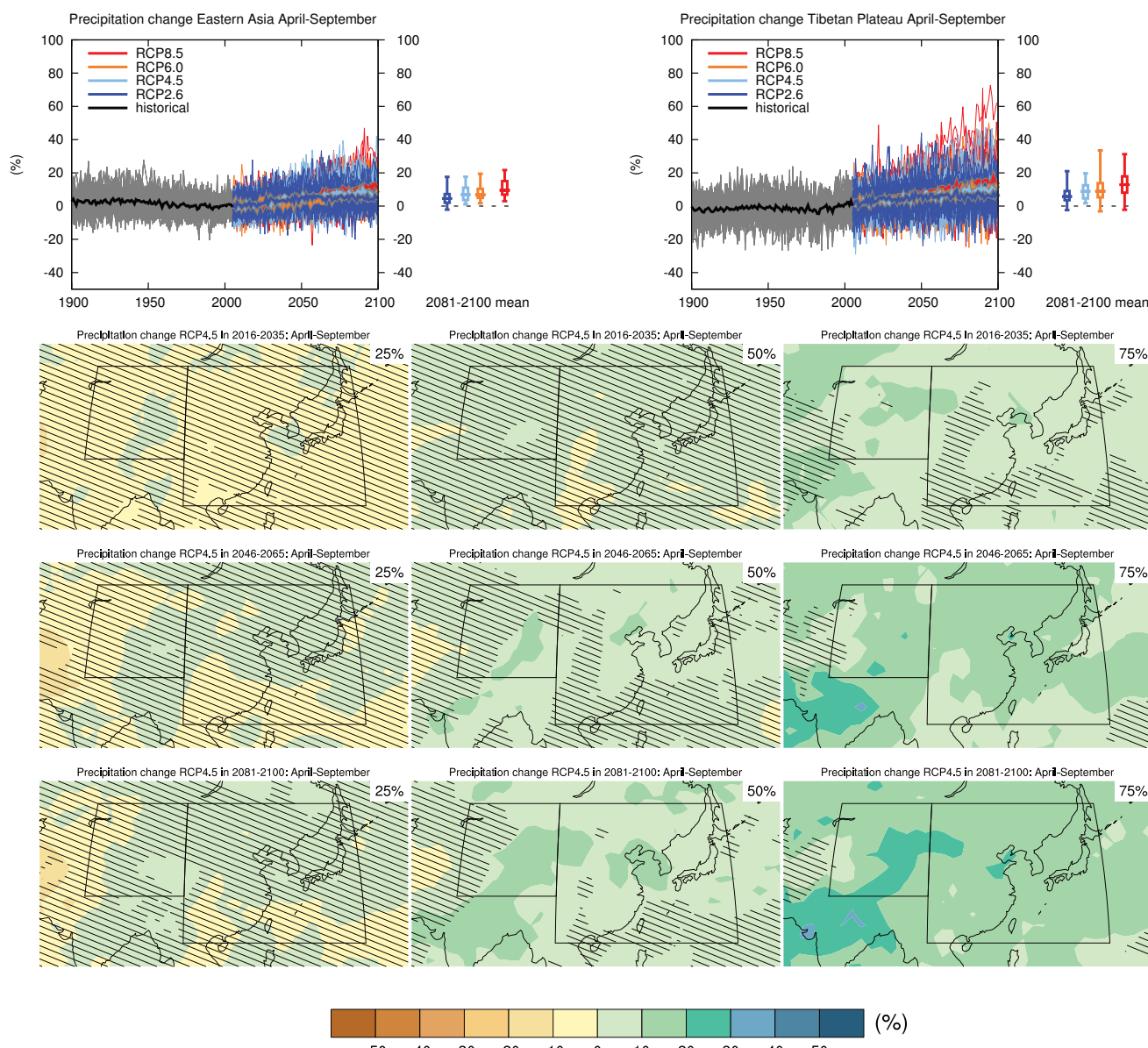


Figure AI.59 | (Top left) Time series of relative change relative to 1986–2005 in precipitation averaged over land grid points in Eastern Asia (20°N to 50°N , 100°E to 145°E) in April to September. (Top right) Same for land grid points on the Tibetan Plateau (30°N to 50°N , 75°E to 100°E). Thin lines denote one ensemble member per model, thick lines the CMIP5 multi-model mean. On the right-hand side the 5th, 25th, 50th (median), 75th and 95th percentiles of the distribution of 20-year mean changes are given for 2081–2100 in the four RCP scenarios.

(Below) Maps of precipitation changes in 2016–2035, 2046–2065 and 2081–2100 with respect to 1986–2005 in the RCP4.5 scenario. For each point, the 25th, 50th and 75th percentiles of the distribution of the CMIP5 ensemble are shown; this includes both natural variability and inter-model spread. Hatching denotes areas where the 20-year mean differences of the percentiles are less than the standard deviation of model-estimated present-day natural variability of 20-year mean differences.

Sections 9.4.1.1, 9.6.1.1, Box 11.2, 14.2.2.2, 14.8.8, 14.8.9 contain relevant information regarding the evaluation of models in this region, the model spread in the context of other methods of projecting changes and the role of modes of variability and other climate phenomena.

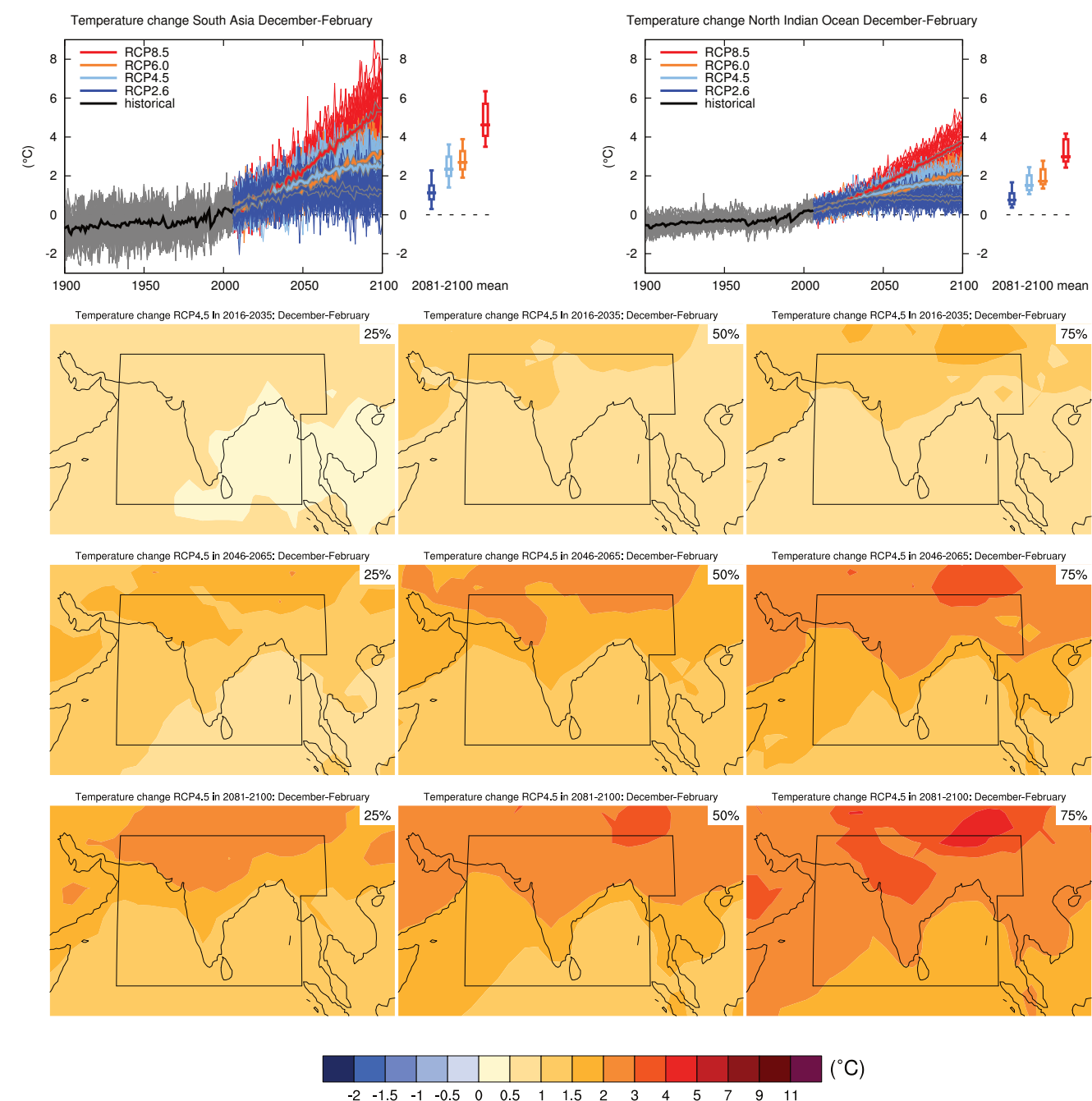


Figure AI.60 | (Top left) Time series of temperature change relative to 1986–2005 averaged over land grid points in South Asia (60°E , 5°N ; 60°E , 30°N ; 100°E , 30°N ; 100°E , 20°E ; 95°E , 20°N ; 95°E , 5°N) in December to February. (Top right) Same for sea grid points in the North Indian Ocean (5°N to 30°N , 60°E to 95°E). Thin lines denote one ensemble member per model, thick lines the CMIP5 multi-model mean. On the right-hand side the 5th, 25th, 50th (median), 75th and 95th percentiles of the distribution of 20-year mean changes are given for 2081–2100 in the four RCP scenarios.

(Below) Maps of temperature changes in 2016–2035, 2046–2065 and 2081–2100 with respect to 1986–2005 in the RCP4.5 scenario. For each point, the 25th, 50th and 75th percentiles of the distribution of the CMIP5 ensemble are shown; this includes both natural variability and inter-model spread. Hatching denotes areas where the 20-year mean differences of the percentiles are less than the standard deviation of model-estimated present-day natural variability of 20-year mean differences.

Sections 9.4.1.1, 9.6.1.1, 10.3.1.1.4, Box 11.2, 14.8.11 contain relevant information regarding the evaluation of models in this region, the model spread in the context of other methods of projecting changes and the role of modes of variability and other climate phenomena.

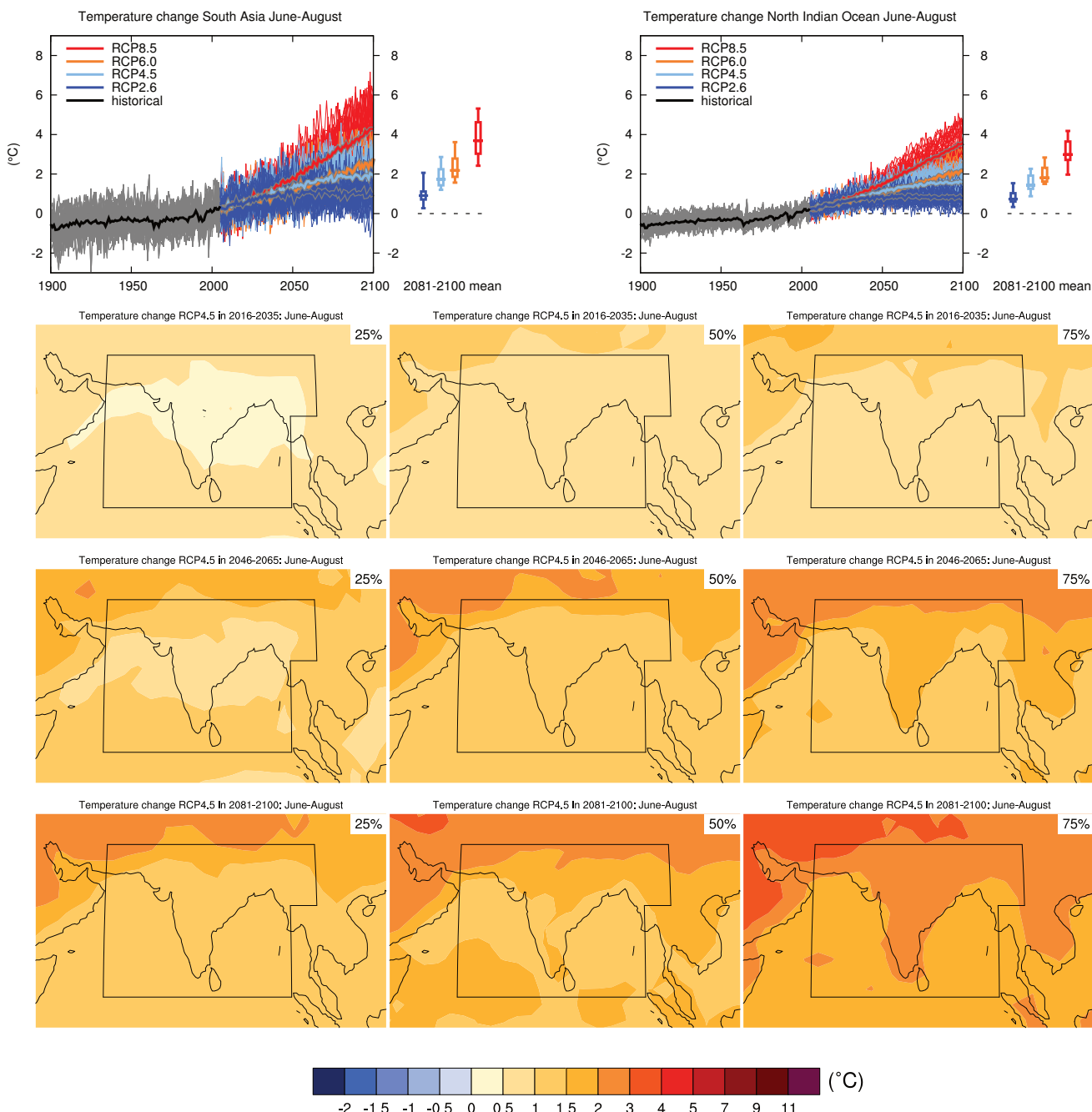


Figure AI.61 | (Top left) Time series of temperature change relative to 1986–2005 averaged over land grid points in South Asia ($60^{\circ}\text{E}, 5^{\circ}\text{N}$; $60^{\circ}\text{E}, 30^{\circ}\text{N}$; $100^{\circ}\text{E}, 30^{\circ}\text{N}$; $100^{\circ}\text{E}, 20^{\circ}\text{E}$; $95^{\circ}\text{E}, 20^{\circ}\text{N}$; $95^{\circ}\text{E}, 5^{\circ}\text{N}$) in June to August. (Top right) Same for sea grid points in the North Indian Ocean (5°N to 30°N , 60°E to 95°E). Thin lines denote one ensemble member per model, thick lines the CMIP5 multi-model mean. On the right-hand side the 5th, 25th, 50th (median), 75th and 95th percentiles of the distribution of 20-year mean changes are given for 2081–2100 in the four RCP scenarios.

(Below) Maps of temperature changes in 2016–2035, 2046–2065 and 2081–2100 with respect to 1986–2005 in the RCP4.5 scenario. For each point, the 25th, 50th and 75th percentiles of the distribution of the CMIP5 ensemble are shown; this includes both natural variability and inter-model spread. Hatching denotes areas where the 20-year mean differences of the percentiles are less than the standard deviation of model-estimated present-day natural variability of 20-year mean differences.

Sections 9.4.1.1, 9.6.1.1, 10.3.1.1.4, Box 11.2, 14.8.11 contain relevant information regarding the evaluation of models in this region, the model spread in the context of other methods of projecting changes and the role of modes of variability and other climate phenomena.

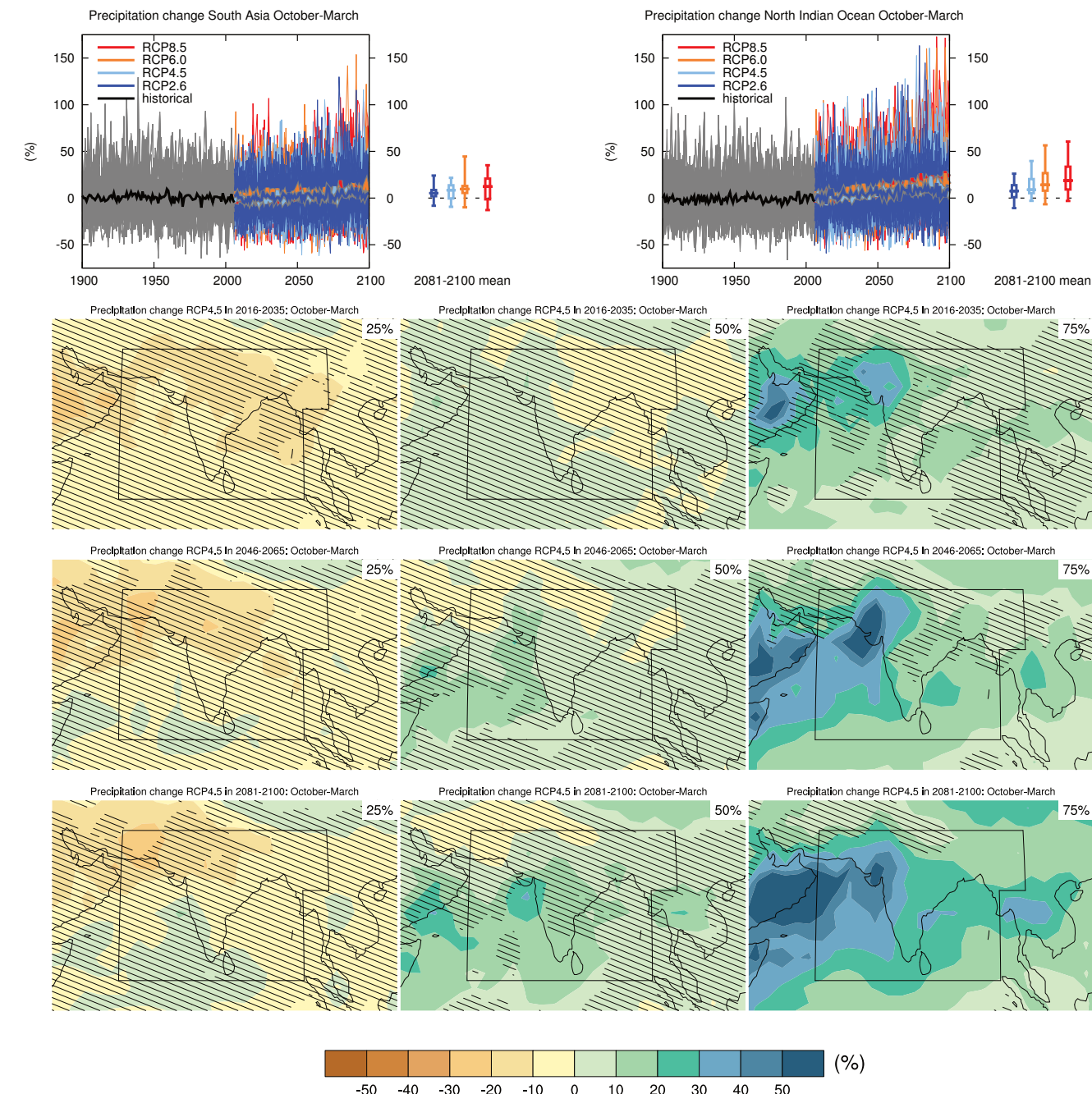


Figure AI.62 | (Top left) Time series of relative change relative to 1986–2005 in precipitation averaged over land grid points in South Asia (60°E , 5°N ; 60°E , 30°N ; 100°E , 30°N ; 100°E , 20°E ; 95°E , 20°N ; 95°E , 5°N) in October to March. (Top right) Same for sea grid points in the North Indian Ocean (5°N to 30°N , 60°E to 95°E). Thin lines denote one ensemble member per model, thick lines the CMIP5 multi-model mean. On the right-hand side the 5th, 25th, 50th (median), 75th and 95th percentiles of the distribution of 20-year mean changes are given for 2081–2100 in the four RCP scenarios.

(Below) Maps of precipitation changes in 2016–2035, 2046–2065 and 2081–2100 with respect to 1986–2005 in the RCP4.5 scenario. For each point, the 25th, 50th and 75th percentiles of the distribution of the CMIP5 ensemble are shown; this includes both natural variability and inter-model spread. Hatching denotes areas where the 20-year mean differences of the percentiles are less than the standard deviation of model-estimated present-day natural variability of 20-year mean differences.

Sections 9.4.1.1, 9.6.1.1, Box 11.2, 14.2.2.1, 14.8.11 contain relevant information regarding the evaluation of models in this region, the model spread in the context of other methods of projecting changes and the role of modes of variability and other climate phenomena.

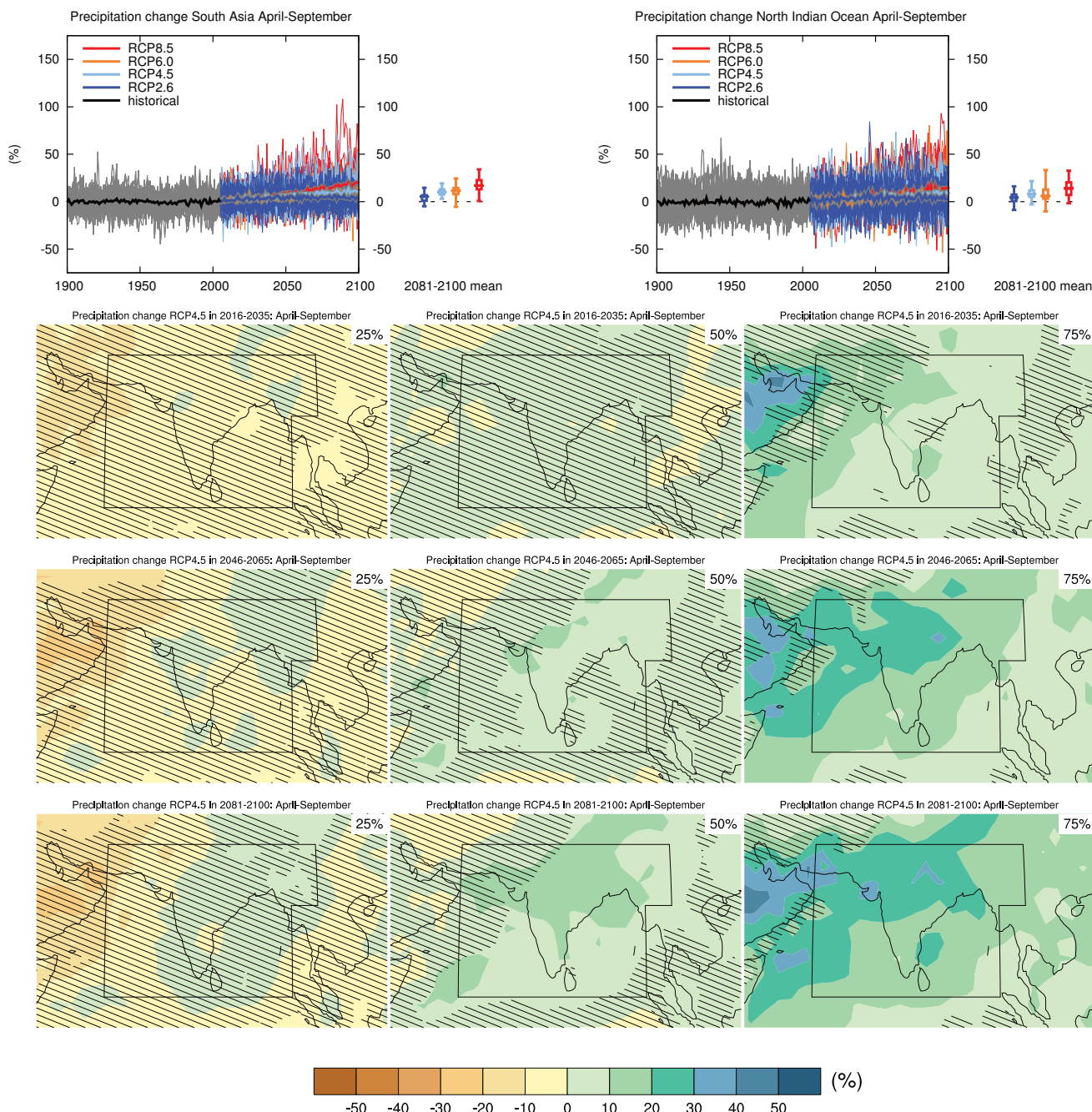


Figure AI.63 | (Top left) Time series of relative change relative to 1986–2005 in precipitation averaged over land grid points in South Asia ($60^{\circ}\text{E}, 5^{\circ}\text{N}$; $60^{\circ}\text{E}, 30^{\circ}\text{N}$; $100^{\circ}\text{E}, 30^{\circ}\text{N}$; $100^{\circ}\text{E}, 20^{\circ}\text{E}$; $95^{\circ}\text{E}, 20^{\circ}\text{N}$; $95^{\circ}\text{E}, 5^{\circ}\text{N}$) in April to September. (Top right) Same for sea grid points in the North Indian Ocean (5°N to 30°N , 60°E to 95°E). Thin lines denote one ensemble member per model, thick lines the CMIP5 multi-model mean. On the right-hand side the 5th, 25th, 50th (median), 75th and 95th percentiles of the distribution of 20-year mean changes are given for 2081–2100 in the four RCP scenarios.

(Below) Maps of precipitation changes in 2016–2035, 2046–2065 and 2081–2100 with respect to 1986–2005 in the RCP4.5 scenario. For each point, the 25th, 50th and 75th percentiles of the distribution of the CMIP5 ensemble are shown; this includes both natural variability and inter-model spread. Hatching denotes areas where the 20-year mean differences of the percentiles are less than the standard deviation of model-estimated present-day natural variability of 20-year mean differences.

Sections 9.4.1.1, 9.6.1.1, Box 11.2, 14.2.2.1, 14.8.11 contain relevant information regarding the evaluation of models in this region, the model spread in the context of other methods of projecting changes and the role of modes of variability and other climate phenomena.

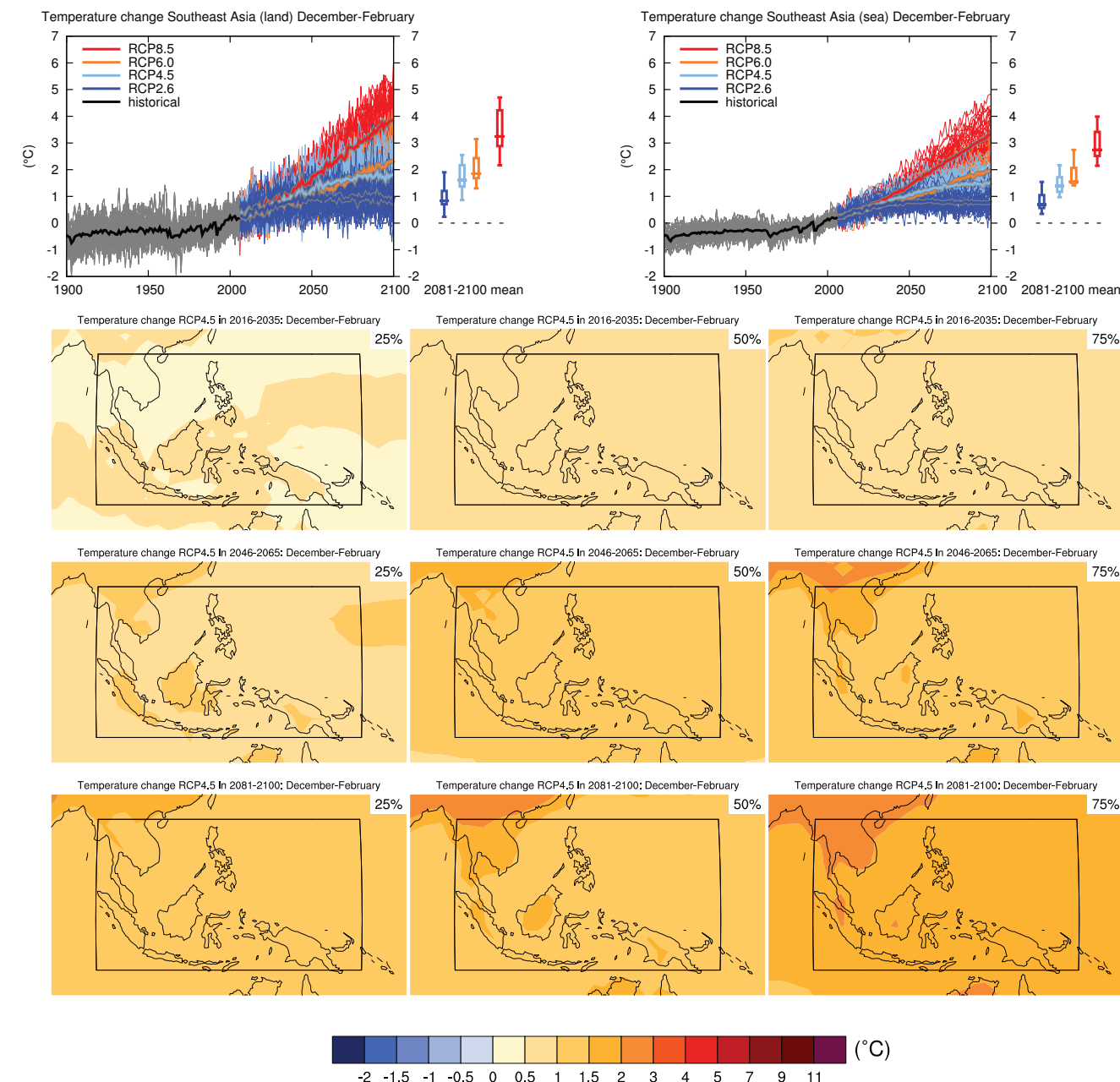


Figure AI.64 | (Top left) Time series of temperature change relative to 1986–2005 averaged over land grid points in Southeast Asia (10°S to 20°N , 95°E to 155°E) in December to February. (Top right) Same for sea grid points. Thin lines denote one ensemble member per model, thick lines the CMIP5 multi-model mean. On the right-hand side the 5th, 25th, 50th (median), 75th and 95th percentiles of the distribution of 20-year mean changes are given for 2081–2100 in the four RCP scenarios.

(Below) Maps of temperature changes in 2016–2035, 2046–2065 and 2081–2100 with respect to 1986–2005 in the RCP4.5 scenario. For each point, the 25th, 50th and 75th percentiles of the distribution of the CMIP5 ensemble are shown; this includes both natural variability and inter-model spread. Hatching denotes areas where the 20-year mean differences of the percentiles are less than the standard deviation of model-estimated present-day natural variability of 20-year mean differences.

Sections 9.4.1.1, 9.6.1.1, 10.3.1.1.4, Box 11.2, 14.8.12 contain relevant information regarding the evaluation of models in this region, the model spread in the context of other methods of projecting changes and the role of modes of variability and other climate phenomena.

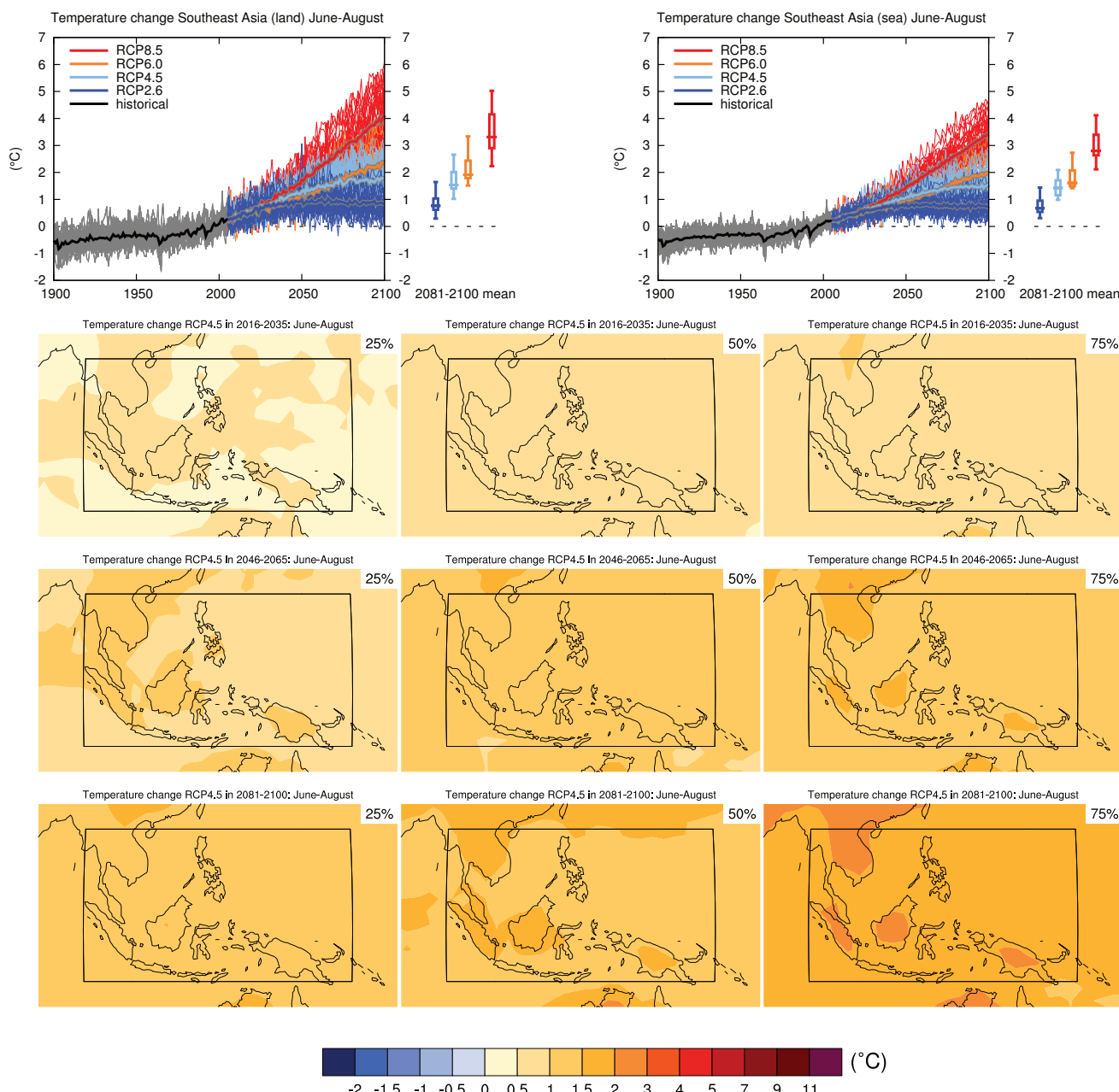


Figure AI.65 | (Top left) Time series of temperature change relative to 1986–2005 averaged over land grid points in Southeast Asia (10°N to 20°N , 95°E to 155°E) in June to August. (Top right) Same for sea grid points. Thin lines denote one ensemble member per model, thick lines the CMIP5 multi-model mean. On the right-hand side the 5th, 25th, 50th (median), 75th and 95th percentiles of the distribution of 20-year mean changes are given for 2081–2100 in the four RCP scenarios.

(Below) Maps of temperature changes in 2016–2035, 2046–2065 and 2081–2100 with respect to 1986–2005 in the RCP4.5 scenario. For each point, the 25th, 50th and 75th percentiles of the distribution of the CMIP5 ensemble are shown; this includes both natural variability and inter-model spread. Hatching denotes areas where the 20-year mean differences of the percentiles are less than the standard deviation of model-estimated present-day natural variability of 20-year mean differences.

Sections 9.4.1.1, 9.6.1.1, 10.3.1.1.4, Box 11.2, 14.8.12 contain relevant information regarding the evaluation of models in this region, the model spread in the context of other methods of projecting changes and the role of modes of variability and other climate phenomena.

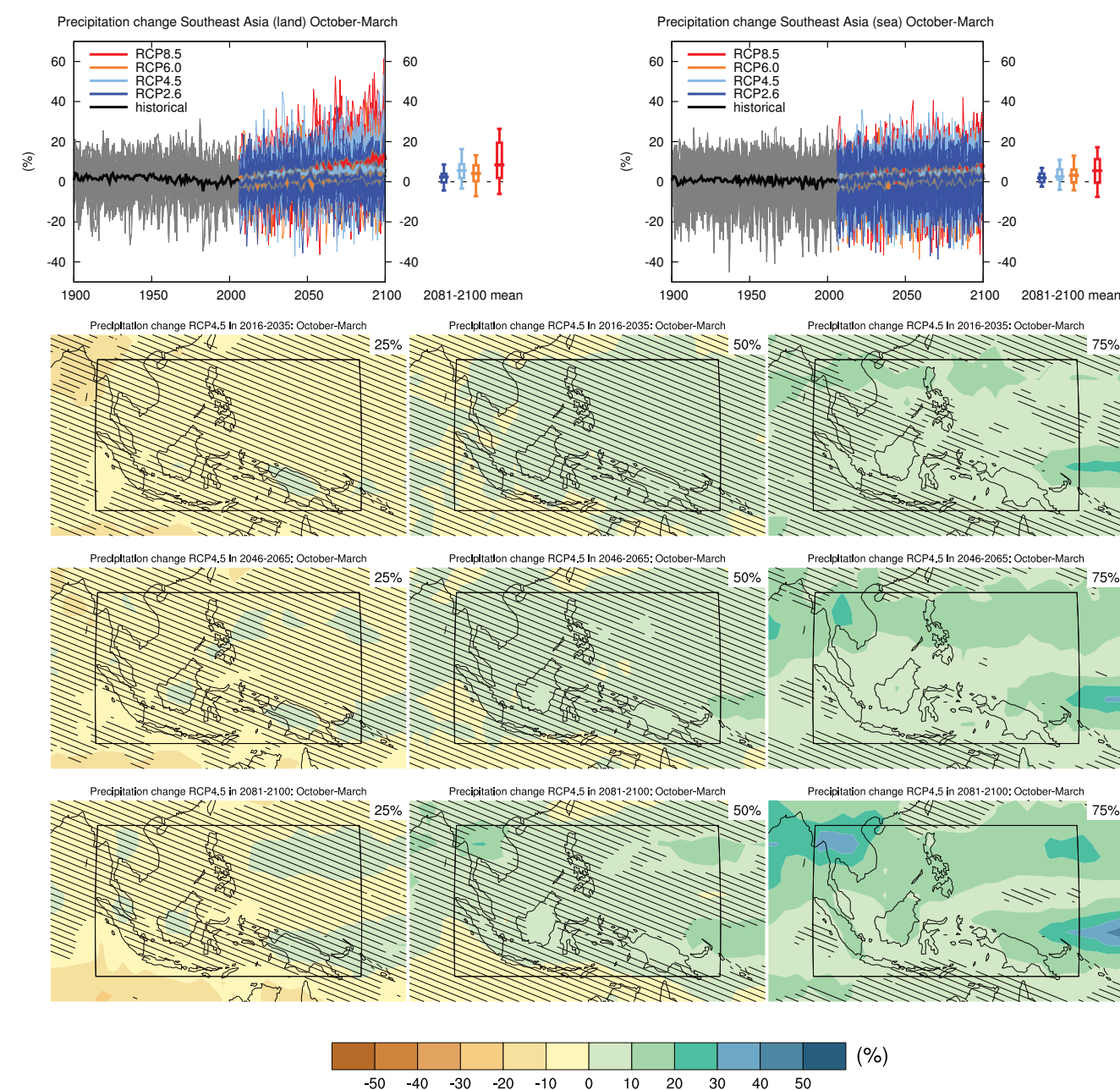


Figure AI.66 | (Top left) Time series of relative change relative to 1986–2005 in precipitation averaged over land grid points in Southeast Asia (10°S to 20°N , 95°E to 155°E) in October to March. (Top right) Same for sea grid points. Thin lines denote one ensemble member per model, thick lines the CMIP5 multi-model mean. On the right-hand side the 5th, 25th, 50th (median), 75th and 95th percentiles of the distribution of 20-year mean changes are given for 2081–2100 in the four RCP scenarios.

(Below) Maps of precipitation changes in 2016–2035, 2046–2065 and 2081–2100 with respect to 1986–2005 in the RCP4.5 scenario. For each point, the 25th, 50th and 75th percentiles of the distribution of the CMIP5 ensemble are shown; this includes both natural variability and inter-model spread. Hatching denotes areas where the 20-year mean differences of the percentiles are less than the standard deviation of model-estimated present-day natural variability of 20-year mean differences.

Sections 9.4.1.1, 9.6.1.1, Box 11.2, 14.2.2.3, 14.2.2.5, 14.8.12 contain relevant information regarding the evaluation of models in this region, the model spread in the context of other methods of projecting changes and the role of modes of variability and other climate phenomena.

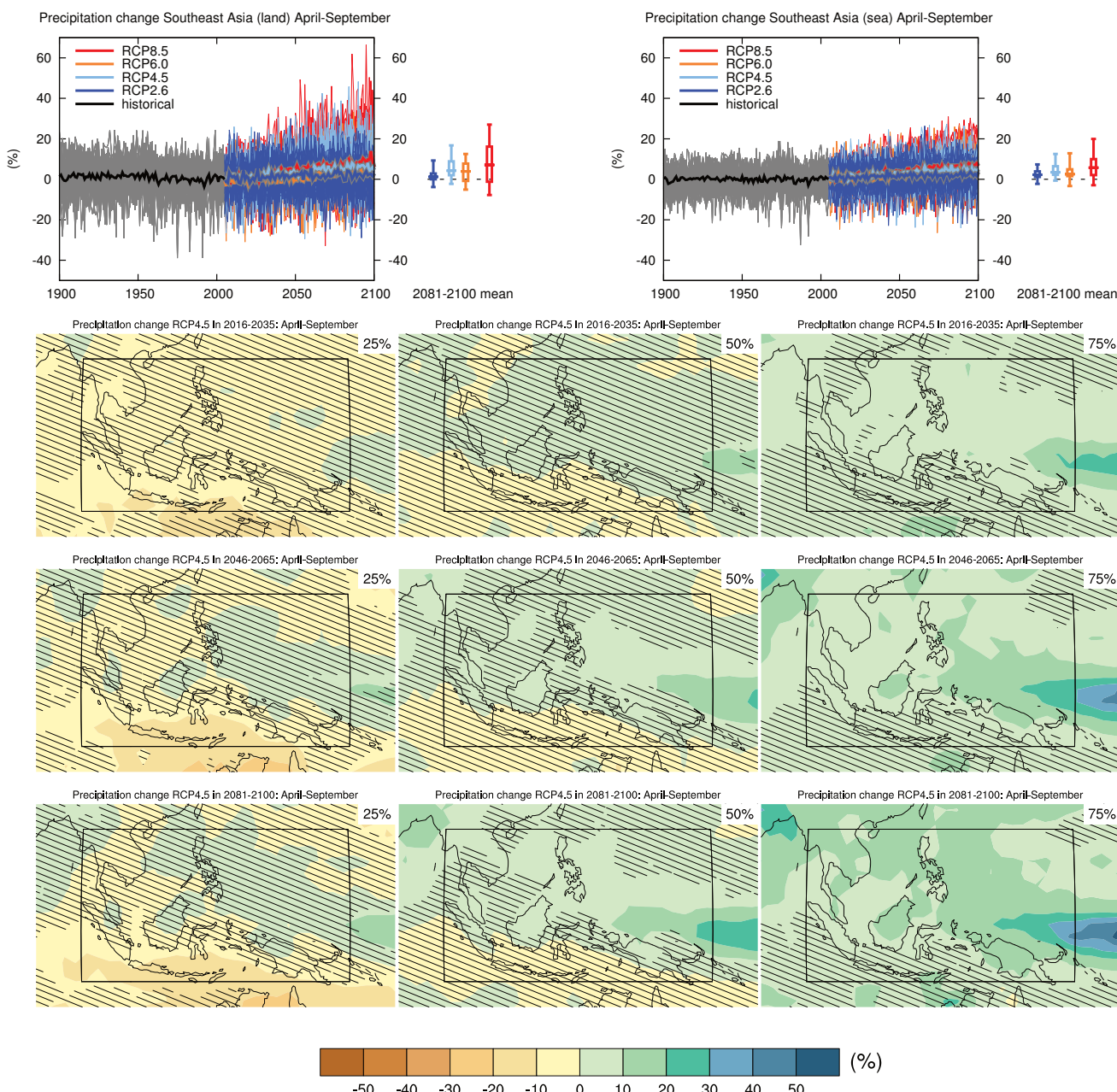


Figure AI.67 | (Top left) Time series of relative change relative to 1986–2005 in precipitation averaged over land grid points in Southeast Asia (10°S to 20°N , 95°E to 155°E) in April to September. (Top right) Same for sea grid points. Thin lines denote one ensemble member per model, thick lines the CMIP5 multi-model mean. On the right-hand side the 5th, 25th, 50th (median), 75th and 95th percentiles of the distribution of 20-year mean changes are given for 2081–2100 in the four RCP scenarios.

(Below) Maps of precipitation changes in 2016–2035, 2046–2065 and 2081–2100 with respect to 1986–2005 in the RCP4.5 scenario. For each point, the 25th, 50th and 75th percentiles of the distribution of the CMIP5 ensemble are shown; this includes both natural variability and inter-model spread. Hatching denotes areas where the 20-year mean differences of the percentiles are less than the standard deviation of model-estimated present-day natural variability of 20-year mean differences.

Sections 9.4.1.1, 9.6.1.1, Box 11.2, 14.2.2.3, 14.2.2.5, 14.8.12 contain relevant information regarding the evaluation of models in this region, the model spread in the context of other methods of projecting changes and the role of modes of variability and other climate phenomena.

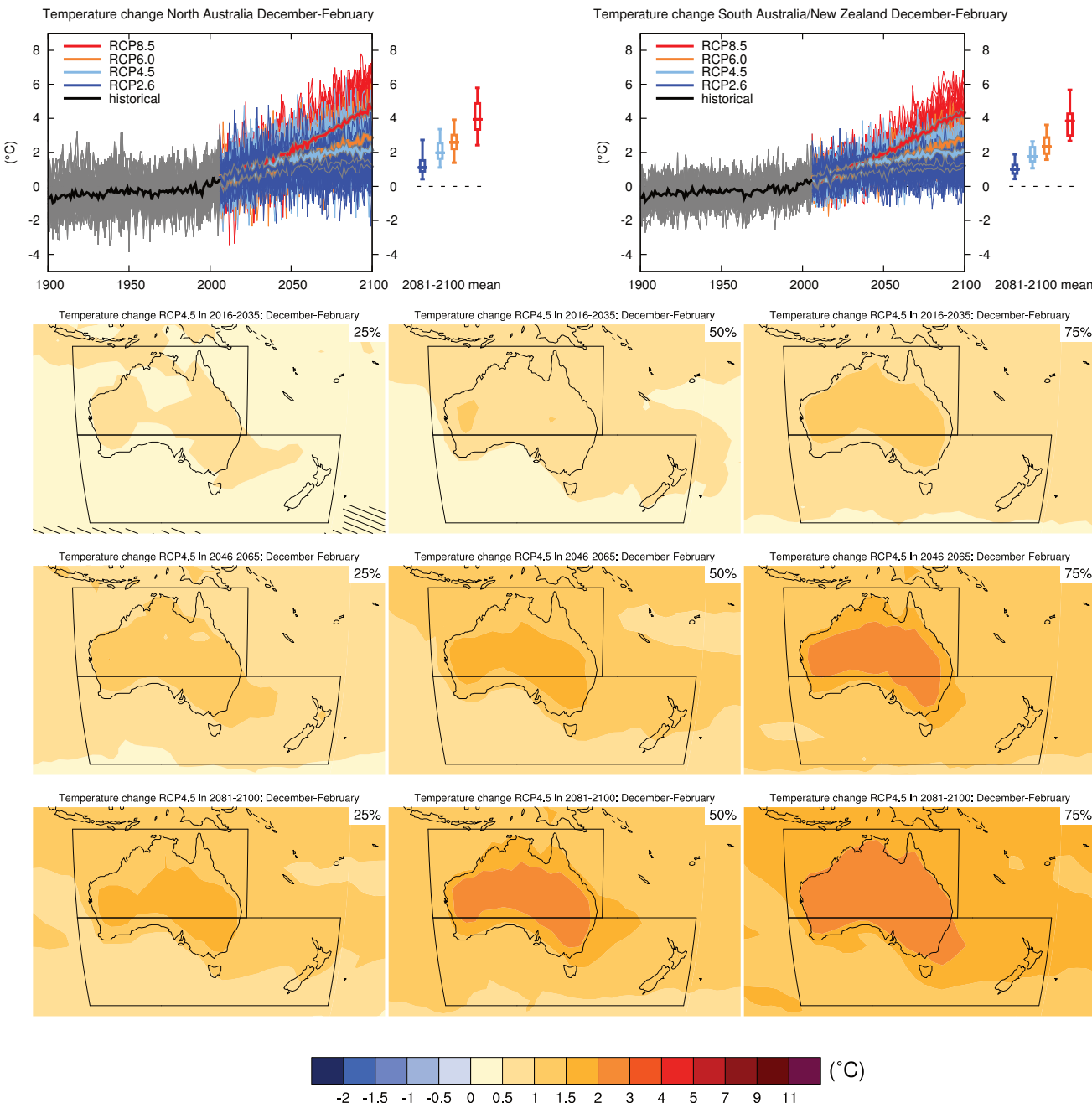


Figure AI.68 | (Top left) Time series of temperature change relative to 1986–2005 averaged over land grid points in North Australia (30°S to 10°S , 110°E to 155°E) in December to February. (Top right) Same for land grid points in South Australia/New Zealand (50°S to 30°S , 110°E to 180°E). Thin lines denote one ensemble member per model, thick lines the CMIP5 multi-model mean. On the right-hand side the 5th, 25th, 50th (median), 75th and 95th percentiles of the distribution of 20-year mean changes are given for 2081–2100 in the four RCP scenarios.

(Below) Maps of temperature changes in 2016–2035, 2046–2065 and 2081–2100 with respect to 1986–2005 in the RCP4.5 scenario. For each point, the 25th, 50th and 75th percentiles of the distribution of the CMIP5 ensemble are shown; this includes both natural variability and inter-model spread. Hatching denotes areas where the 20-year mean differences of the percentiles are less than the standard deviation of model-estimated present-day natural variability of 20-year mean differences.

Sections 9.4.1.1, 9.6.1.1, 10.3.1.1.4, Box 11.2, 14.8.13 contain relevant information regarding the evaluation of models in this region, the model spread in the context of other methods of projecting changes and the role of modes of variability and other climate phenomena.

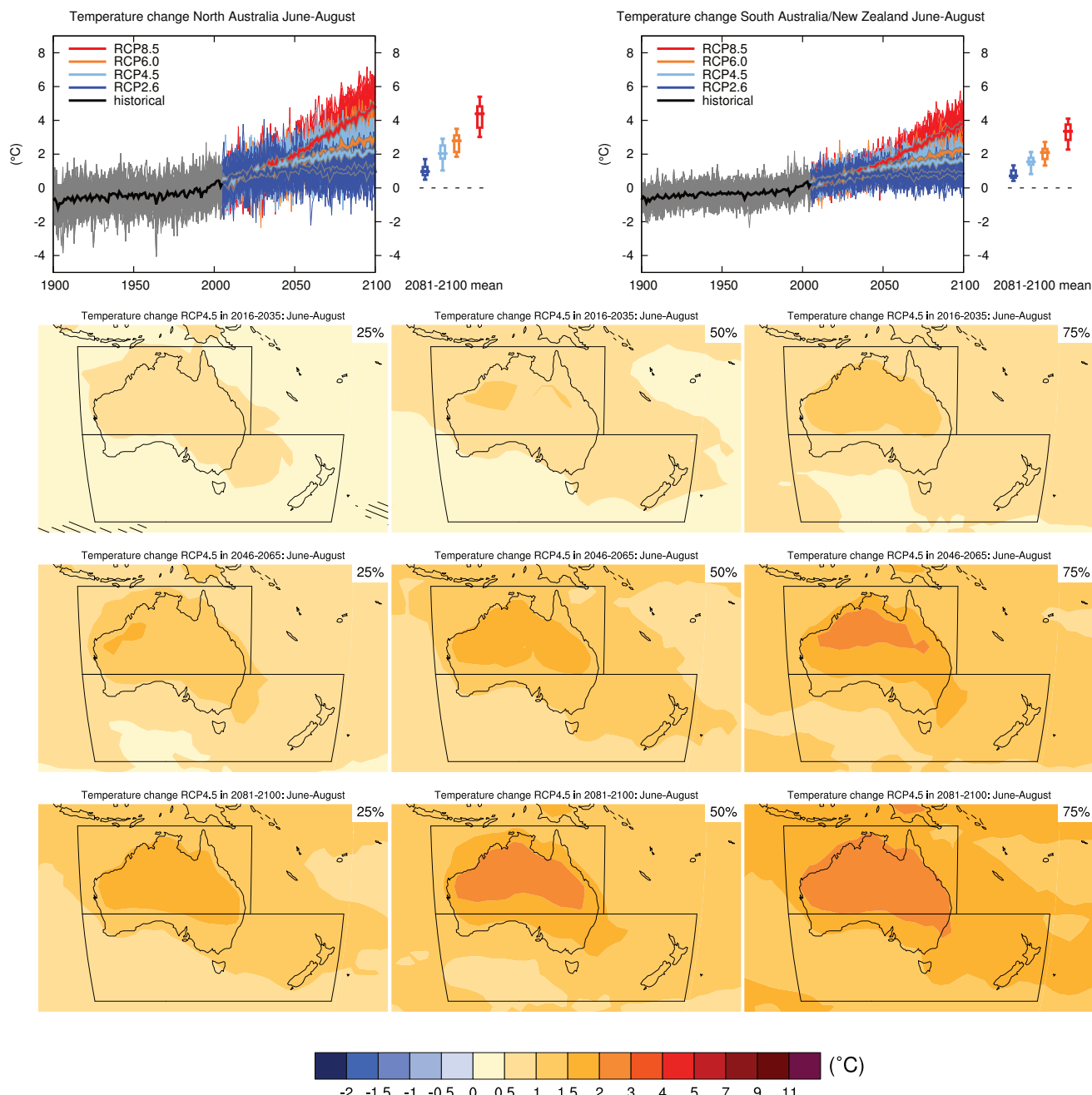


Figure Al.69 | (Top left) Time series of temperature change relative to 1986–2005 averaged over land grid points in North Australia (30°S to 10°S , 110°E to 155°E) in June to August. (Top right) Same for land grid points in South Australia/New Zealand (50°S to 30°S , 110°E to 180°E). Thin lines denote one ensemble member per model, thick lines the CMIP5 multi-model mean. On the right-hand side the 5th, 25th, 50th (median), 75th and 95th percentiles of the distribution of 20-year mean changes are given for 2081–2100 in the four RCP scenarios.

(Below) Maps of temperature changes in 2016–2035, 2046–2065 and 2081–2100 with respect to 1986–2005 in the RCP4.5 scenario. For each point, the 25th, 50th and 75th percentiles of the distribution of the CMIP5 ensemble are shown; this includes both natural variability and inter-model spread. Hatching denotes areas where the 20-year mean differences of the percentiles are less than the standard deviation of model-estimated present-day natural variability of 20-year mean differences.

Sections 9.4.1.1, 9.6.1.1, 10.3.1.1.4, Box 11.2, 14.8.13 contain relevant information regarding the evaluation of models in this region, the model spread in the context of other methods of projecting changes and the role of modes of variability and other climate phenomena.

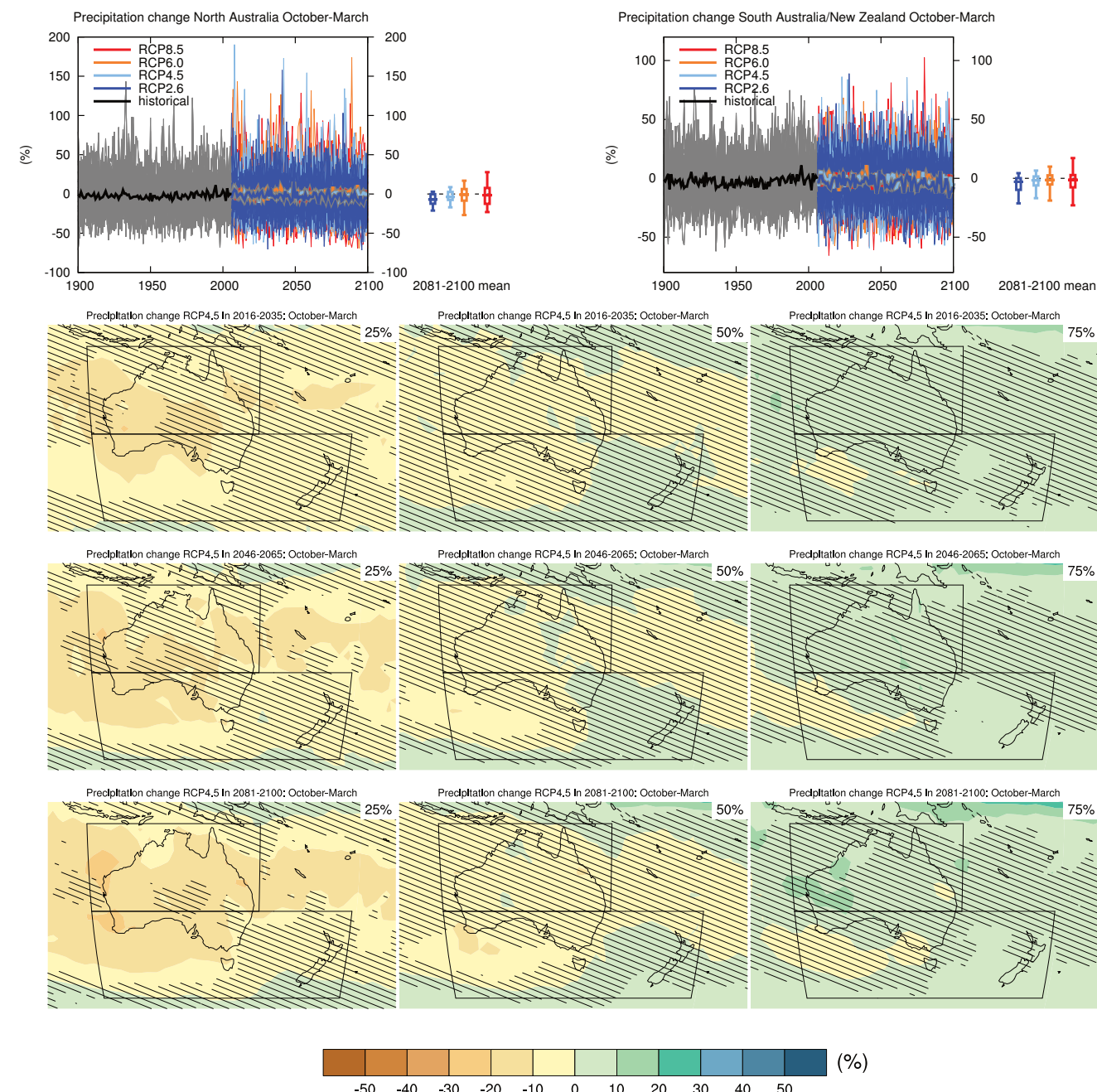


Figure AI.70 | (Top left) Time series of relative change relative to 1986–2005 in precipitation averaged over land grid points in North Australia (30°S to 10°S , 110°E to 155°E) in October to March. (Top right) Same for land grid points in South Australia/New Zealand (50°S to 30°S , 110°E to 180°E). Thin lines denote one ensemble member per model, thick lines the CMIP5 multi-model mean. On the right-hand side the 5th, 25th, 50th (median), 75th and 95th percentiles of the distribution of 20-year mean changes are given for 2081–2100 in the four RCP scenarios. Note different scales.

(Below) Maps of precipitation changes in 2016–2035, 2046–2065 and 2081–2100 with respect to 1986–2005 in the RCP4.5 scenario. For each point, the 25th, 50th and 75th percentiles of the distribution of the CMIP5 ensemble are shown; this includes both natural variability and inter-model spread. Hatching denotes areas where the 20-year mean differences of the percentiles are less than the standard deviation of model-estimated present-day natural variability of 20-year mean differences.

Sections 9.4.1.1, 9.6.1.1, Box 11.2, 14.2.2.4, 14.8.13 contain relevant information regarding the evaluation of models in this region, the model spread in the context of other methods of projecting changes and the role of modes of variability and other climate phenomena.

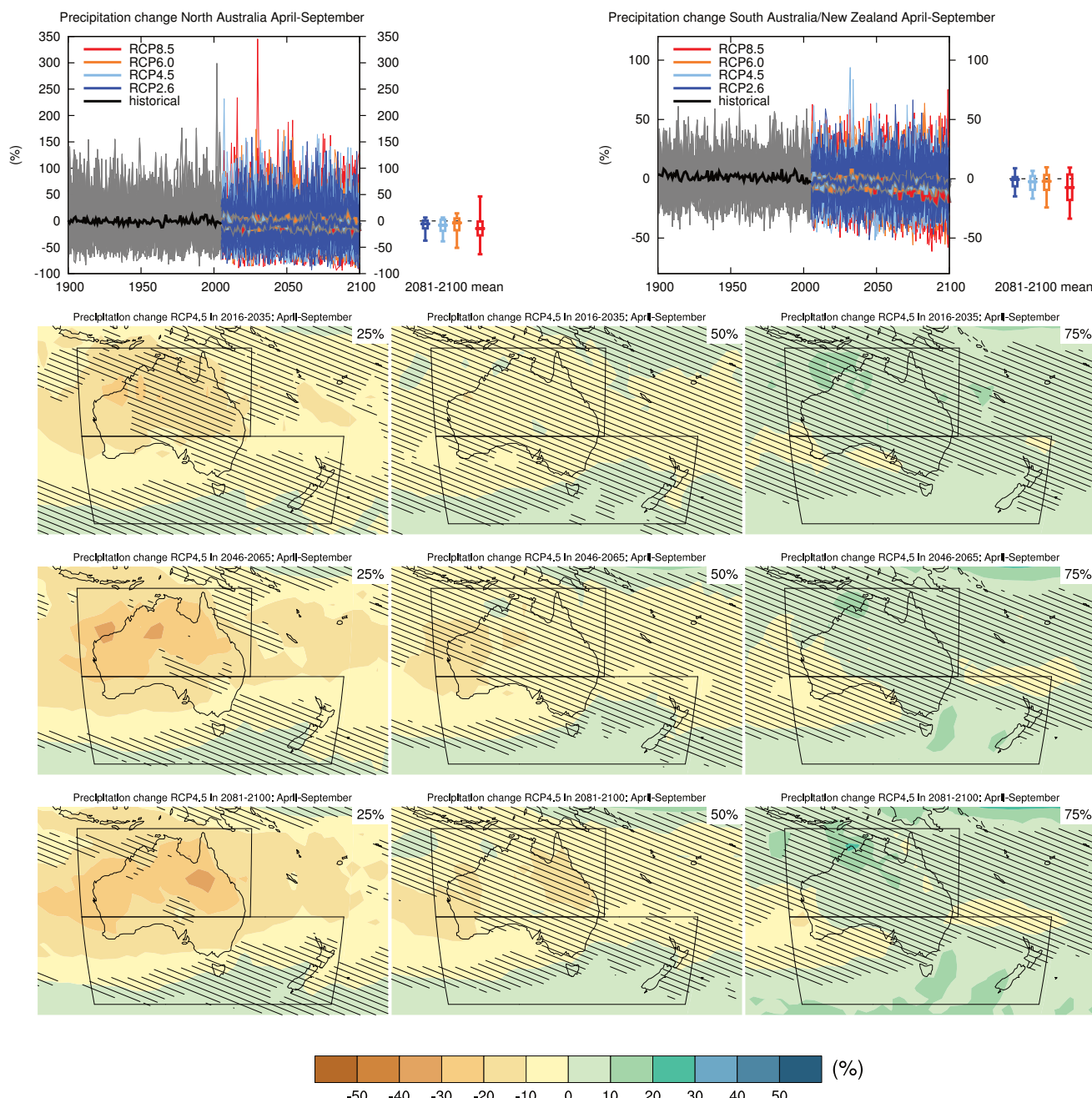


Figure AI.71 | (Top left) Time series of relative change relative to 1986–2005 in precipitation averaged over land grid points in North Australia (30°S to 10°S , 110°E to 155°E) in April to September. (Top right) Same for land grid points in South Australia/New Zealand (50°S to 30°S , 110°E to 180°E). Thin lines denote one ensemble member per model, thick lines the CMIP5 multi-model mean. On the right-hand side the 5th, 25th, 50th (median), 75th and 95th percentiles of the distribution of 20-year mean changes are given for 2081–2100 in the four RCP scenarios. Note different scales.

(Below) Maps of precipitation changes in 2016–2035, 2046–2065 and 2081–2100 with respect to 1986–2005 in the RCP4.5 scenario. For each point, the 25th, 50th and 75th percentiles of the distribution of the CMIP5 ensemble are shown; this includes both natural variability and inter-model spread. Hatching denotes areas where the 20-year mean differences of the percentiles are less than the standard deviation of model-estimated present-day natural variability of 20-year mean differences.

Sections 9.4.1.1, 9.6.1.1, Box 11.2, 14.2.2.4, 14.8.13 contain relevant information regarding the evaluation of models in this region, the model spread in the context of other methods of projecting changes and the role of modes of variability and other climate phenomena.

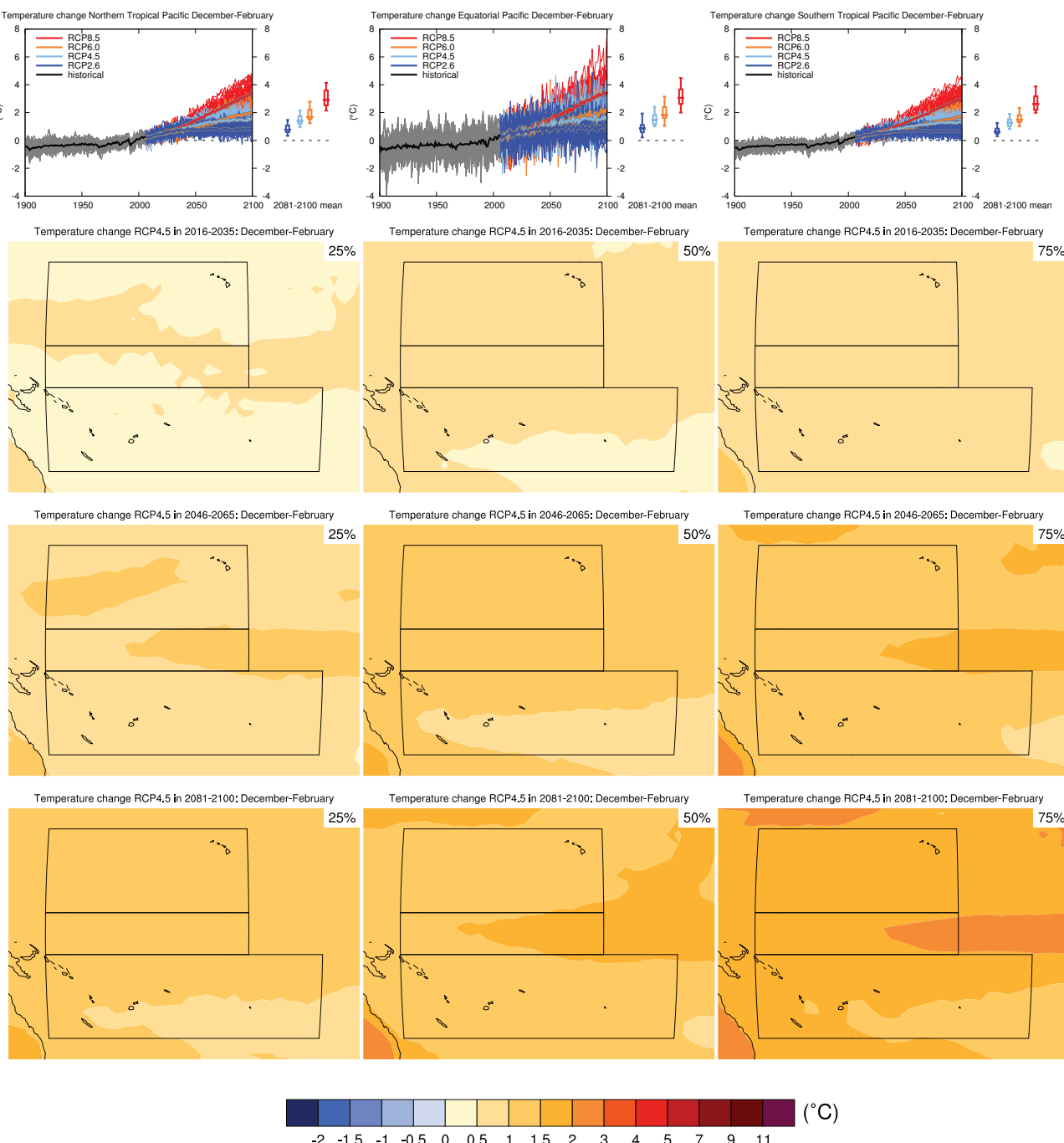


Figure AI.72 | (Top left) Time series of temperature change relative to 1986–2005 averaged over all grid points in the Northern Tropical Pacific (5°N to 25°N , 155°E to 150°W) in December to February. Top middle: same for all grid points in the Equatorial Pacific (5°S to 5°N , 155°E to 150°W). (Top right) Same for all grid points in the Southern Tropical Pacific (5°S to 5°N , 155°E to 150°W). Thin lines denote one ensemble member per model, thick lines the CMIP5 multi-model mean. On the right-hand side the 5th, 25th, 50th (median), 75th and 95th percentiles of the distribution of 20-year mean changes are given for 2081–2100 in the four RCP scenarios.

(Below) Maps of temperature changes in 2016–2035, 2046–2065 and 2081–2100 with respect to 1986–2005 in the RCP4.5 scenario. For each point, the 25th, 50th and 75th percentiles of the distribution of the CMIP5 ensemble are shown; this includes both natural variability and inter-model spread. Hatching denotes areas where the 20-year mean differences of the percentiles are less than the standard deviation of model-estimated present-day natural variability of 20-year mean differences.

Sections 9.4.1.1, 9.6.1.1, 10.3.1.1.4, Box 11.2, 12.4.3.1, 14.4.1, 14.8.14 contain relevant information regarding the evaluation of models in this region, the model spread in the context of other methods of projecting changes and the role of modes of variability and other climate phenomena.

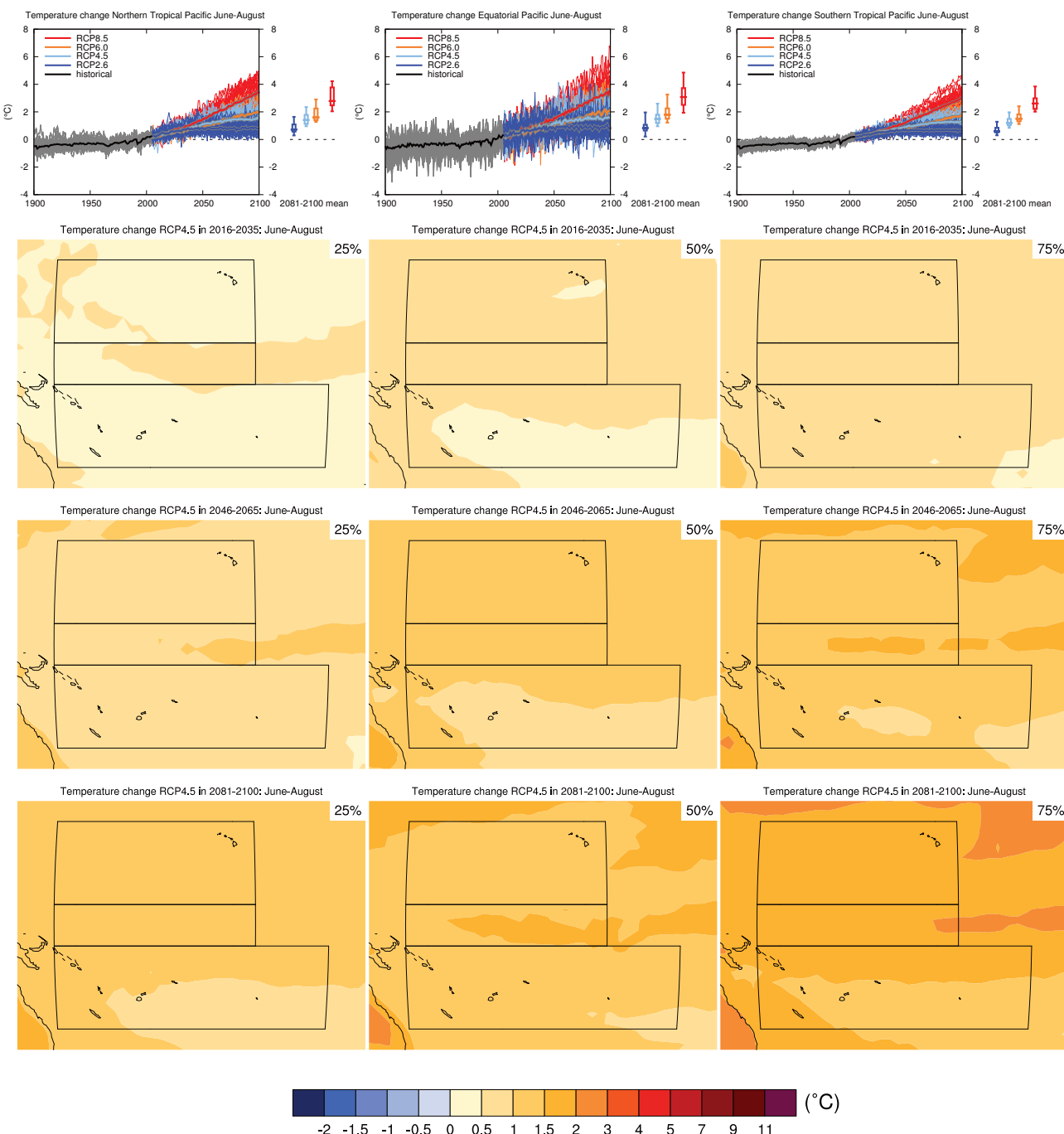


Figure AI.73 | (Top left) Time series of temperature change relative to 1986–2005 averaged over all grid points in the Northern Tropical Pacific (5°N to 25°N , 155°E to 150°W) in June to August. Top middle: same for all grid points in the Equatorial Pacific (5°S to 5°N , 155°E to 150°W). (Top right) Same for all grid points in the Southern Tropical Pacific (5°S to 5°N , 155°E to 150°W). Thin lines denote one ensemble member per model, thick lines the CMIP5 multi-model mean. On the right-hand side the 5th, 25th, 50th (median), 75th and 95th percentiles of the distribution of 20-year mean changes are given for 2081–2100 in the four RCP scenarios.

(Below) Maps of temperature changes in 2016–2035, 2046–2065 and 2081–2100 with respect to 1986–2005 in the RCP4.5 scenario. For each point, the 25th, 50th and 75th percentiles of the distribution of the CMIP5 ensemble are shown; this includes both natural variability and inter-model spread. Hatching denotes areas where the 20-year mean differences of the percentiles are less than the standard deviation of model-estimated present-day natural variability of 20-year mean differences.

Sections 9.4.1.1, 9.6.1.1, 10.3.1.1.4, Box 11.2, 12.4.3.1, 14.4.1, 14.8.14 contain relevant information regarding the evaluation of models in this region, the model spread in the context of other methods of projecting changes and the role of modes of variability and other climate phenomena.

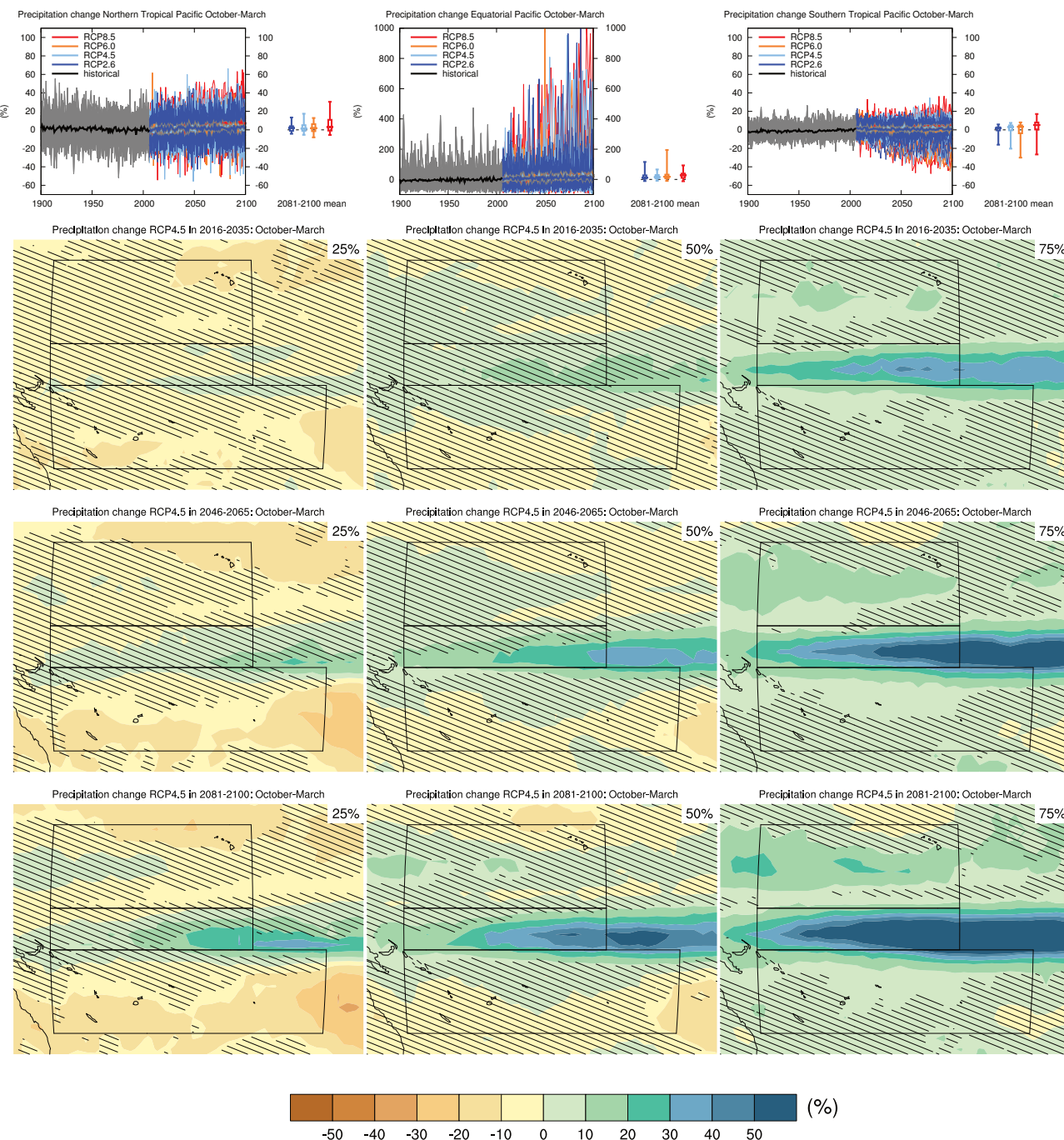


Figure AI.74 | (Top left) Time series of relative change relative to 1986–2005 in precipitation averaged over all grid points in the Northern Tropical Pacific (5°N to 25°N , 155°E to 150°W) in October to March. Top middle: same for all grid points in the Equatorial Pacific (5°S to 5°N , 155°E to 150°W). (Top right) Same for all grid points in the Southern Tropical Pacific (5°S to 5°N , 155°E to 150°W). Thin lines denote one ensemble member per model, thick lines the CMIP5 multi-model mean. On the right-hand side the 5th, 25th, 50th (median), 75th and 95th percentiles of the distribution of 20-year mean changes are given for 2081–2100 in the four RCP scenarios. Note different scales.

(Below) Maps of precipitation changes in 2016–2035, 2046–2065 and 2081–2100 with respect to 1986–2005 in the RCP4.5 scenario. For each point, the 25th, 50th and 75th percentiles of the distribution of the CMIP5 ensemble are shown; this includes both natural variability and inter-model spread. Hatching denotes areas where the 20-year mean differences of the percentiles are less than the standard deviation of model-estimated present-day natural variability of 20-year mean differences.

Sections 9.4.1.1, 9.6.1.1, 11.3.2.1.2, Box 11.2, 12.4.5.2, 14.8.14 contain relevant information regarding the evaluation of models in this region, the model spread in the context of other methods of projecting changes and the role of modes of variability and other climate phenomena.

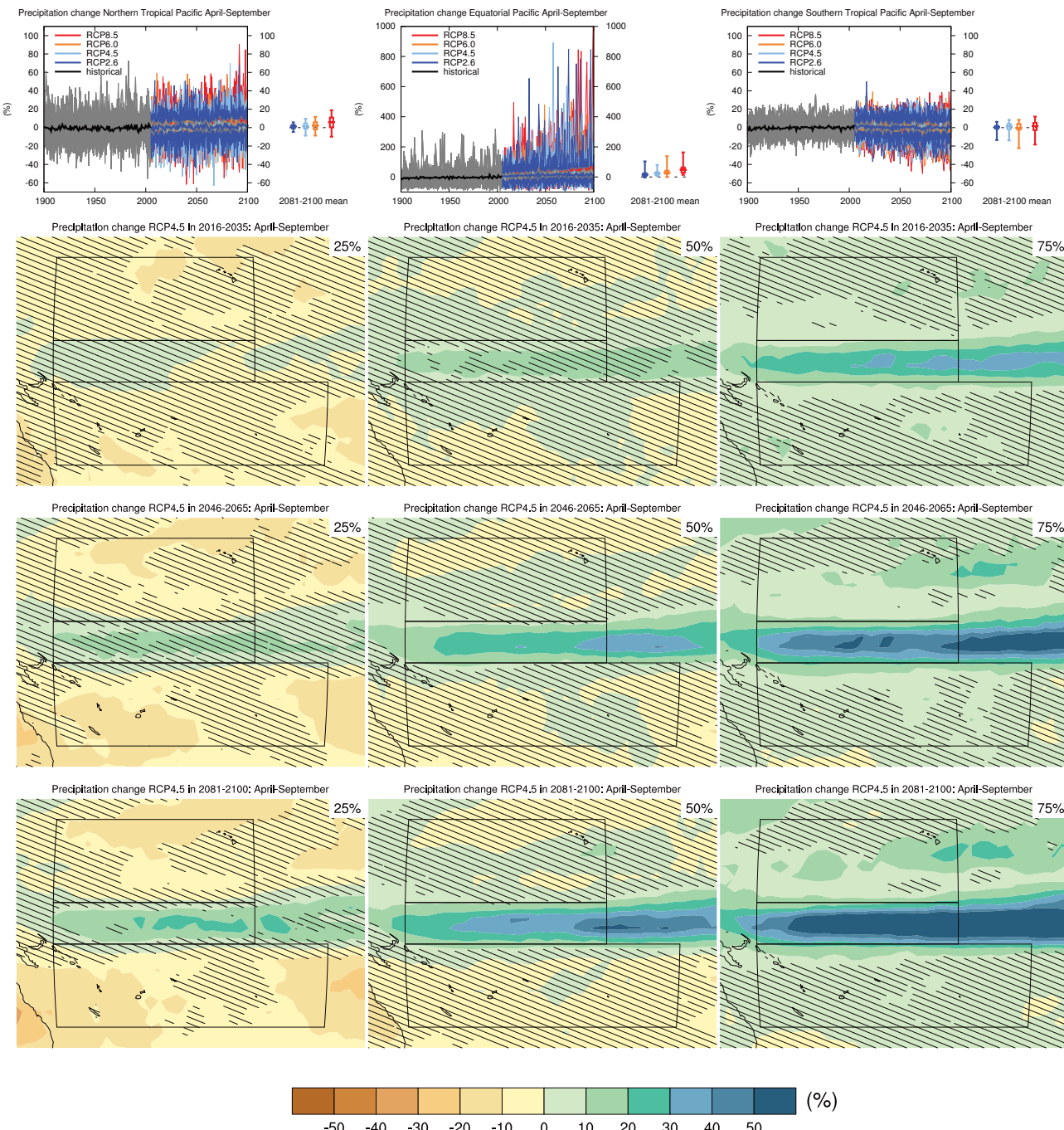


Figure AI.75 | (Top left) Time series of relative change relative to 1986–2005 in precipitation averaged over all grid points in the Northern Tropical Pacific (5°N to 25°N , 155°E to 150°W) in April to September. Top middle: same for all grid points in the Equatorial Pacific (5°S to 5°N , 155°E to 150°W). (Top right) Same for all grid points in the Southern Tropical Pacific (5°S to 5°N , 155°E to 150°W). Thin lines denote one ensemble member per model, thick lines the CMIP5 multi-model mean. On the right-hand side the 5th, 25th, 50th (median), 75th and 95th percentiles of the distribution of 20-year mean changes are given for 2081–2100 in the four RCP scenarios. Note different scales.

(Below) Maps of precipitation changes in 2016–2035, 2046–2065 and 2081–2100 with respect to 1986–2005 in the RCP4.5 scenario. For each point, the 25th, 50th and 75th percentiles of the distribution of the CMIP5 ensemble are shown; this includes both natural variability and inter-model spread. Hatching denotes areas where the 20-year mean differences of the percentiles are less than the standard deviation of model-estimated present-day natural variability of 20-year mean differences.

Sections 9.4.1.1, 9.6.1.1, 11.3.2.1.2, Box 11.2, 12.4.5.2, 14.8.14 contain relevant information regarding the evaluation of models in this region, the model spread in the context of other methods of projecting changes and the role of modes of variability and other climate phenomena.

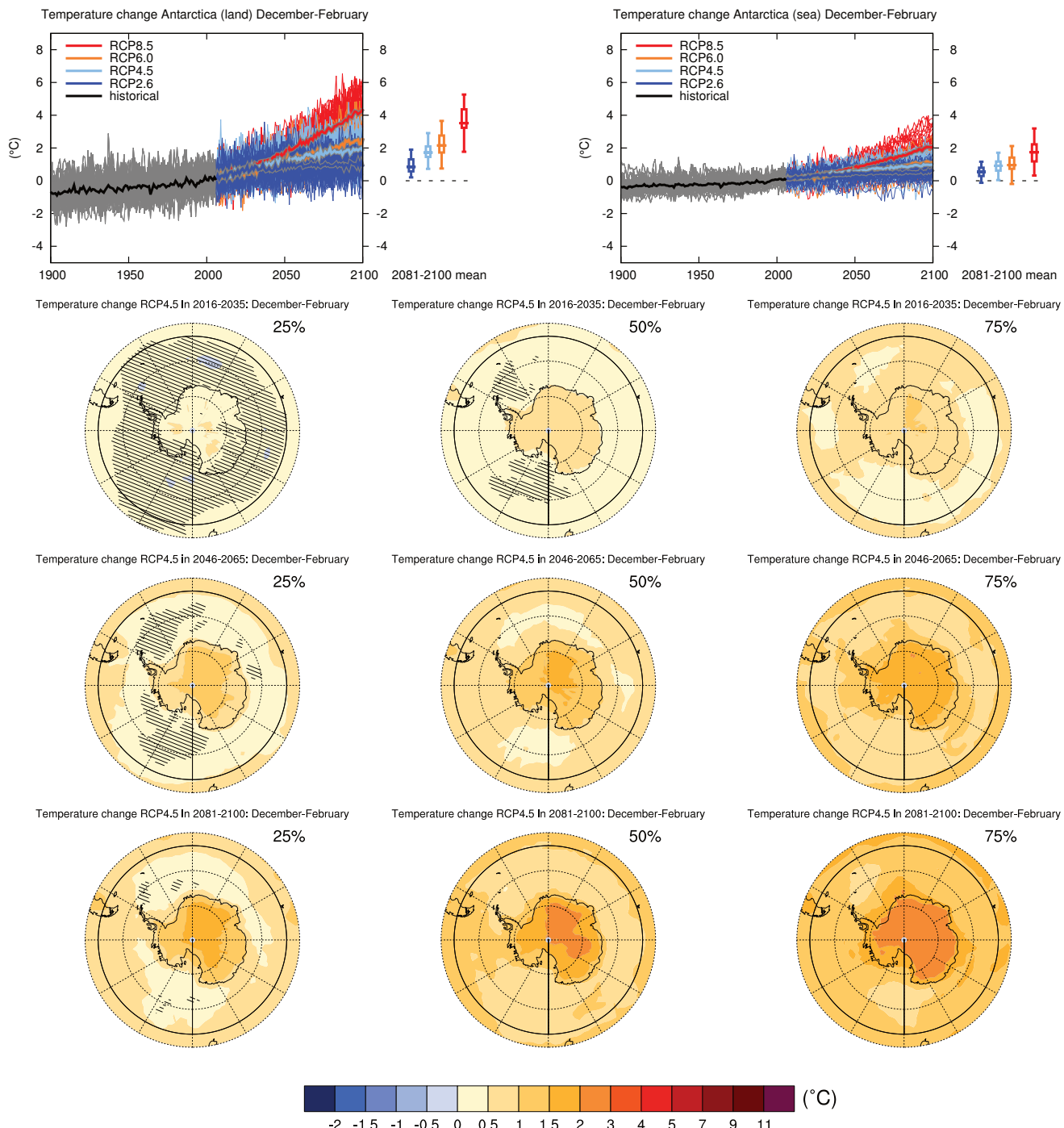


Figure AI.76 | (Top left) Time series of temperature change relative to 1986–2005 averaged over land grid points in Antarctica (90°S to 50°S) in December to February. (Top right) Same for sea grid points. Thin lines denote one ensemble member per model, thick lines the CMIP5 multi-model mean. On the right-hand side the 5th, 25th, 50th (median), 75th and 95th percentiles of the distribution of 20-year mean changes are given for 2081–2100 in the four RCP scenarios.

(Below) Maps of temperature changes in 2016–2035, 2046–2065 and 2081–2100 with respect to 1986–2005 in the RCP4.5 scenario. For each point, the 25th, 50th and 75th percentiles of the distribution of the CMIP5 ensemble are shown; this includes both natural variability and inter-model spread. Hatching denotes areas where the 20-year mean differences of the percentiles are less than the standard deviation of model-estimated present-day natural variability of 20-year mean differences.

Sections 9.4.1.1, 9.6.1.1, 10.3.1.1.4, Box 11.2, 12.4.3.1, 14.8.15 contain relevant information regarding the evaluation of models in this region, the model spread in the context of other methods of projecting changes and the role of modes of variability and other climate phenomena.

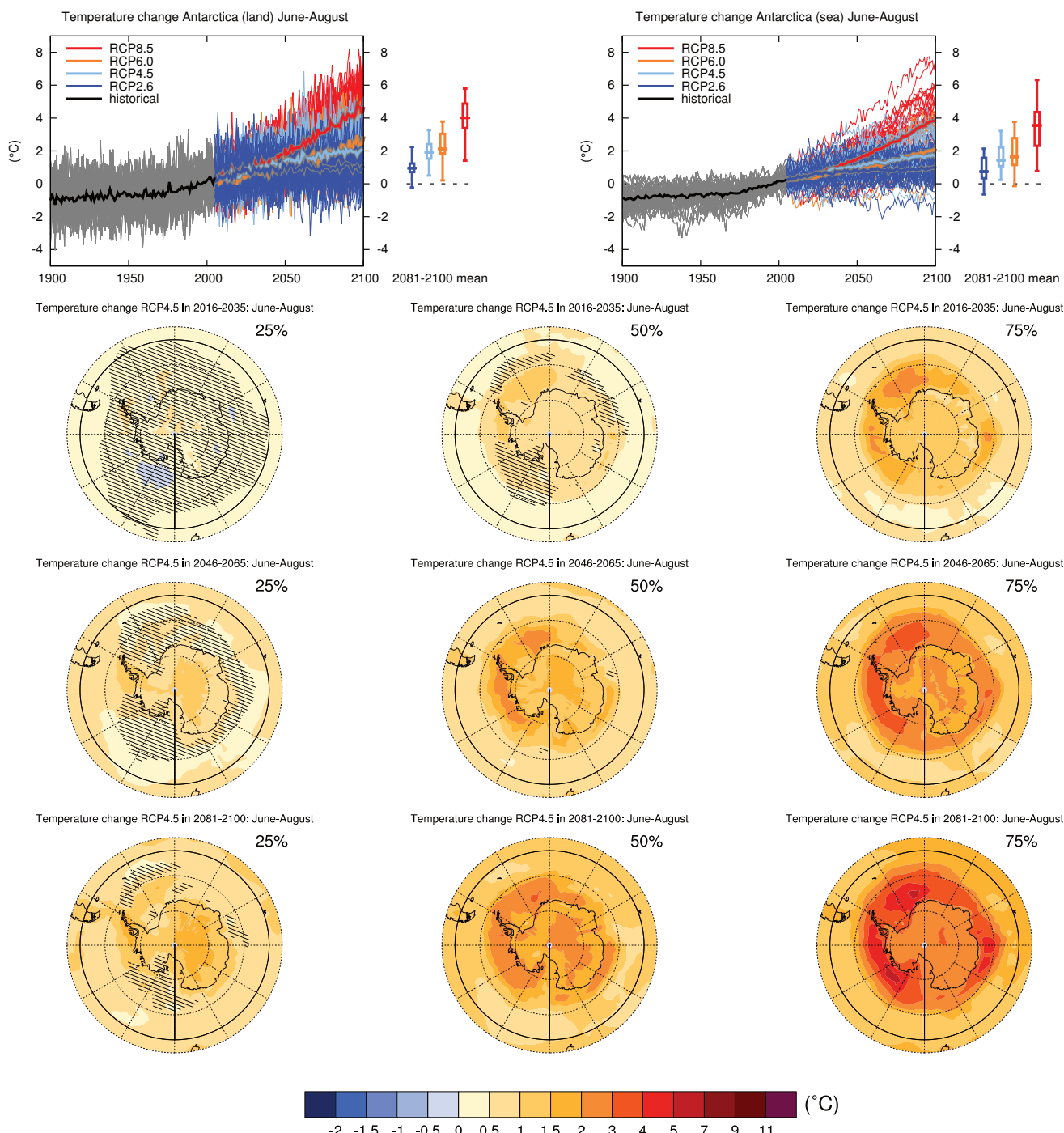


Figure AI.77 | (Top left) Time series of temperature change relative to 1986–2005 averaged over land grid points in Antarctica (90°S to 50°S) in June to August. (Top right) Same for sea grid points. Thin lines denote one ensemble member per model, thick lines the CMIP5 multi-model mean. On the right-hand side the 5th, 25th, 50th (median), 75th and 95th percentiles of the distribution of 20-year mean changes are given for 2081–2100 in the four RCP scenarios.

(Below) Maps of temperature changes in 2016–2035, 2046–2065 and 2081–2100 with respect to 1986–2005 in the RCP4.5 scenario. For each point, the 25th, 50th and 75th percentiles of the distribution of the CMIP5 ensemble are shown; this includes both natural variability and inter-model spread. Hatching denotes areas where the 20-year mean differences of the percentiles are less than the standard deviation of model-estimated present-day natural variability of 20-year mean differences.

Sections 9.4.1.1, 9.6.1.1, 10.3.1.1.4, Box 11.2, 12.4.3.1, 14.8.15 contain relevant information regarding the evaluation of models in this region, the model spread in the context of other methods of projecting changes and the role of modes of variability and other climate phenomena.

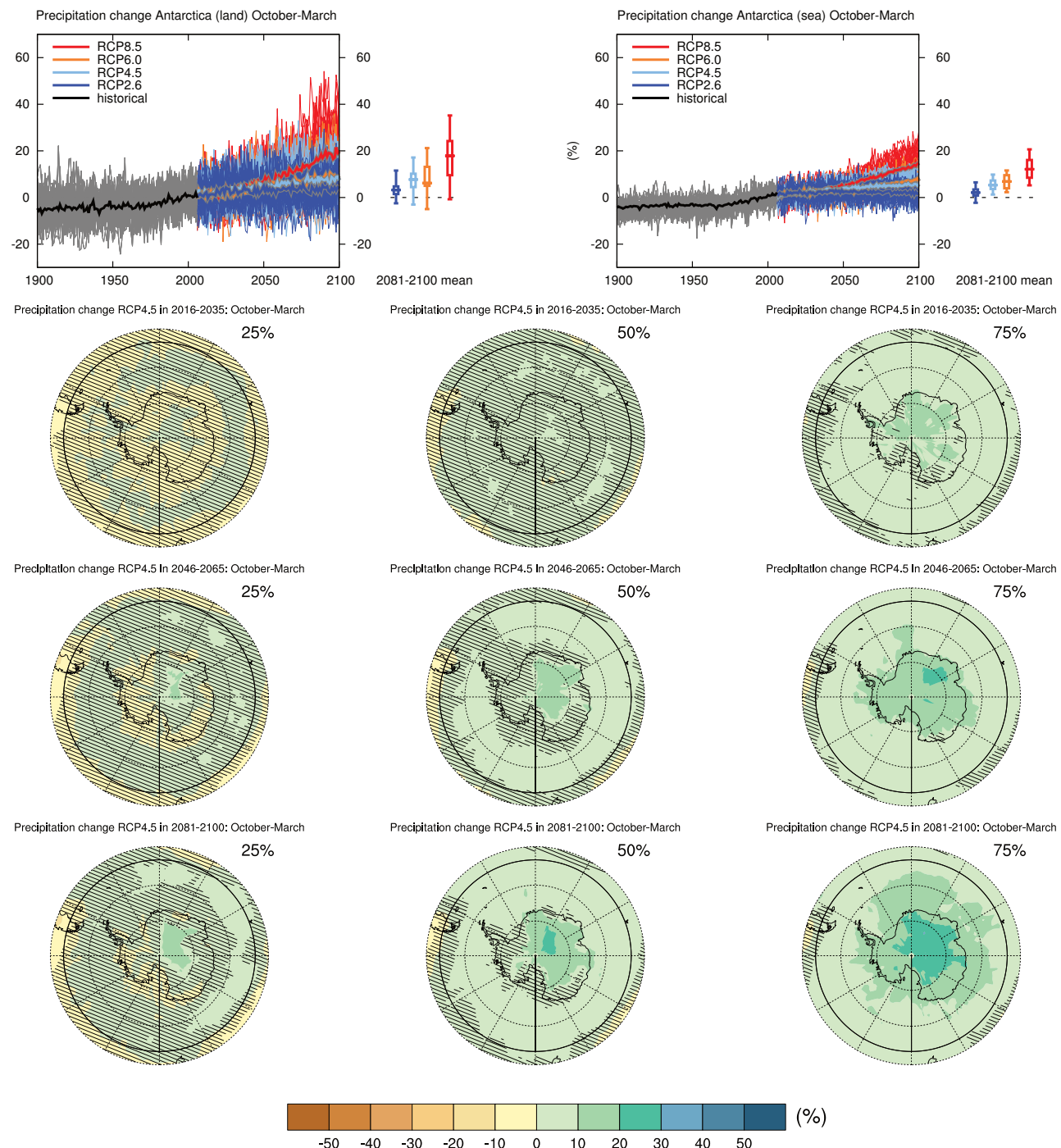


Figure AI.78 | (Top left) Time series of relative change relative to 1986–2005 in precipitation averaged over land grid points in Antarctica (90°S to 50°S) in October to March. (Top right) Same for sea grid points. Thin lines denote one ensemble member per model, thick lines the CMIP5 multi-model mean. On the right-hand side the 5th, 25th, 50th (median), 75th and 95th percentiles of the distribution of 20-year mean changes are given for 2081–2100 in the four RCP scenarios.

(Below) Maps of precipitation changes in 2016–2035, 2046–2065 and 2081–2100 with respect to 1986–2005 in the RCP4.5 scenario. For each point, the 25th, 50th and 75th percentiles of the distribution of the CMIP5 ensemble are shown; this includes both natural variability and inter-model spread. Hatching denotes areas where the 20-year mean differences of the percentiles are less than the standard deviation of model-estimated present-day natural variability of 20-year mean differences.

Sections 9.4.1.1, 9.6.1.1, 10.3.2.2, Box 11.2, 12.4.5.2, 14.8.15 contain relevant information regarding the evaluation of models in this region, the model spread in the context of other methods of projecting changes and the role of modes of variability and other climate phenomena.

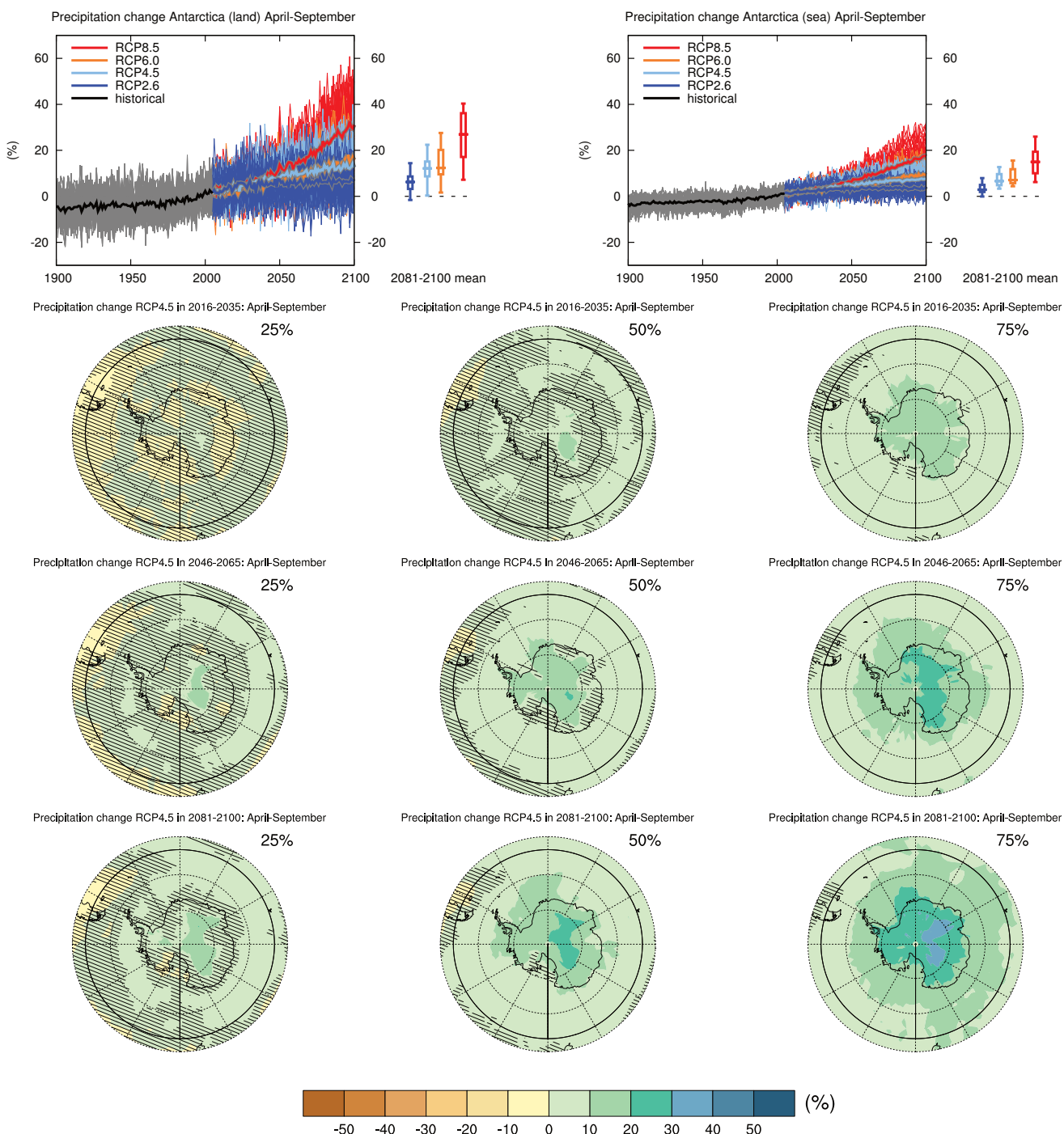


Figure AI.79 | (Top left) Time series of relative change relative to 1986–2005 in precipitation averaged over land grid points in Antarctica (90°S to 50°S) in April to September. (Top right) Same for sea grid points. Thin lines denote one ensemble member per model, thick lines the CMIP5 multi-model mean. On the right-hand side the 5th, 25th, 50th (median), 75th and 95th percentiles of the distribution of 20-year mean changes are given for 2081–2100 in the four RCP scenarios.

(Below) Maps of precipitation changes in 2016–2035, 2046–2065 and 2081–2100 with respect to 1986–2005 in the RCP4.5 scenario. For each point, the 25th, 50th and 75th percentiles of the distribution of the CMIP5 ensemble are shown; this includes both natural variability and inter-model spread. Hatching denotes areas where the 20-year mean differences of the percentiles are less than the standard deviation of model-estimated present-day natural variability of 20-year mean differences.

Sections 9.4.1.1, 9.6.1.1, 10.3.2.2, Box 11.2, 12.4.5.2, 14.8.15 contain relevant information regarding the evaluation of models in this region, the model spread in the context of other methods of projecting changes and the role of modes of variability and other climate phenomena.

